HYDROLOGICAL RESPONSES TO CURRENT AND PROJECTED LAND-USE/LAND COVER CHANGES OF THE WELMEL RIVER WATERSHED, GENALE DAWA BASIN, ETHIOPIA

MSc THESIS

SOLOMON ESHETE AYALEW

HAWASSA UNIVERSITY, HAWASSA, ETHIOPIA

NOVEMBER, 2021

HYDROLOGICAL RESPONSES TO CURRENT AND PROJECTED LAND-USE/LAND COVER CHANGES OF THE WELMEL RIVER WATERSHED, GENALE DAWA BASIN, ETHIOPIA

SOLOMON ESHETE AYALEW

A THESIS SUBMITTED TO

FACULTY OF BIOSYSTEM AND WATER RESOURCE ENGINEERING,
DEPARTMENT OF WATER RESOURCE AND IRRIGATION ENGINEERING

INSTITUTE OF TECHNOLOGY

HAWASSA UNIVERSITY

HAWASSA, ETHIOPIA

IN PARTIAL FULFILLMENT OF THE REQUIREMENTS FOR

THE DEGREE OF MASTER OF SCIENCE IN WATER RESOURCE ENGINEERING AND MANAGEMENT

NOVEMBER, 2021

APPROVAL SHEET

HAWASSA UNIVERSITY

INSTITUTE OF TECHNOLOGY

DEPARTMENT OF WATER RESOURECE ENGINEERING AND MANAGEMENT

Advisors Approval Form

(Submission Sheet-1)

This is to certify that the thesis entitled as **"Hydrological Responses to Current and Projected Land-use/Land Cover Changes of the Welmel River Watershed, Genale Dawa Basin, Ethiopia''** has been approved by the Faculty of Biosystem and Water Resource Engineering for partial fulfilment of the Degree of Master of Science with specialization in Water Resource Engineering and Management and has been carried out by Solomon Eshete Ayalew,ID.NO:WRKMK/008/08, under my/our supervision. Therefore, I/we recommend that the student has fulfilled the requirements and hence hereby can submit the thesis to the department.

Approved by:

Major Advisor: Abraham W/Mikael (PhD) _____ _____

Name Signature Date

Co-Advisor: Tewodros Assefa (PhD) _____ _____

Name Signature Date

EXAMINER'S APPROVAL SHEET-I

SCHOOL OF GRADUATE STUDIES

HAWASSA UNIVERSITY EXAMINERS' APPROVAL SHEET-1

(Submission Sheet-2)

We, the undersigned, members of the Board of Examiners of the final open defense by Solomon Eshete Ayalew have read and evaluated his thesis entitled **"Hydrological Responses to Current and Projected Land-use/Land Cover Changes of the Welmel River Watershed, Genale Dawa Basin, Ethiopia''**, and examined the candidate. This is, therefore, to certify that the thesis has been accepted in partial fulfillment of the requirements for the degree.

_____	_____	_____
Name of Major Advisor	Signature	Date
_____	_____	_____
Name of the Chairperson	Signature	Date
_____	_____	_____
Name of Internal Examiner	Signature	Date
_____	_____	_____
Name of External Examiner	Signature	Date
_____	_____	_____
SGS Approval	Signature	Date

Final approval and acceptance of the thesis is contingent upon the submission of the final copy of the thesis to the School of Graduate Studies (SGS) through the Department/School Graduate committee (DGC/SGC) of the candidate's department.

Stamp of SGS

Date: _____

DEDICATION

This thesis manuscript is dedicated to my Mother**,** *ABEBECH WORKU,* for her love and Sacrifice in the success of my life.

DECLARATION

I, Solomon Eshete Ayalew, declare that this thesis is my own original work and that it has not been presented and will not be presented by me to any other university for similar or any other degree award.

Name: Solomon Eshete

Email: se61921@gmail.com

Signature: _____

Date: _____

ACKNOWLEDGEMENTS

First of all, I would like to present my thanks to my almighty GOD for being with me and helping me to complete this work. I would like to express my deepest gratitude to my Advisors Dr. Abraham W/Mikael and Dr. Tewodros Assefa for their professional advice and valuable suggestions throughout my study. I express my gratitude to Netherlands Initiative for Capacity development in Higher Education (NICHE) project, for their financial support. I extend my thanks to the National Meteorology Agency of Ethiopia and the Ministry of Water, Energy and Irrigation for providing me with all the necessary meteorological and hydrological as well as spatial data, which were important to my work. I would like special thanks to Firew Abebe who is a Development Agent in the study area for his endless help during site data collection. I further extend my gratitude to my friends Henok mekonen, Hailu Nega and Kalayu Kiros for their help during my work.

ABBREVIATIONS AND ACRONYMS

Arc SWAT	SWAT-Integrated with ArcGIS
CA-Markov	Cellular Automata Markov
DEM	Digital Elevation Model
FAO	Food and Agricultural Organization
GPS	Global Information System
HRU	Hydrologic Response Unit
LULC	Land Use/Land Cover
LULCC	Land Use/Land Cover Change
MCM	Markov Chain Model
NGOs	Non-Governmental Organizations
RS	Remote Sensing
SCS	Soil Conservation Service
SWAT	Soil and Water Assessment Tool
SWAT CUP	Soil and Water Assessment Tool Calibration Uncertainty Procedures
USDA-ARS	US Department of Agriculture-Agriculture Research Service
DMC	Double Mass Curve
GIS	Geographic Information System
ERDAS	Earth Resources Data Analysis System
USGS	United States Geological Survey

TABLE OF CONTENTS

LIST OF TABLES

LIST OF FIGURES

ABSTRACT

Land use/land cover change is one of the important concerns in many regions of the world. It is recognized that dramatic LULC change can significantly impact regional climate, ecosystem stability, water balance, stream silt up, socioeconomic practices, and biodiversity. The main objective of this study was to assess the hydrological responses to historical and future Land Use/Land Cover Change at basin and sub-basin levels of the Welmel River watershed, which is located in the Genale-Dawa Basin South Eastern Ethiopia using hydrological SWAT model. The study analyses the historical LULC change between the years 1990, 2005 and 2020 and the future year of 2035 and 2050. The hydrological responses to LULC changes in the Watershed were analyzed using the historical and future LULC maps. Images were processed using ERDAS Imagine 2014 and CA-Markov chain model was used for the prediction of the LULC map of 2035 and 2050. Discharge data from 1990 to 2006 and 2007 to 2014 were used for calibration and validation respectively with three years of warm-up period and climate data from 1990 to 2020 time period. The main finding of this study revealed that the coverage of agriculture/settlement increased by a rate of change of 6.85km^2/year, while forestland was declined by the rate of change of 9.16km^2/year over the last 31 years between 1990 and 2020. In the coming 31 years (by 2050), if the current trend of LULC change continues, agriculture/settlement land is expected to increase by the rate of change of 6.73km^2/year, while forestland is expected to diminish by a rate of change of 8.78km^2/year. As a result of LULC change, surface runoff has increased by 25.32% while lateral flow, groundwater flow, water yield, evapotranspiration and percolation declined by 19.91%, 17.17%, 2.38%, 0.36% and 17.17% respectively between 1990 and 2020. If the current rates of LULC change continue, surface runoff is expected to increase by a relative change of 18.47% while lateral flow, groundwater flow, water yield, evapotranspiration and percolation are expected to decline by 26.84%, 17.51%, 2.09%, 1.91% and 17.47% respectively by 2050. Average annually, surface runoff in all 29 sub-basins has increased by 39.90mm and groundwater flow decreased by 34.57mm. The average annual stream flow increased with a relative change of 6.18% from 1990 to 2020 and is expected to increase by 12.69% by 2050. The average wet annual flow from 1990 to 2020 increased by 10.21%, while the average dry annual flow decreased by 6.34%. The average wet and dry annual stream flow is expected to increase and decline by 19.67 % and 6.86% respectively in 2050. Therefore, the Woredas in and around the Welmel River Watershed and the Bale Mountains National Park should integrate to design and implement a proper strategy for protecting and managing the existing forest and woodlands in addition to rehabilitating the degraded areas to maintain the hydrological balance of the watershed.

Key words: *Welmel Watershed, Land-use/land cover change, SWAT model, Water balance*

1. INTRODUCTION

1.1. Background

Land use/land cover change is one of the important concerns in many regions of the world (Taelman *et al.,* 2016; Belward *et al.,* 2015). It is recognized that dramatic LULC change can significantly impact regional climate, ecosystem stability, water balance, stream silt up, socioeconomic practices, and biodiversity (Alam *et al.,* 2019; Temesgen *et al.,* 2017; Dayamba *et al.,* 2016; Mengistie *et al.,* 2013). The intensity, speed, and degree of LULC changes are now faster compared to the past because of the development of society, and the rapid increase in population resulted in disturbing a large number of landscapes on Earth (Lambin and Meyfroidt, 2011). For instance, at least 50% of Earth's ice-free land surface of the planet transformed by human actions (Hooke *et al.,* 2012). On the global scale, urban land area increased by 346.4 thousand km^2 and growth by 1.3% from 1992 to 2016 (He *et al.*, 2019). Considering the current trends in population density change, by 2030, the urban land cover will increase by 1.2 million km^2 (Seto *et al*., 2012).

The dynamic nature of Land use/land cover change arising from an increasing population and expansion of agricultural land is also happening at an alarming rate in Ethiopia. Expansion and intensification of agriculture, growth of urban areas and extraction of timber and other natural resources will likely accelerate over the coming decades to satisfy the demands of an increasing population. This change of LULC in a rural and urban area is the result of deforestation, agricultural land expansions, human settlements and other factors derived from the population growth and environmental problem. Many literatures showed that population growth is the main factor for the land-use change in urban or rural areas (Tesfa and Bogale, 2015; Hagos, 2014; Asimamaw, 2013; Dereje, 2010; Kassa, 2009). Previous studies in different parts of Ethiopia have shown a rapid expansion of

cultivated land at the expense of forestlands in the country (Ebrahim and Mohamed, 2017; Temesgen *et al.,* 2014; Tesfay *et al.,* 2013; Solomon *et al.,* 2010). Evidence from several studies shows a high conversion of forest vegetation land to agricultural and pasture land (Mango *et al.,* 2011; Eleni *et al.,* 2013). According to the Food and Agriculture Organization (FAO) of the United Nations (2010), in East Africa, nearly 13 million hectares of original forest were lost in 20 years period, and the remaining forest is fragmented and continually under threat. On the other hand, the recent data on forest resources of Ethiopia reported in FAO (2010) puts Ethiopia among countries with a forest cover of 10-30%. According to this report, Ethiopia's forest cover is 12.2 million ha (11%). It further indicated that the forest cover shows a decline from 15.11million ha in 1990 to 12.2 million ha in 2010, during which 2.65% of the forest cover was deforested.

Excessive pressure on land resources aimed at providing food, water and shelter have resulted in a significant change of land cover which consequently modified the hydrological regimes (Gyamfi *et al.,* 2016; Savenije *et al.,* 2014). The activities of land use/land cover changes influence the hydrological processes such as interception rates, soil moisture storage, evapotranspiration loss, infiltration and groundwater recharge, leading to modifications in basin water resources (Tesfay *et al.,* 2019; Temesgen *et al.,* 2018; Tekalegn *et al.,* 2017; Tesfay *et al.,* 2013). Moreover, LULC changes affect the spatial and temporal variability of the watershed hydrology through modifying stream flow, surface runoff, base-flow and evapotranspiration (Liu *et al.,* 2017; Rahman *et al.,* 2015). The conversion of forest into urban and agricultural areas results in higher surface runoff and reduced groundwater recharges (Gyamfi *et al*., 2016; Baker and Miller, 2013).

The Ethiopian highlands, covering 45% of the country, is affected by severe LULC and land degradation problems (Temesgen *et al.,* 2018; Nigussie *et al.,* 2014; Nyssen *et al.,* 2014). Because of the high increase of population, a rapid expansion of cultivable lands has significantly reduced land with natural vegetation (Ariti *et al.,* 2015; Tesfay Gebretsadkan *et al.,* 2013; Nigussie *et al.,* 2017). In the Bale Mountain Eco-Region, Ethiopia, the Welmel River Watershed, which is one of the contributors of the Genale Dawa Basin, is currently characterized by severe land degradation. The natural vegetation has been replaced by cultivable and grazing lands (Girma *et al.,* 2019; Adane and Getachew, 2017; Sisay *et al.,* 2016). Thus, estimating current and future LULC changes and the responses of hydrology to the changes can be essential to the decision-making of environmental management and future planning. Hydrological models are generally used to evaluate the effects of LULC changes on hydrological processes. These models simulate the spatial as well as temporal responses of various LULC changes on the hydrological components in a river basin (Garg *et al.,* 2019; Mulatu *et al*., 2019; Temesgen *et al*., 2018; Yan *et al*., 2018; Zhou *et al*., 2013).

1.2. Statement of the problem

Welmel River Watershed, Genale-Dawa Basin is a prominent ecosystem resource of the basin since the watershed lies along Mena-Harenna-Angetu forest and Bale Mountains National Park. However, land use/land cover change, and its impact on hydrology is one of the major threats in the watershed. Currently, the watershed area in the basin is under increasing threat from forest degradation, overgrazing of livestock, expansion of the agricultural area, disturbance of the water systems, unsustainable fuel wood and timber extraction, fire and rapid immigration with unplanned and unrestricted settlement(Farm-Africa-SOS Sahel Ethiopia, 2010; Alemtsehay , 2010; Sisay *et al.,* 2015). Excessive

pressure on land resources aimed at providing food, water and shelter has resulted in a significant change of land cover which consequently modified the hydrological regimes (Gyamfi *et al.,* 2016; Savenije *et al.,* 2014). Alteration of existing land management practices in a catchment affects the hydrological processes and consequently the overall water availability in rivers (Kiptala *et al.,* 2013).

Analyzing and understanding the effect of LULC changes is important for policymaking, planning and implementation of natural resource management (Reddy and Gebreselassie, 2011). There are some studies conducted regarding LULC changes in the study River Watershed, but the impact of such LULC changes on hydrology is not studied specifically in the Welmel Watershed. Those studies were focused on land use and land cover change detection and deforestation modeling in the Bale Mountain Eco-Region, Ethiopia. For instance, Girma *et al.* (2019); Adane and Getachew, (2017); Sisay *et al. (*2016) conducted modeling of LULC in the study area. Moreover, a number of studies have assessed the hydrological responses to LULC changes in different parts of the watershed in Ethiopia. Though, most of those studies have focused specifically at the watershed level. Accordingly, the responses of hydrology to LULC change is commonly more evident at a sub-basin level (Marhaento *et al.,* 2017; Schilling *et al.,* 2014; Wagner *et al.,* 2013), whereas their impact on the water budget elements is relatively small at a larger basin level due to compensating effects (Alemayehu *et al.,* 2019; Schilling *et al.,* 2014). As a result, information about how and by how much LULC changes will influence the hydrology at the sub-basin level is important for planning appropriate mitigation measures (Marhaento *et al.,* 2017). Based on this, this research aimed to evaluate the hydrological responses to historical and projected LULC changes of the Welmel River Watershed.

1.3. Objectives of the study

1.3.1. General objective

The main objective of this study was to assess the hydrological responses to historical and future land use/land cover changes at basin and sub-basin levels in the Welmel River watershed, Ethiopia.

1.3.2. Specific objectives

The specific objectives of this study were to:

- Detect the land use/land cover changes over the last 31 years (1990-2020).
- Predict future land use/land cover changes for the year 2050.
- Assess the responses of hydrological components to historical and future LULC changes.

1.4. Research Questions

This study addressed the following research questions:

- ✓ Are there changes in different categories of historical and future LULC in the watershed? If so, which of the LULC types show the most increasing and declining during the study period?
- ✓ Does the land use/land cover change affect the hydrological components at the basin and sub-basin level in the Welmel Watershed?
- ✓ What is the response of wet and dry season stream flow to land use/land cover change in magnitudes of Welmel Watershed?

1.5. Significance of the Study

This study was accomplished through a strategy that combines the hydrological model (SWAT) to simulate the hydrological processes, GIS and remote sensing methods to

analyze the Land Use/Land Cover change and future Land Use/Land Cover change was predicted using the CA-Markov chain model. Land use/land cover change data is important for setting up the historical and present conditions and foreseeing the future patterns of the land use/land cover changes and evaluating the responses of hydrology to the LULC change. Therefore, the discoveries from this study will help hydrologists and land resource managers and NGOs to have information about the study area. The findings of this study will be documented for future use by policymakers, local land managers and any responsible/interested bodies who can carry out development interventions on water and land resource management programs. Furthermore, the study results will be used by students, researchers and other interested bodies as baseline information for future studies.

1.6. Scope of the Study

The study was conducted in Genale-Dawa River Basin, specifically in Welmel River Watershed. The focus of this study was evaluating responses of hydrological components to historical and predicted land use/land cover change using CA-Markov chain and hydrological SWAT models. Responses of hydrological components to historical LULC changes were evaluated using 1990, 2005 and 2020 LULC maps in reference with the baseline LULC map of 1990, while responses to the predicted LULC changes using 2020, 2035 and 2050 LULC map with the baseline of 2020 LULC map. Although the hydrology of the watershed can be affected by factors of climate change and variability, this study only focuses on the responses of hydrological components to LULC changes. Moreover, the study was not considered the driving forces of land use/land cover changes in the study area. This research also limited in detecting the impact of LULC change on HRU as considered only at the basin and sub-basin levels.

2. LITERATURE REVIEW

2.1. Land-Use/Land Cover Change

Land is the platform on which most human activities are performed and is the source of many materials needed for such activities. Land cover and land use are the two interrelated ways of observing the earth's surface. Land use describes activities, arrangements, and inputs often associated with people that take place on the land and represent the current use of property such as residential homes, shopping centers, row crops, tree nurseries, state parks, and reservoirs. Land cover describes the natural and anthropogenic features that can be observed on the Earth's surface, i.e., forests, tidal wetlands, developed/built areas, grasslands, and water (Kaul *et al.,* 2012). A change in land cover refers to the conversion of one land cover type to a new cover type or modification within one land cover category. On the other hand, land-use change refers to a conversion of land use due to the interference of human beings for different purposes such as for settlement, infrastructural development, agriculture and recreational uses (Caldas *et al.,* 2015).

The relationship between land use and land cover can be described as: change in land use can affect and be affected by land cover; however, the change in either of them is not necessarily the product of the other. A single land-use system may correspond to a single land cover or it may involve several distinct covers (Briassoulis, 2011). For instance, a farming system may involve several distinct covers such as cultivated land, woodlots, improved pasture and settlements. On the other hand, a single class of cover may support multiple uses. For example, the area covered by natural forest can be used for hunting and gathering, fuel wood collection, recreation and wildlife preservation (Briassoulis, 2011; Verheye, 2011). LULC change refers to the human modification and conversion of the earth's terrestrial surface (Hamza and Aiayi, 2012; Shrestha, 2012). Modification occurs

when the change affects only the characteristics of the land cover without causing a complete shift from one LULC type to the other. On the other hand, conversion of LULC occurs when one LULC type is completely replaced by another (Binyam *et al.,* 2015).

2.2. Land-Use/Land Cover Change in Ethiopia

Most studies conducted shown that, the land in Ethiopia is being used by small holders who farm for subsistence. With the rapid population growth and in the absence of agricultural intensification, small holders require more land to grow crops and earn a living, which results in deforestation and land-use conversions from other types of land cover to crop land (Asmamaw, 2013). More than 90% of the Ethiopian high lands were once forested, today small area is covered by trees and the percentage of forest cover is less than 4% (Hurni *et al*., 2010). This is evidence of a high incidence of degradation of vegetation in the past, which has continued to the present. The land use and land cover change from the 1980s to 2000s showed a continuous decline of shrub lands and forest cover, but improvements in vegetation cover in some areas. The expansion of cultivated land continued to very steep slopes and marginal lands (Alemayehu, 2010).

In the highland parts of Ethiopia there was expansion of agriculture at the expense of vegetated lands mainly shrub land, woodland and forestlands since the 1860s and expansion of agriculture at the expense of vegetated lands worsened since 1980s (Hiywot, 2014). In the Gilgel Gibe catchment in the south western part of Ethiopia agricultural land and urban area increased continuously in 1987, 2001 and 2010. Forest cover increased between 1987 and 2001 but decreased between 2001 and 2010. In the opposite range land decreased in the first period but then increased in the second period. Water body decreased continuously through all these years (Wakjira *et al.,* 2016). Birhan & Assefa, (2017) in the Northern highlands of Ethiopia investigated that cultivated land, urban area and bare land

increased continuously in 1964, 1986 and 2014. Forest cover decreased dramatically between 1964 and 2014 as a result of population growth, cultivated land and rural settlement expansion, and growing demand for the forest for extraction of fuel and construction materials. Similarly, Efrem, (2010) in the semi-arid areas of the central Rift Valley of Ethiopia, during the period 1973-2000 cultivated land has increased at the expense of other LULC changes. In the Bale mountain eco-region of Ethiopia, land use/land cover change was undertaken dramatically especially between 1985 and 2015, as a result of farm land and settlement expansion were found to be major drivers of land use and land cover change in the region (Sisay *et al*., 2016).

Studies undertaken in different parts of Ethiopia reported population growth as a major cause for LULCC. Population growth was the major cause for the expansion of agriculture and reduction of vegetation covers in Ethiopian highlands (Alemayehu, 2010), Borena Wereda South Wello Highland (Abate and Singh, 2011); Nono Wereda, Central Ethiopia (Messay, 2011), West Guna Mountain South Gondar (Lewoye, 2014) and Northwest lowland of Ethiopia (Binyam *et al.*, 2015).

2.3. Responses of Hydrological Components to LULC Changes

Land Use/Land Cover changes are the most common cause of loss of biological productivity and biodiversity in aquatic and terrestrial ecosystems. The LULC change affects the climate of an area which in turn affects natural resources such as water, wetlands and biodiversity (IPCC, 2007; Gibbard *et al.*, 2005). Land use and land cover changes influence hydrological processes by altering interception rates, soil water, evapotranspiration, infiltration, and groundwater, leading to changes in Surface runoff and stream flow. Increasing land-use conversion especially for urbanization, deforestation, grassland depletion can potentially lead to an increase in stream flow and flood frequency

(Schilling *et al.,* 2014). During storm events, greater Surface runoff can exceed the flow carrying capacity of the stream within the watershed which may increase the risk of potential flooding.

Higher porosity increases infiltration and percolation rates and the water-holding capacity of the soil. Infiltration rates are positively related to litter and grass basal cover, being up to 9 times faster with 100% litter cover than for bare soil. Therefore, deforestation increases surface runoff and reduces recharge by affecting the above condition especially if the area is steeply sloped and recharging zone (Orkodjo, 2014). Land use/land cover affects runoff in the form of accelerated or retarded overland flow as a result of slow or fast infiltration rate and initial abstraction due to canopy cover. Initial abstraction is a parameter that accounts for all losses before runoff and consists mainly of interception, infiltration, evaporation, and surface depression storage (the storage of water in low areas, such as ponds, and wetlands). In theory, all Rainfall minus Initial Abstraction will generate the runoff from a specified Catchment (Caletka *et al.,* 2020).

The amount and type of vegetative land cover is one determinant of the water yield of a drainage basin. Forests produce higher rates of evapotranspiration and interception (the storage of water on leaf surfaces) than do grass or shrub lands, all of which influence the amount of water that is available for direct drainage into streams or for aquifer recharge (Farley *et al.,* 2005). Trees have lower surface albedo, higher surface aerodynamic roughness, higher leaf surface area, and deeper roots than other types of vegetation, with each characteristic tending towards an increase in evapotranspiration of water and a decrease in stream flow discharge. The conversion of the land surface from native cover to managed cropland affects the evapotranspiration, infiltration and overland runoff

characteristics of a watershed. Crops need less soil moisture than forests; therefore, the rainfall satisfies the shortage of soil moisture in agricultural lands more quickly than in forests there by generating more runoff. The increased removal of native vegetation and soil compaction decreases soil infiltration capacity. Hence, this leads to an increase in the hydrological component of surface runoff (Kotei *et al.*, 2013).

Depending on the type of product being grown, croplands tend to have a percentage of bare ground even during the peak of the growing season and may be completely bare before being planted. In both instances, most of the precipitation that lands on these denuded areas will be discharged directly into the stream channel rather than infiltrating into the soil or evaporating/transpiring from the plant surfaces. As a result, conversion to cropland tends to increase water yield compared to native vegetation (Fisher and Mustard, 2004). There is a growing consensus for the need to understand and improve water resources management to meet new challenges posed by increasing demand and diminishing water supply. However, the options, processes and impacts of desired change are less clear (Hajkowicz, 2009). Therefore, a good understanding of the processes causing land-use change and their effects on the hydrology of small sub-catchment is essential. Such understanding includes both assessments of the anticipated rate and spatial pattern of land-use change as well as knowledge of the underlying human and biophysical drivers.

2.4. Remote Sensing and GIS in LULC Change Detection

Remote Sensing is defined as the science of obtaining information about an object, area, or phenomenon through the analysis of data acquiring by a device that is not in contact with the object, area, or phenomenon under investigation (Razak and Firdaus, 2013). It provides a large amount of data about the earth's surface for detailed analysis and change detection with the help of sensors. Most of the data inputs to the hydrological (SWAT) model are

directly or indirectly extracted from remotely sensed data. Some of the important data used in the hydrological modeling that are obtained from remote sensing include digital elevation model (DEM) and land use/land cover maps. Some of the applications of remote sensing technology in mapping and studying the land use and land cover changes are; mapping and classifying the land use and land cover, assessing the spatial arrangement of land use and land cover, allowing analysis of time-series images used to analyze landscape history, report and analyze results of inventories including inputs to Geographic Information System (GIS), provide a basis for model building.

LULC is changing rapidly in most parts of the world. In this situation, accurate, meaningful and availability of data is highly essential for planning and decision making. Remote sensing is particularly attractive for the land cover data among the different sources (Stefanov *et al.*, 2001) reported that in the 1970's satellite remote sensing techniques have started to be used as a modern tool to detect and monitor land cover change at various scales with useful results. Information of land use/land cover change which is extracted from remotely sensed data is vital for updating land cover maps and the management of natural resources and monitoring phenomena on the surface (Girum and Tesfa, 2018). The importance of land cover mapping is to show the land cover changes in the watershed area and to divide the land use and land cover into different classes of land use and land cover. For this purpose, remotely sensed imagery plays a great role in obtaining information on both temporal trends and spatial distribution of watershed areas and changes over the time dimension for projecting land cover changes but also to support changes impact assessment (Atasoy *et al.,* 2006). To monitor the rapid changes of land cover, to classify the types of land cover, and to obtain timely land cover information, multi-temporal remotely sensed images are considered effective data sources.

2.5. Modeling and Prediction of LULC

Models are useful for sorting out the complex groups of socio-economic and biophysical forces that influence the rate and spatial pattern of LULC change and for estimating the impacts of changes in LULC change. Moreover, models can support the prediction of future LULC changes under different scenario conditions, based on past evidence (recent past). Assessing and predicting LULCC would help for effective environmental management and sustainable resources use (Nath *et al.,* 2020). There are many LULC change models with their strong sides and limitation though there is no clearly prioritized approach to model LULC changes (Eskider *et al.,* 2017). However, the Markov Chain and Cellular Automata Analysis (CA-Markov) model, a hybrid of the cellular automata and Markov models, is the most commonly used spatially explicit model in recent literature because of its consideration to the spatial and temporal components of the LULC dynamic (Behera *et al*., 2012; Temesgen *et al.,* 2017). It is a discrete-time stochastic model, describing the probabilistic movement of one state (LULC type) to another state (LULC type) (Eskider *et al.,* 2017). The 'Cellular Automata' and 'Markov Chain' models are considered to be advantageous for modeling land-use changes (Mishra and Rai, 2016; Parsa *et al*., 2016). A disadvantage of the Markov chain model is its inability to provide a spatial distribution of the LULC occurrences, but rather an estimate of the magnitude of these changes (Maviza and Ahmed, 2020; Yang *et al.,* 2012). Cellular automata (CA) however, have the ability to change and control complex spatially distributed processes, with a strong ability to simulate the spatio-temporal characteristics of complex systems (Yang *et al.,* 2014; Guan *et al.,* 2011).

The CA-Markov model is the integration of cellular automata and transition probability matrix created by the cross-tabulation of two dissimilar images. This integration of the CA-

Markov model offers a strong method in spatial and temporal dynamic modelling. In other words, the CA-Markov chain can simulate and predict any transitions among any number of categories (Abdulrahman and Ameen, 2020). The CA-Markov model uses Markov Chain analysis outputs, particularly the transition area file, to apply a contiguity filter to enable the development of other land use characteristics from time two into a later time period (Parsa *et al.,* 2016). The CA-Markov is able to develop a weighting spatial on the particular areas which have approximately the same to the existing land use based on classes, and it is not random (Subedi *et al*., 2013). Hence, the CA-Markov model is considered a strong approach because of the quantitative estimation and the spatial and temporal dynamic it has for modeling the LULC dynamic (Mishra and Rai, 2016; Parsa *et al.,* 2016; Subedi, 2013). GIS and remote sensing is easy to fir with the CA-Markov model to facilitate tasks and reduce the cost and time needed (Mishra and Rai, 2016; Parsa *et al.,* 2016). For LULCC prediction CA-Markov utilizes two historic LULC images and uses Markov Chain analysis outputs particularly transition areas matrix, transition suitability image collection matrix and a set of conditional probability images as input to predict the future LULC (Habtamu *et al.,* 2021). The former represents the probability that each land use/land cover category will change to every other category over the specified number of time units, while the latter represents the number of pixels that are expected to change from each land use/land cover type to each other land use/land cover type over the specified number of time units (Mishra and Rai, 2016). The conditional probability images report the probability that each land cover type would be found at each pixel after the specified number of time units (IDRISI Selva help system).

The CA model generally uses the following formula (Camara *et al.*, 2020; Subedi *et al.*, 2013).

$$S\,(t, t+1) = f(s\,(t)) \qquad (1)$$

Where $S\,(t+1)$ is the system status at the time of $(t, t+1)$, functioned by the state probability of any time (N). The Markov chain model is often used in LULC monitoring, ecological modelling, simulation changes, trends of the LULC, and to predict the extent of the land use change and the stability of future land development in the area of concern (Parsa *et al.*, 2016; Subedi *et al.*, 2013). The Markov chain model pronounces the LULC change from one time to another to predict future change (Kumar *et al.*, 2014). Equation (1) explains the calculation of the prediction of LULC changes (Markov chain model):

$$S\,(t, t+1) = Pij \times S\,(t) \qquad (2)$$

Where $S\,(t)$ is the system status at the time of t, $S\,(t+1)$ is the system status at the time of $t+1$; Pij is the transition probability matrix in a state which is calculated as follows (Kumar *et al.*, 2014; Sang *et al.*, 2011):

$$\| Pij \| = \begin{Vmatrix} P1, & p1,2 & p1,N \\ P1,2 & P2,2 & P2,N \\ \cdots & \cdots & \cdots \\ PN,1 & PN,2 & PN,N \end{Vmatrix} \qquad (3)$$

$$(0 \leq Pij \leq 1) \qquad (4)$$

Where P is the transition probability; Pij stands for the probability of transforming from present state i to another state j in succeeding time; PN is the state probability of any time. The high transition has probabilities near (1) and the low transition will have a probability near (0) (Kumar *et al.*, 2014). Markov Chain concludes precisely how much land would be estimated to change from the latest date to the predicted date. The transition probabilities

file is the result of this process, which is a matrix that registers the probability that each land use/land cover class will change to every other class (Mishra *et al.,* 2014).

2.6. Hydrological Model

Hydrologic models use mathematical and empirical expressions that define quantitative relationships between inputs such as temperature, precipitation and outputs (e.g. discharge) to define a hydrological cycle. They are vital for decision-makers who need to evaluate various management alternatives under different land use/land cover changes. They have been developed for many different reasons and have many different forms. However, hydrological models are in general designed to meet one of the two primary objectives. The one objective of the watershed hydrologic modeling is to get a better understanding of the hydrologic processes in a watershed and of how changes in the watershed may these phenomena. The other objective is for hydrologic prediction (Arnold *et al.,* 1993). They are also providing valuable information for studying the potential impacts of land use land cover changes or climate change in the area. Based on the process description, the hydrological models can be categorized into three main parts (Dhami & Pandey, 2013).

Lumped models: parameters in these hydrologic models typically do not vary spatially within the basin and thus, basin response is evaluated only at the outlet, without explicitly accounting for the response of individual sub-basins. This model is empirically based on integrating over some time and space scales. The high non-linear response of watersheds appears linear. Parameters of lumped models often do not represent physical features of hydrologic processes and usually involve a certain degree of empiricism. Though they are conceptually simple and easy to program and apply, they require substantial calibration data and they are not useful outside of the range of calibration. Examples include WATBAL, SRM, HYRROM, SWM4, IHACRES, and others.

Distributed models: Parameters of distributed models are fully allowed to vary in space at a resolution usually chosen by the user. These are broken down into small time and space increments. The physical processes occurring in the watershed may be explicitly simulated and then integrated to produce the watershed response. Examples in this category are MIKE-SHE, Wetspa, CASC2D, WATFLOOD, and others. They can be used to analyze changing conditions such as land-use changes, project alternatives, and climate change and they are extendible beyond the calibration range. However, they are data-intensive and code development is difficult. Distributed models generally require large amounts of (often unavailable) data for parameterization in each grid cell. However, the governing physical processes are modeled in detail, and if properly applied, they can provide the highest degree of accuracy.

Semi-distributed models: parameters of semi-distributed models are partially allowed to vary in space by dividing the basin into a number of smaller sub-basins. They are a mixture of empirical and physically-based approaches. They lie between lumped and distributed models. They have the advantage of increased spatial resolution and better process descriptions over simple lumped parameter models. They also maintain the computational advantage over fully distributed, physics-based models. Some of the examples of a Semi-distributed model include SWAT, HEC-HMS, HPV, TOPMODEL, and others.

3. MATERIALS AND METHODS

3.1. Description of the Study Area

3.1.1. Location

Welmel River is located in the South-Eastern part of Ethiopia in Genale Dawa Basin. The River originates from the northeastern of the Bale Mountains and drains to the Genale-Dawa River. Geographically, the Welmel watershed is located 6º 8’0’’N - 6º 50’0’’N and 39º 27’0’’E - 39º 55’0’’E latitude and longitude respectively with an elevation ranging from 1035 to 4290 m a.s.l. The watershed covers a total land area of 1,461.54km^2 in the Genale-Dawa River basin and is composed of Delo Mena, Arena Buluq, Adaba, Meda Welabu and Goba District. The river flow year-round southeast direction; the upper catchment area where the river originates is well covered with Moist Evergreen Mountain or Afro Mountain forest vegetation type (MoWR, 2007).

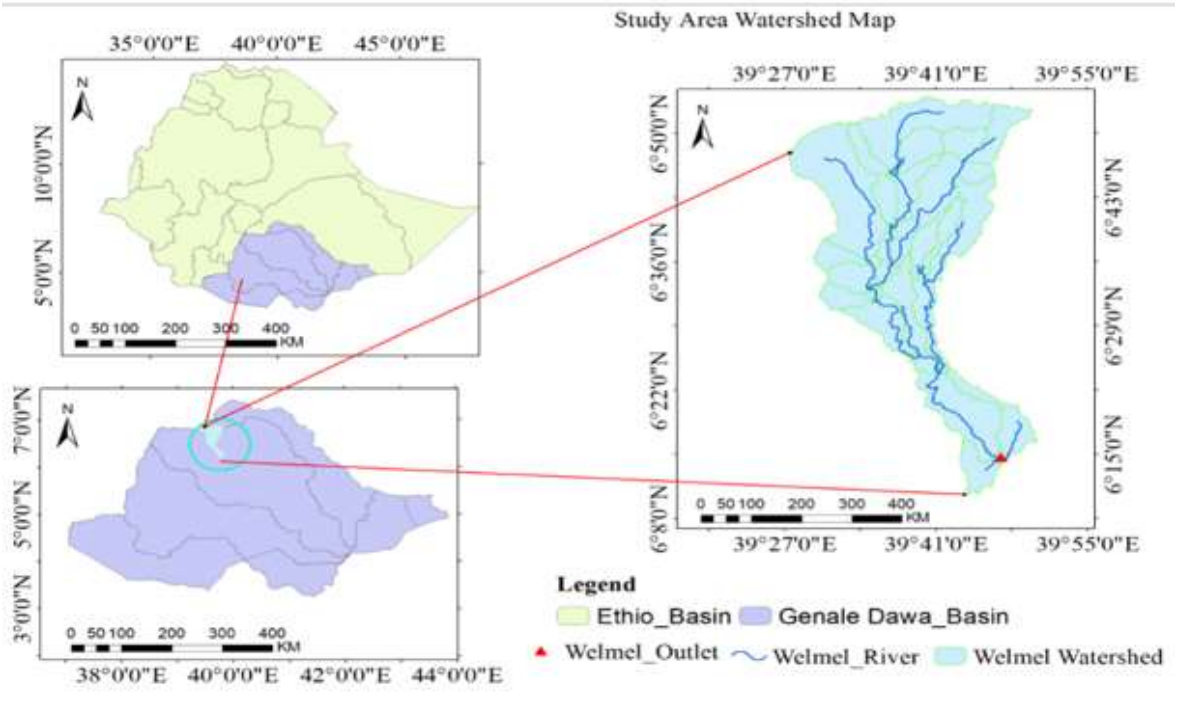

Figure 3-1: Map of the Study area

3.1.2. Topography

The landform of upstream of the catchment is complex comprising of sloppy terrain towards the river shore, a wider plateau at the top ascending away in both directions towards higher ridges. The upland of the woodland and the river shore natural forest vegetation of the study area are under severe pressure due to increasing farm expansion and the energy needs of the population. The land configuration of the watershed accounts for about 39.61% of the total area is found in the slope < 5%, 30.48% is found between 5 and 12% and 15.52% of the total area is found between 12 and 20%. The remaining area is found in the slope > 20% (Figure 3.2). The land surfaces rise from about 1035m above mean sea level (lowland area) to a high range of mountains and plateaus with elevation above 4290 m above mean sea level. The central and southern part of the watershed is relatively lowland; the general land elevation progressively decreases from north to south. The central part terrains are a gentle sloping which is more or less a lowland plain.

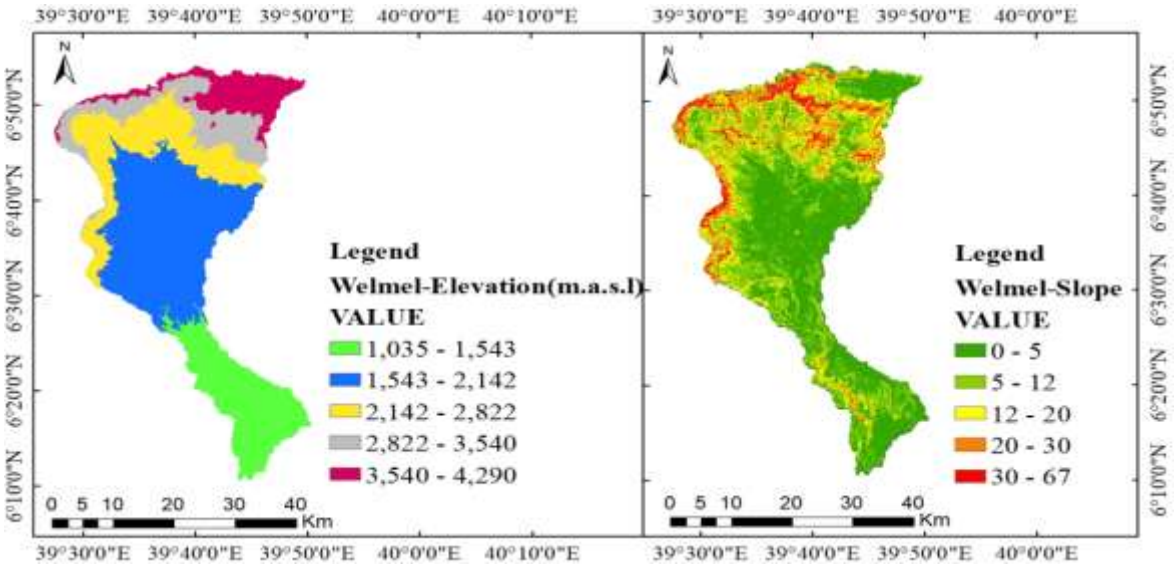

Figure 3-2: Topography map of Welmel Watershed with elevation and slope

3.1.3. Climate

The study area is characterized by two (Bimodal) rainy seasons March to May and August to November. The rainfall distribution shows that the peak rainy month for the first and second seasons are May and October respectively. The study area receives annual average minimum and maximum rainfall of 836.38mm at Rira and 940.3mm at Delomena station. With regard to temperature, the annual average maximum temperature ranges from 29.35℃ to 20.59℃ and minimum temperature ranges from 15.87℃ to 9.65℃ at Delomena and Rira station, respectively.

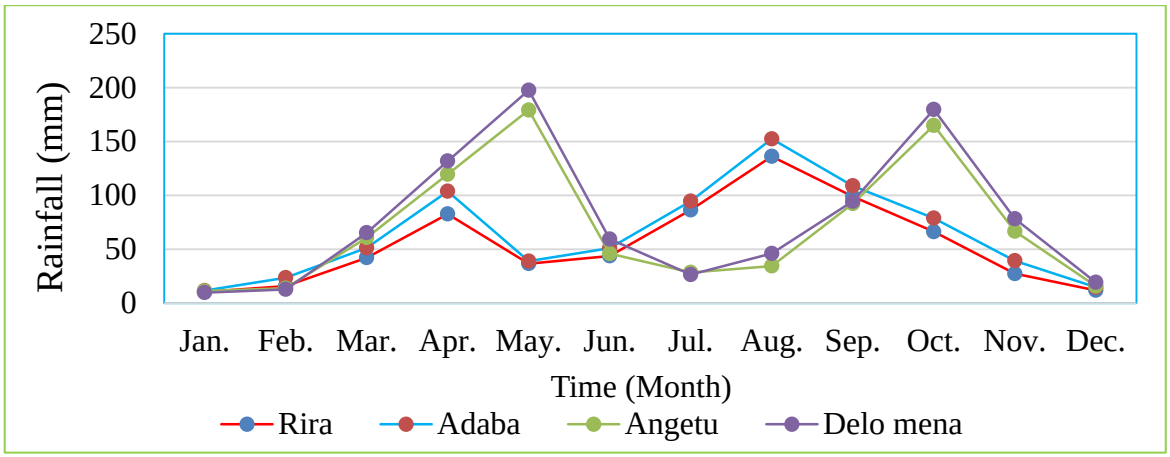

Figure 3-3: Monthly average rainfall of individual stations

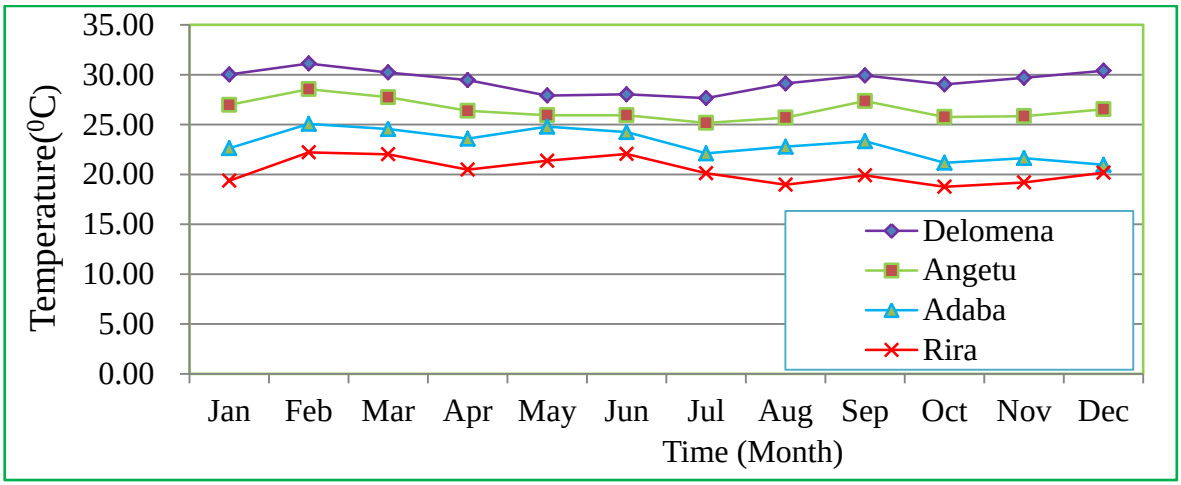

Figure 3-4: Monthly average maximum temperature of individual stations

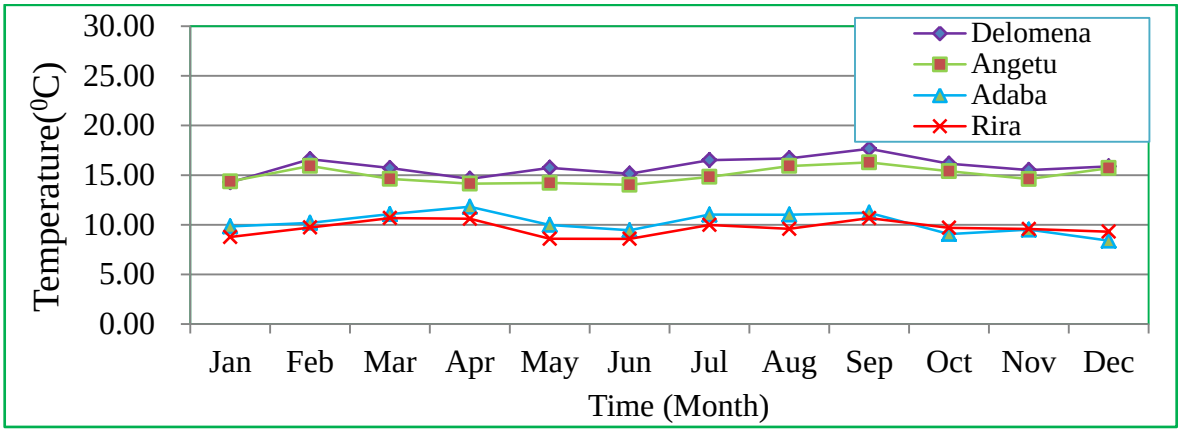

Figure 3-5: Monthly average minimum temperature of individual stations

3.1.4. Soil

According to Atlas of Bale zone, July 2004 in the study area, there are about six major soil types, which are Chromic Cambisol, Chromic Luvisol, Dystric Cambisol, Eutric Cambisol, Regosol and Rhodic Nitisol. Chromic Cambisol cover 578.03Km^2 (40.16%), Chromic Luvisol cover 180.68Km^2 (12.36%), Dystric Cambisol cover 17.99km^2 (1.24%), Eutric Cambisol cover 46.34km^2 (3.17%), Regosol covers 69.73km^2 (4.77%) and Rhodic Nitisol covers 559.77km^2 (38.30%) of the total area. The distribution of the Rhodic Nitisol is observed mostly in the plain that ranges in the slope of less than 5%. Dystric Cambisol has a little share followed by Eutric Cambisol when it is compared with the other types of soils of the study area. This result was almost consistent with the soil types identified by Abdulkerim and Sarma, (2016), in Weyib River Basin, Bale Mountainous southeastern Ethiopia.

3.1.5. Land-Use/Land Cover

The Land Use/Land Cover of the study area includes forest land; rangeland, Scrubland/bushland, woodland, agricultural land and scattered rural settlement. This includes the vegetation of the common natural vegetation of the LULC category that is found in the area is Coniferous forest, Dominated by Juniperus procure (Gatira) and

Podocarpous gracilior (Birbirsa), Juniperus forest associated with Hagen Abyssinia and Olean trees. The middle catchment area is well covered with forest vegetation type. At lower altitudes, the dominant vegetation is woodland type. The lower area is dominantly characterized by agriculture (agriculture/settlement). The types of crops grown in the area include; maize, teff, sorghum and sesame among annual crops and coffee and fruits among perennial crops (Teketay, 2001; IBC, 2005; MoWR; 2007; Mulugeta and Tadesse, 2010).

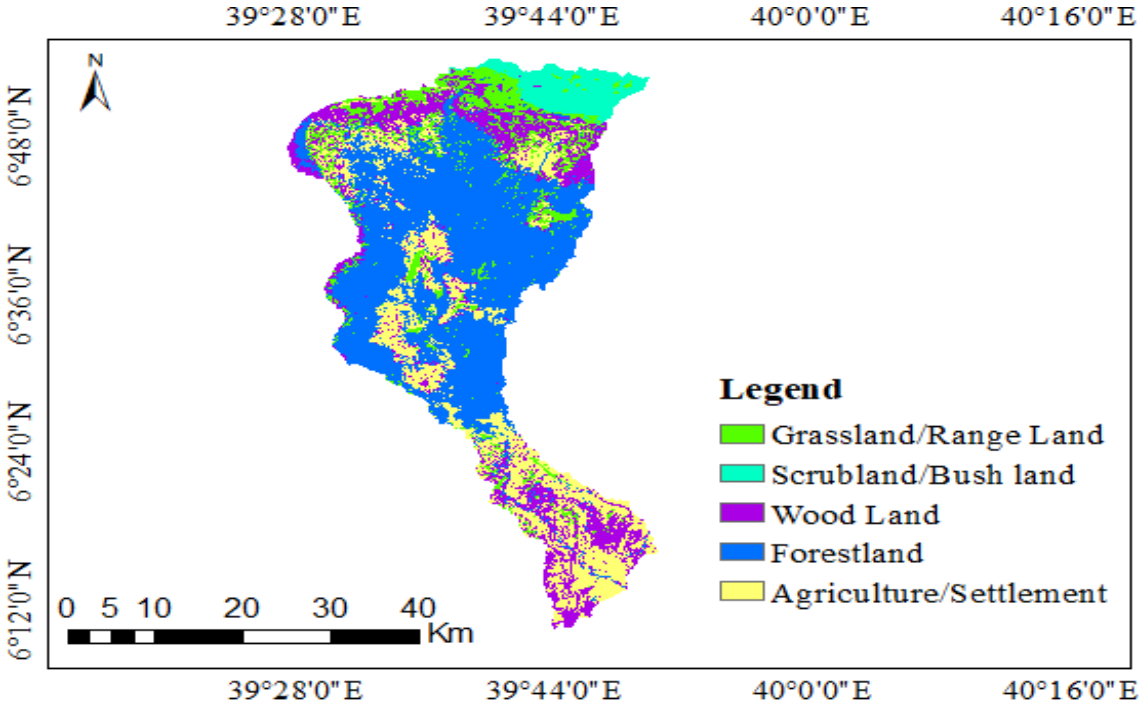

Figure 3-6: Current (2020) LULC map of Welmel Watershed

Agricultural land is covers from the middle to downstream parts of the river watershed. It is the land cover under the crop cultivation of annual crops. The downstream and southeastern part of the watershed area is largely characterized by cultivation land use and woodland. The middle part of the catchments is dominantly characterized by forest following by cultivation land. Crops like sorghum, maize, sesame and teff are grown by two rain-fed seasons March to June and September to December. Cultivation intensity increases gradually from the center and goes to the south, southeastern, northeastern and northwestern parts of the command area.

3.2. Data Collection and Analysis

3.2.1. Detection of Historical LULC Changes

3.2.1.1. Land-use/land covers map

The Landsat satellite imageries of the study area of the years 1990, 2005 and 2020 were downloaded from free USGS Glovis website (http://earthexplorer.usgs.gov) and used for land use/land cover change detection of the area. The first reason why these years' images selected was, there were events of resettlement program by the Derge government in 1985/1986 and implementation of participatory forest management by Farm Africa and SOS Sahel starting from 2005/2006 (Adane and Getachew, 2017). The second reason was the availability of discharge data starting from 1990 at Melka Amana gauged station. The 1990, 2005 and 2020 (Table 3.1 and Figure 4.1) dataset was generated from Landsat5, landsat7 and landsat8 respectively which comprised of the Landsat Thematic Mapper (TM), Enhanced Thematic Mapper Plus (ETM+) and Operational Land Imager/Thermal Infrared Sensor (OLI/TIRS). All images used in this study had 30m spatial resolution and below 10% cloud cover. To reduce the effect of cloud cover and seasonal variation on the classification result, Landsat satellite images of the same season (January to February) was used because three months from December to February are dry season in the study area and have relatively cloud-free sky.

Table 3-1: shows details of Landsat satellite imagery data

year	Spacecraft	Sensor ID	Path/Row	Acquisitions Date (mm-dd-yy)	Cloud cover (%)
	Landsat 5	TM	167/55	01/25/1990	<10
1990	Landsat 5	TM	167/56	01/25/1990	<10
	Landsat 5	TM	168/55	02/17/1990	<10
	Landsat 7	ETM+	167/55	01/10/2005	<10
2005	Landsat 7	ETM+	167/56	01/10/2005	<10
	Landsat 7	ETM+	168/55	01/01/2005	<10
	Landsat 8	OLI/TIRS	167/55	01/09/2020	<10
2020	Landsat 8	OLI/TIRS	167/56	01/25/2020	<10
	Landsat 8	OLI/TIRS	168/55	01/16/2020	<10

Landsat satellite images of 1990, 2005 and 2020 were used to analyze present and future LULC changes of the Welmel River Watershed. The watershed area comprises 167/055, 167/056 and 168/055 scenes.

3.2.1.1.1. Image pre-processing and classification

Satellite image pre-processing of image extraction, layer stacking, mosaicking and image sub-setting were performed before image classification to create multi-band composite images since the study area lies on three scenes. The LULC of the study area were forest, woodland, scrubland/bushland, grassland/rangeland and agriculture/settlement. Rivers, streams and springs were not included in the classification. This is due to the resolution problem of the image (30m), the very low likelihood of identifying springs and rivers from riverine vegetation (Adane and Getachew, 2017).

Table 3-2: Description of LULC types in Welmel River Watershed

Class name	Description
Forestland	Areas that are covered with dense growth of trees with closed canopies. It was made to include human-made plantation forest, riverine forests, dry ever green forest and moist mountain forest.
Woodland	The land covered with both open and closed (high) woodland with dominant species of Acacia-Commiphora vegetation (Eyayu *et al.*, 2010).
Scrubland/bushland	The land area covered by Asta scrubland, Erica bushes, alpine vegetation (vegetation with small white leaves found at top of Sanette Platue and habitats of Ethiopian Wolf. It includes Lobelia rhynchopetalum and Helichrysum species) and ground covered by Artemesia afra, Alchemilla johnstoni and Knifofia (Adane and Getachew, 2017).
Grassland/rangeland	Both communal and\or private grazing lands that are used for livestock grazing. The land is basically covered by small grasses, grass-like plants and herbaceous species. It also includes land covered with a mixture of small grasses, grass-like plants and shrubs less than 2m and it is used for grazing.
Agriculture/settlement	Includes areas allotted to rain-fed cereal crops (e.g. Corn, Barley, Teff, and Wheat), cash crops (chat) and horticultural crops particularly vegetables (e.g. onion, potato and cabbage). Crop cultivation is both annuals and perennials, mostly in subsistence farming and the land covered by rural villages and scattered rural settlements (Adane and Getachew, 2017).

It was difficult to identify settlements especially rural settlements from agricultural land on a 30m spatial resolution image and in most cases, the two are spatially integrated. Therefore settlements were grouped under agricultural land covers. This classification is in

agreement with (Adane and Getachew, 2017; Temesgen *et al.,* 2014) who grouped agriculture and settlement under one class for the same reason listed above. In this study for LULC change detection, Landsat images were first pre-processed to enhance the quality and visibility of features (Henok *et al.,* 2021). The unsupervised classification was first carried out to have an idea of representing the overall LULC clusters of pixels. Then supervised classification was employed to categorize the images using ground truths (training areas) which was defined based on the results of unsupervised classification (the cluster of pixels) and ancillary data (Google Earth) (Saah *et al*., 2019).

Table 3-3: Land Use/Land Cover of the study area

Land use/land cover	**Land use according to SWAT database**	**SWAT code**
Agricultural land/Settlement	Agricultural Land-Generic	AGRL
Forest	Forest mixed	FRST
Scrubland/Bushland	Range Brush	RNGB
Grassland/Rangeland	Range-grass	RNGE
Woodland	Forest Deciduous	FRSD

In this study for classification purposes, ERDAS Imagine 2014 and ArcGIS 10.4.1 were used for pre-classification of geometric and atmospheric correction, image classification, and mapping.

3.2.1.1.2. Accuracy assessment

Accuracy assessment is an important step in the image classification process to achieve the first specific objective of this study. The accuracy assessment of the classified map is the comparison of the classified image and the sampling points from the Google Earth Imageries and existing land cover maps (Yesserie, 2009). The most widely used classification accuracy is in the form of error matrix which can be used to derive a series of

descriptive and analytical statistics (Manandhar, 2009). The columns of the matrix depict the number of pixels per class for the reference data, and the rows show the number of pixels per class for the classified image. From this error matrix, overall accuracy, user's and producer's accuracy were determined. The overall accuracy is used to indicate the accuracy of the whole classification (i.e., number of correctly classified pixels divided by the total number of pixels in the error matrix), whereas the other two measures indicate the accuracy of individual classes. A user's accuracy is regarded as the probability that a pixel classified on the map actually represents that class on the ground or reference data, whereas product's accuracy represents the probability that a pixel on reference data has been correctly classified.

The accuracy assessment for the years 1990 and 2005 of this study was performed using a Google Earth by integrating with ERDAS Imagine 2014. In the case of 2020 classified image of accuracy assessment was performed by collecting a total of 115 Ground Control Points using GPS. After the LULC maps were classified, change detection analysis was conducted to examine the extent of LULC changes that occurred during the study period and make useful decisions. Mulatu *et al.* (2019) stated that percent changes of individual LULC classes were computed as follows to determine the extent of change between periods:

$$\text{Percent change (\%)} = \left(\frac{A2 - A1}{A1}\right) \text{X } 100 \qquad (5)$$

Where A1 is the area in year 1 and A_2 is the area in year 2 of a LULC Class (km^2). While the rate of change of the classified LULC maps (Mulatu *et al*., 2019; Temesgen *et al*., 2017) estimated as follows:

$$\text{Change rate} = \frac{A-B}{Z} \qquad (6)$$

Where Change Rate is the rate of change (km^2/year); A is the area of LULC (km^2) at time t −2; B is the area of LULC (km^2) at time t −1; and Z is the time interval between A and B (years).

3.2.2. Prediction of Future LULC Changes

This study employed cellular automata (CA-Markov) model with a combination of the Markov chain model to simulate future LULC changes of 2035 and 2050 for the Welmel Watershed. CA-Markov model requires three types of data inputs to predict LULC change prediction (Hyandye & Martz, 2017). These are the basis temporal LULC image, Markov transition areas file and transition suitability images collection generated using the Markov chain model. Basis temporal LULC was prepared following the satellite image classification. The Markov transition area files were generated by running a Markov module before executing a CA-Markov module during the implementation of the Markovian LULC change modeling.

The LULC maps of 1990 and 2005 were used as inputs for the preparation of Markov chain outputs of transition areas matrix, transition suitability image collection matrix, a set of conditional probability images and for the model validation. The transitional probability matrix contains the probability of changing of each LULC category to every other category and the transitional area matrix contains the number of pixels that are expected to be converted from one LULC category to other categories over a specific period of time. On the other hand, the output conditional probability images represent the probability of each LULC class to be found in each pixel over time. The 1990 and 2005 historical LULC maps were used to produce a simulated LULC map of 2020 for the validation of the model by

comparing it with the actual LULC map of 2020 through the KIA (Kappa Index of Agreement) approach (Hua, 2017). In this case, the LULC map of 2005 was used as the base map for the prediction of the 2020 LULC map.

Hence, the validation result indicates a high level of agreement between observed and projected LULC maps of 2020. Based on this, the result of various Kappa indices of agreement (KIA or K standard) and the respective statistics were computed. The result is usually between 0 and 1. The level of agreement for Kappa indices is as follows: Kappa ≤ 0.5 indicates rare agreement; 0.5 ≤ Kappa ≤ 0.75 indicates a medium level of agreement; 0.75 ≤ Kappa < 1 indicates a high level of agreement; and Kappa = 1 denotes perfect agreement (Singh *et al.,* 2018; Keshtkar and Voigt, 2016). Kappa for no information (K_{no}) indicates the proportion classified correctly relative to the expected proportion classified correctly by simulation, with no ability to specify the quantity of location accurately and Kappa for location ($K_{location}$) measures the validation between the classified maps and the simulated map based on a specified location, while Kappa for standard ($K_{standard}$) indicates the proportion assigned correctly versus the proportion that is correct by chance (Araya, and Cabral, 2010).

The following equations express the statistics for the kappa variations according to Omar *et al.* (2014):

$$\text{Kno} = \frac{(\text{M(m)N(n)})}{\text{P(p)}-\text{N(n)}} \tag{7}$$

$$\text{Klocation} = \frac{(\text{M(m)N(m)})}{\text{P(m)}-\text{N(m)}} \tag{8}$$

$$\text{Kstandard} = \frac{(\text{M(m)N(n)})}{\text{P(p)}-\text{N(m)}} \tag{9}$$

Where no information is defined by N (n), medium grid cell level information by M (m), and perfect grid cell-level information across the landscape by P (p).

The Kappa statistics of Kstandard = 0.81, Kno = 0.86, and Klocation = 0.86 were obtained in the validation process which indicates a high level of agreement between projected and actual LULC map of 2020, which indicates the model prediction was reliable. After successful validation of the model, the techniques were repeated using the transition probabilities of 2005 and 2020 maps to predict LULC maps of 2035 and 2050, using the LULC map of 2005 as a base map. The predicted LULC change was evaluated using LULC map of 2020, 2035 and 2050 with the baseline LULC map of 2020.

3.2.3. Evaluation of Hydrological Responses

Various criteria can be used for choosing the right hydrological model for a specific problem. These criteria are always project-dependent since every project has its own specific requirements and needs. Further, some criteria are also user-depended (and therefore subjective). Among the various project-dependent selection criteria, there are four common, fundamental ones that must be always answered (Cunderlik, 2003): -

- ✓ the model prediction capacity
- ✓ Availability of input data required by the model to provide within the time and cost constraints of the project.
- ✓ Availability of the model and its Price

Based on this, SWAT Model was used for this research to simulate the responses of hydrological components to LULC changes.

3.2.3.1. Description of SWAT Model

The Soil and Water Assessment Tool (SWAT) is a semi-distributed hydrological model that was developed by the Agricultural Research Service of the United States Department of Agriculture (USDA-ARS). It is a physically-based model designed to predict the impact of land management practices on water, sediment and agricultural chemical yields in large complex watersheds with varying conditions over long periods of time (Neitsch *et al*., 2012). A physically-based SWAT hydrological model was used to delineate the watershed into a number of sub-basins. Each sub-basin is divided into hydrologic response units (HRUs) (Kumar *et al.,* 2017). HRUs are portion of areas within the sub-basin that are comprised of unique land cover, soil and slope combinations (Kushwaha and Jain, 2013; Arnold *et al*., 2012; Arnold *et al.*, 2011). The model predicts the impacts at the sub-basin (sub-watershed) or further at the Hydrologic Response Units (HRUs) (Ghoraba, 2015). It simulates river basin hydrological processes such as surface runoff and sediment yield at a daily time-step, based on information regarding weather, topography, soil properties, vegetation, and land management practices (Ghaffari *et al.,* 2010).

The criterion used to select the model is based on the benefits it provides to meet the objectives of the study area. The SWAT model is embodied in ArcGIS that can integrate various readily available geospatial data to accurately represent the characteristics of the watershed. One of the main advantages of SWAT is that it can be used to model watersheds with less monitoring data. For simulation, SWAT needs digital elevation model; land use and land cover map, soil data and climate data of the study area. The model is based on the principle of water balance algorithm as defined: -

$$SWt = SWo + \sum_{i=1}^{t}(Rday - Qsurf - Ea - Wseep - Qgw) \quad (10)$$

Where SWt is the final soil water content (mm), SW_o is the initial water content (mm), t is the time (days), R_{day} is the amount of precipitation on day i (mm), Q_{surf} is the amount of surface runoff on day i (mm), E_a is the amount of evapotranspiration on day i (mm), W_{seep} is the amount of water entering the vadose zone from the soil profile on day i (mm) and Q_{gw} is the amount of return flow on day i (mm).

The model has eight major components: hydrology, weather, sedimentation, soil temperature, crop growth, nutrients, pesticides and agricultural management (Neitsch *et al.,* 2005). Major hydrologic processes that can be simulated by this model include evapotranspiration, surface runoff, infiltration, percolation, shallow aquifer and deep aquifer flow, and channel routing (Arnold *et al.,* 1998). Stream flow is determined by its components (surface runoff and groundwater flow from shallow aquifer). Based on this, for this study, we have put a brief description of the SWAT components of computation procedures that are related to the topics of this study.

Surface Runoff: Surface runoff refers to the portion of rainwater that is not lost to interception, infiltration, and evapotranspiration (Harssema, 2005). Surface runoff occurs whenever the rate of precipitation exceeds the rate of infiltration. SWAT offers two methods for estimating the surface runoff: the Soil Conservation Service (SCS) curve number method (USDA-SCS) or the Green & Ampt infiltration method (Green and Ampt) (Bauwe *et al.,* 2016). The Green and Ampt method needs sub-daily time step rainfall which made it difficult to be used for this study due to the unavailability of sub-daily rainfall data. Therefore, the SCS curve number method was adopted for this study. The general equation for the SCS curve number method is expressed by the equation:

$$Q_{surf} = \frac{(Rday - Ia)2}{(Rday - Ia + S)}, \qquad \text{true if Rday} \geq \text{Ia} \qquad (11)$$

Where, Qsurf is the accumulated runoff or rainfall excess (mm), R_{day} is the rainfall depth for the day (mm water), Ia is an initial abstraction that includes surface storage, interception and infiltration before runoff (mm water) and S is retention parameter (mm water). The retention parameter varies spatially due to changes with land surface features such as soils, land use, slope and management practices. This parameter can also be affected temporally due to changes in soil water content. It is mathematically expressed as:

$$S = 25.4 \text{ x } [(\frac{100}{CN}) - 10] \quad (12)$$

Where, *CN* is the curve number for the day and its value is the function of land use practice, soil permeability and soil hydrologic group. The initial abstraction, *Ia* is commonly approximated as 0.2*S* and equation 7 becomes:

$$Q_{surf} = [(R_{day} - 0.2S)]^2 / (R_{day} + 0.8S) \quad (13)$$

For the definition of hydrological groups, the model uses the U.S. Natural Resource Conservation Service (NRCS) classification. The classification defines a hydrological group as a group of soils having similar runoff potential under similar storm and land cover conditions. Thus, soils are classified into four hydrologic groups (A, B, C, and D) based on infiltration which represents high, moderate, slow, and very slow infiltration rates, respectively.

Ground Water Flow: To simulate the groundwater, SWAT partitions groundwater into two aquifer systems: a shallow, unconfined aquifer which contributes return flow to streams within the watershed and a deep, confined aquifer which contributes return flow to streams outside the watershed (Arnold *et al.,* 1993). In SWAT the water balance for a shallow aquifer is calculated with equation:-

$$aq_{sh,\,i} = aq_{sh,i-1} + W_{rchrg} - Q_{gw} - W_{revap} - W_{deep} - W_{pump,\,sh} \quad (14)$$

Where, $aq_{sh,i}$ is the amount of water stored in the shallow aquifer on day i (mm), $aq_{sh,i-1}$ is the amount of water stored in the shallow aquifer on day i-1 (mm), W_{rchrg} is the amount of recharge entering the aquifer on day i (mm), Q_{gw} is the groundwater flow, or base flow, or return flow, into the main channel on day (mm), W_{revap} is the amount of water moving in to the soil zone in response to water deficiencies on day i (mm), W_{deep} is the amount of water percolating from the shallow aquifer into the deep aquifer on day i(mm), and W_{pump}, *sh* is the amount of water removed from the shallow aquifer by pumping on day i (mm).

Water yield: - is one of the vital parameters calculated for sustainable water resources management of the watershed. Water yield in a catchment is calculated by the equation (15) (Arnold *et al.*, 2012).

$$Qyld = Qsrf + Qlat + Qgw – Tloss \quad (15)$$

Where Qyld is the amount of water yield (mm); Qsrf is the surface runoff (mm); Qlat is the amount of water contributed by lateral flow (mm); Qgw is the ground water flow contribution (mm); Tloss is the loss of water through transmission process (mm).

3.2.4. Input Data for SWAT Model

3.2.4.1. Digital Elevation Model

The input data for SWAT were LULC map described under specific objective one, DEM, soil map and Hydro-meteorological data. Digital Elevation Model (DEM) is one of GIS input data in SWAT that can be used by Arc SWAT for automatic delineation of the catchment, to calculate the flow accumulation and determine the sub-basin parameters such as elevation and slope and defines the location of the streams network in a basin using SWAT watershed delineator tools. The DEM used for this research work has a resolution of 30m by 30m. It was obtained from the Ministry of Water, Irrigation and Energy of

Ethiopia. The DEM of Welmel watershed was clipped from Ethio-DEM using the area of interest and converted to grid by using the ArcGIS10.4 software to be used in Arc SWAT as input.

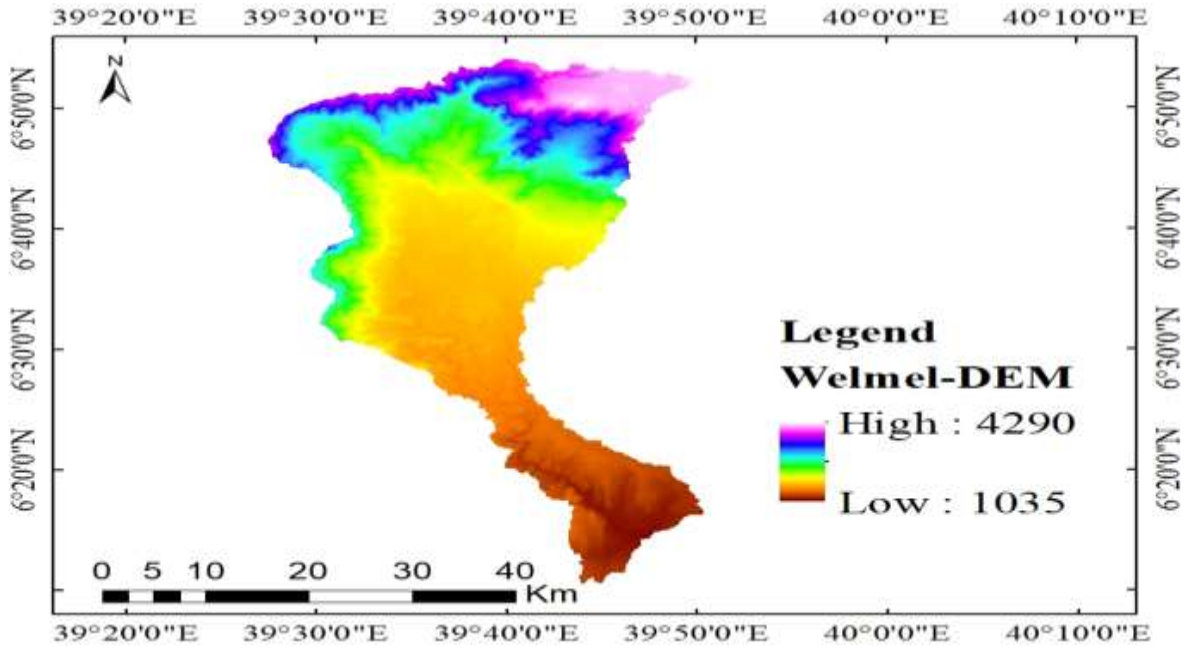

Figure 3-7: Digital Elevation Model of the Welmel Watershed

3.2.4.2. Soil Map

The soil map of the study area was obtained from the Ministry of Water, Irrigation and Energy of Ethiopia.

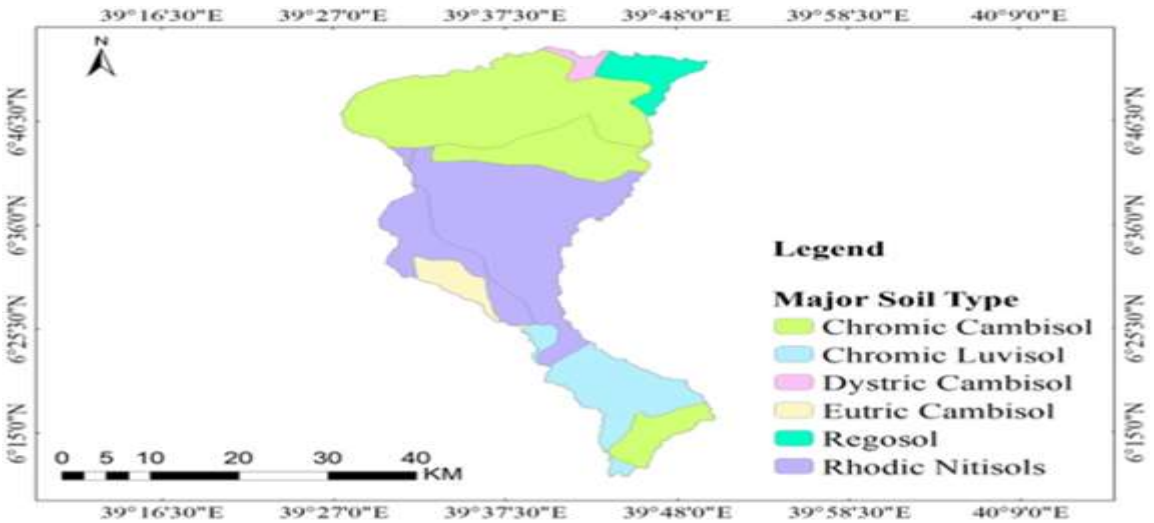

Figure 3-8: Major soil Types of Welmel Watershed

The soil map used for this research work has a resolution of 30m by 30m. Major soil properties for the Welmel River watershed for the SWAT model were obtained from the Genale-Dawa river basin integrated resources development master plan of the Ministry of Water, Irrigation and Energy of Ethiopia of 2007. To integrate the soil map with the SWAT model, a user soil database that contains the properties of soils was prepared for each soil layer and added to the SWAT user soil databases using the data management tool in ArcGIS. Physical properties of soil Name, soil hydraulic group (A, B, C, or D), maximum rooting depth of soil profile, fraction of porosity, depth from the soil surface to bottom of layer, moist bulk density. Also, available water capacity of the soil layer, saturated hydraulic conductivity, organic carbon content, clay content, silt content, sand content, rock fragment content, moist soil albedo, soil erodibility (K) factor for the study area of soils were organized and used for input data for SWAT model.

Table 3-4: Major soil Types of Welmel Watershed

Type of soil	Symbol	Area in Km^2	Coverage in %
Chromic Cambisol	CHROMICCAM	587.03	40.16
Chromic Luvisol	CHROMICLUV	180.68	12.36
Dystric Cambisol	DYSTRICCAM	17.99	1.24
Eutric Cambisol	EUTRICCAM	46.34	3.17
Regosol	REGO	69.73	4.77
Rhodic Nitisol	RHODICNITI	559.77	38.30

3.2.4.3. Discharge Data

Discharge data is required for performing sensitivity analysis, calibration and validation of the SWAT model for the proposed periods of 31 years of this study. The daily stream flow data of Welmel River at Melka Amana gauged station was collected from the Ministry of Water, Irrigation and Energy of Ethiopia for the year 1990 to 2014. Then the daily stream

flow was changed into monthly and arranged as per the requirement of the SWAT model for both calibration and validation.

3.2.4.4. Weather Data

SWAT model requires daily meteorological data, which include daily precipitation, maximum and minimum temperatures, solar radiation, wind speed and relative humidity. The model allows these daily data either the measured values directly or generated values from the weather generator during the simulation. The meteorological data required for this study from four (4) recording stations in and around the watershed were collected from the National Meteorological Agency of Ethiopia and Bale Robe Branch. The data series were from January 01/1990 to December 31/2020. These four (4) Meteorological Stations were selected by creating the Thiessen Polygon method using ArcGIS.

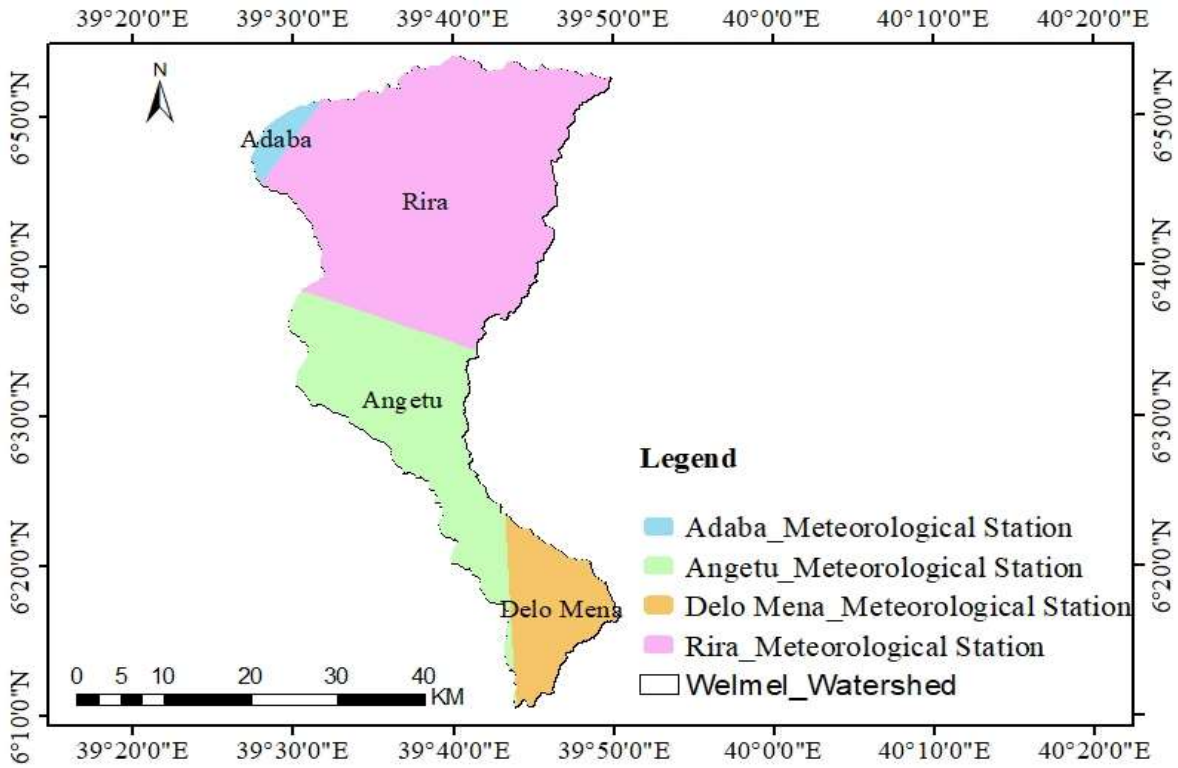

Figure 3-9: Thiessen Polygon for Meteorological stations

Table 3-5: Influencing factors of stations

Station Name	Area of influence(Km^2)	Influencing factor
Delo mena	165.89	0.11
Adaba	28.26	0.02
Angetu	394.8	0.27
Rira	872.59	0.6
Total	1461.54	1.00

The meteorological data that was collected were precipitation, maximum and minimum temperature, relative humidity, sunshine hours and wind speed of the study area. However, weather data like wind speed; sunshine hours and relative humidity were not obtained for all selected stations except Delo Mena meteorological station, due to this limitation, using the weather generator simulation method was used.

Table 3-6: Summary of Meteorological Data and Stations

Station Name	Lat(deg)	Lon(deg)	Alt(m)	Periods of Weather Data(1990-2020)				
				RF	T°	RH	WS	SR
Delo Mena	6.42	39.83	1295	yes	yes	yes	yes	Yes
Adaba	7.0	39.38	2420	yes	yes	No	No	No
Angetu	6.4	39.58	1450	yes	yes	No	No	No
Rira	6.77	39.72	2900	yes	yes	No	No	No

Key: RF: Rainfall, T°: Temperature, RH: Relative Humidity, WS: Wind speed and SR: Solar radiation

3.2.5. Filling Missing Hydro-Meteorological Data

Hydro-meteorological data can be missed due to measurement errors caused by natural or human-induced factors. Missed data less than 5%, can be filled by any method and the normal annual rainfalls at surrounding gauges are within 10% of the normal annual precipitation at the stations concerned, then the arithmetic procedure could be adopted to estimate the missing data (Adilah and Hannani, 2021). The Normal Ratio Method could be adopted for any surrounding gauge that exceeds 10% of the gauge that is under

consideration (Caldera *et al.,* 2016). For this study, arithmetic and Normal Ratio Method for one station which has less than 10% and exceeds 10% missing data were adopted to fill the missing data of rainfall and temperature from nearest stations for other stations respectively. The percentage of difference of the missing data was computed using the formula (Anmut *et al.,* 2019):

$$\text{Percent Difference} = \left(\frac{\text{Nx}-\text{Ni}}{\text{Nx}}\right) \text{x}100 \quad (16)$$

Where, Px = Estimate for the target station(x), Pi = Rainfall values of rain gauges used for estimation, m= Number of surrounding stations, Nx = Normal annual precipitation of the X station, Ni = Normal annual precipitation of the surrounding stations and di = Distance from each location to the point being estimated.

Arithmetic Mean Method:

If the normal annual rainfalls at surrounding gauges are within 10% of the normal annual precipitation at the stations concerned, then the arithmetic procedure could be adopted to estimate the missing data (Adilah and Hannani, 2021). This assumes equal weights from all nearby rain gauge stations and uses the arithmetic mean of the precipitation data.

$$P_X = \frac{1}{m}\sum_{i=1}^{m} pi \quad (17)$$

Normal Ratio (NR) Method:

This method is used if the normal annual precipitation of any surrounding gauges exceeds 10% of the gauge that is under consideration. This weighs the effect of each surrounding station.

$$px = \frac{1}{m}\sum_{i=1}^{m}\left(\frac{Nx}{Ni}\right) \text{Pi} \quad (18)$$

3.2.6. Homogeneity and Consistency Test

The homogeneity of the data was assessed using XLSTAT2016 software. XLSTAT was obtained from the https://www.xlstat.com website. The Statistician Excel add-in performs a range of statistical analyses within the Microsoft Excel environment. Double mass curve is a simple, visual and practical method and it is widely used in the study of the consistency and long-term trend test of hydro-meteorological data. The method was first employed to analyze the consistency of precipitation records to correct the measurements, which were sometimes subject to considerable inconsistencies driven by non-representative forces (e.g., relocation of rain gauges or changes in exposure of them (Gao *et al.*, 2017). Therefore, the homogeneity and Consistency of rainfall and flow data for this study were tested by using XLSTAT2016 software and the Double mass curve (DMC) method respectively.

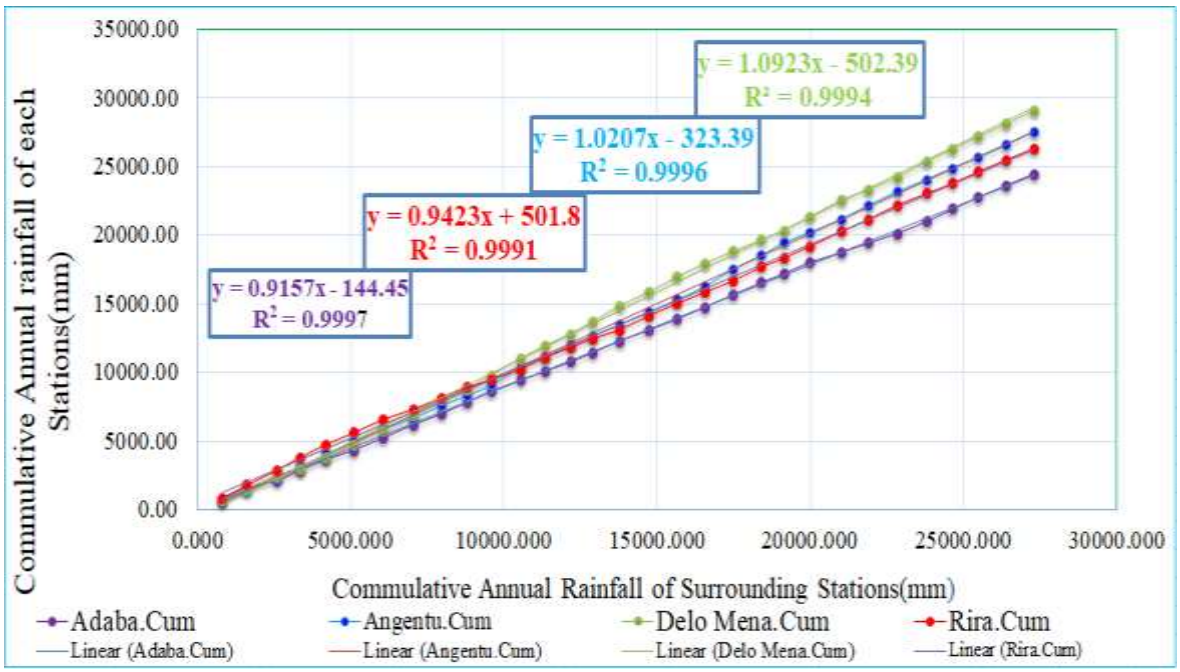

Figure 3-10: Consistency test of selected precipitation stations

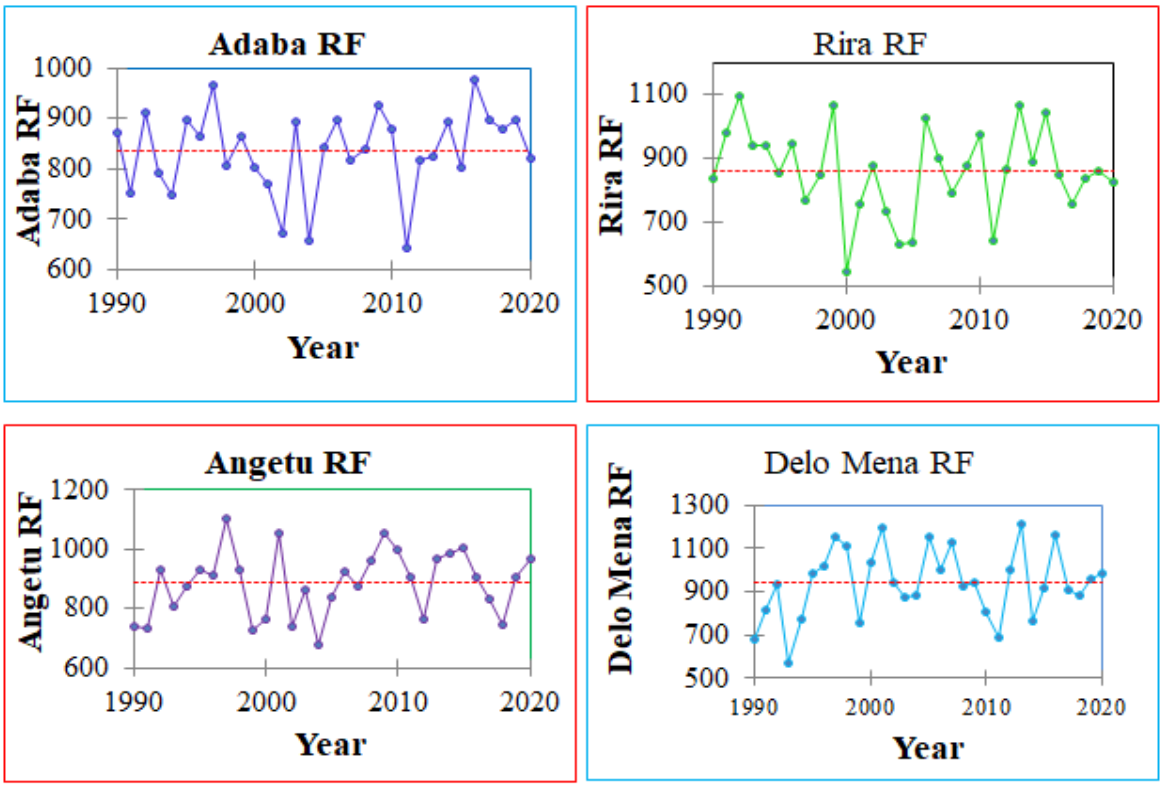

Figure 3-11: Homogeneity test (using Pettit's) of annual rainfall

3.3. SWAT Model Setup

3.3.1. Watershed Delineation

In this study, watershed delineation was carried out using the extension of ArcSWATv2012.10.4.21 and ArcGISv10.4.1. The watershed and sub-watershed delineation was performed using 30m x 30m resolution DEM. The watershed was delineated by setting and creating the SWAT project first. The watershed delineation process consists of five major steps, DEM setup, stream definition, outlet and inlet definition, watershed outlets selection and definition, and calculation of sub-basin parameters. The outlet of the watershed was manually added to fix it at the river gauging station. For the stream definition, the threshold-based stream definition option was used to define the minimum size of the sub-basin. The HRU threshold is employed to further discretize each sub-watershed considering the landscape heterogeneity found from its land

use, soil, and slope. Thresholds from 5% to 15% are commonly used in watershed modeling (Han *et al.,* 2012; Sexton *et al.,* 2010). Based on this, with the threshold area of 7,300ha, 29 sub-basins were generated in Welmel Watershed and area of 1461.54 Km^2.

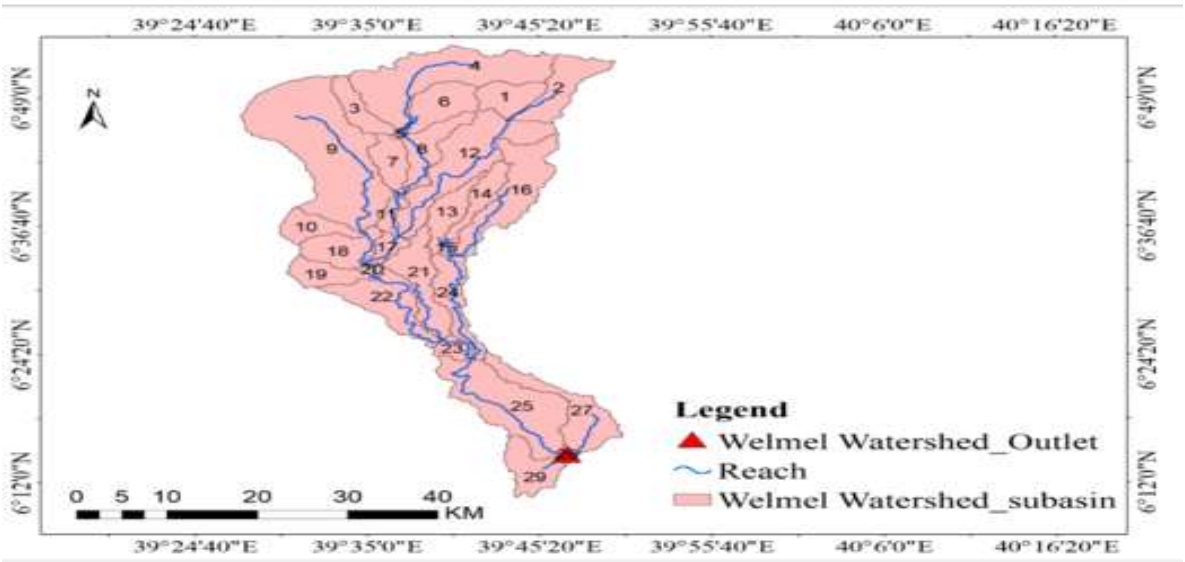

Figure 3-12: Welmel Watershed and sub-basin

3.3.2. HRU Definition

Hydrologic Response Units are land areas within the sub-basin that are covered with unique land use, soil and slope. The HRUs can be defined either by assigning only one HRU for each sub-basin considering the dominant soil/land use/slope combinations or by assigning multiple HRUs for each sub-basin considering the sensitivity of the hydrologic process based on a certain threshold value of soil/land use/slope combinations. During the creation of HRU, the slope was classified to a reasonable range. Based on the slope of the area, the slope was classified into five classes. The classes were 0 to 5%, 5 to 12%, 12-20%, 20-30% and 30 to 67%. The slope gradient was calculated from Aster DEM in the ArcGIS environment. It was reclassified into four slope categories, i.e., gentle slopes (0%-5%), moderate slopes (5%-15%), steep slopes (15%-30%), and very steep slopes (>30%) (FAO, 1990).

For this study, multiple methods were adopted as it describes better the heterogeneity within the watershed and as it accurately simulates the hydrologic processes. To model multiple HRUs, a threshold level must be determined to eliminate minor land uses/soil/slope in each sub-basin. A threshold value is used to remove minor land use/land covers in sub-basins, minor soil within a Land Use/Land Covers area and minor slope classes in a soil class within a soil on a specific Land Use/Land Covers area. The Arc-SWAT interface user's manual (Asimamaw, 2013; Karki *et al.*, 2020) suggests that 5% land use threshold, 10% soil threshold and 10% slope threshold values. Based on these suggestions and properties of the study area of the watershed, 5% land use, 10% soil and 10% slope threshold values were used for the HRU definition of this study.

3.3.3. Model Warm-up Period

A warm-up period is used to allow the model to run for a sufficient period before the simulation period to initialize important model variables or allow important processes to reach a dynamic equilibrium. Model developers recommend using warm-up periods of two (2) to three (3) years for hydrological processes and five (5) to ten (10) years for sediment and nutrient-related processes (Daggupati *et al.*, 2015). Based on these recommendations, the measured data of average monthly stream flow data of three (3) years from January 1990 to December 1992 was used for the model warm-up period for this Study.

3.3.4. Sensitivity Analysis

Sensitivity analysis is a method of identifying the most important parameters for calibration and validation of the SWAT model (Arnold *et al.*, 2012; Tang *et al.*, 2012). The average monthly stream flow data from 1990 to 2014 of the Welmel Watershed at Melka Amana gauging station was used to identify the sensitive parameters. In this study

sensitivity analysis was conducted using global sensitivity analysis available in SWAT CUP (Calibration and uncertainty program) and the Sequential Uncertainty Fitting (SUFI-2) algorithm within the SWAT-CUP was employed for calibration and validation (Nauman and Zulkafli, 2021; Abbaspour *et al.,* 2017). To provide a measure and significance of sensitivity, indices of t-Stat and p-value were used respectively. Therefore, higher t-test in absolute values measures high sensitivity while a p-value of 0 is more significant.

3.3.5. Model Calibration

Model calibration is a process in which a generalized model is adjusted so that the model predictions better represent site-specific hydrologic and water quality processes and conditions. The term calibration refers to a procedure where the difference between model simulation and observation is minimized. During calibration, model parameters are optimized to increase accuracy and reduce model prediction uncertainty. Calibration is performed by carefully selecting model parameter values, adjusting them within their recommended ranges, and comparing predicted output variables with observed data for a given set of conditions (Moriasi *et al.*, 2012). Since the crucial goal of model calibration is to optimize unknown parameter values in the model, this process is also called parameter optimization (Šimunek *et al.*, 2012). A model is considered to be successfully calibrated when it replicates observed data within an adequate level of accuracy and precision (Daggupati *et al.,* 2015; Moriasi *et al.* 2015).

Following the sensitivity analysis result, model calibration was done to obtain optimum values for sensitive parameters. SWAT provides three options for calibration: auto-calibration, manual calibration and a combination of these two methods. For this study, first manual calibration was employed. In this procedure, parameters values were adjusted

by changing the parameters within the allowable ranges either by replacing the initial value or addition or by multiplication of the initial value as designed in the interface (Arnold *et al.,* 2012). The calibration was done on monthly time steps using the average measured stream flow data of 14 years of the Welmel River watershed covering from January 1993 to December 2006 time period. Then, auto calibration was performed for sensitivity flow parameters.

3.3.6. Model Validation

Validation demonstrates that a given site-specific calibrated model can make sufficiently accurate simulations in a new modeling situation. It is the process of checking the representation of the parameters by simulating the observed data with an independent data set without further adjustment of the calibrated parameter values (Arnold *et al.,* 2012; Vilaysane *et al.,* 2015). Therefore, in this study, the measured data of average monthly stream flow data of 8 years from January 2007 to December 2014 was used for the model validation process.

3.3.7. Model Performance Evaluation

Model performance was assessed to evaluate the model simulation outputs in reference to the observed data. The coefficient of determination (R^2) and the Nash-Sutcliffe Efficiency simulation efficiency (ENS), R^2 ranges from zero to one with zero indicating poorness and one goodness of the model. Higher values indicate less error variance values greater than 0.6 are considered acceptable (Arnold *et al.*, 2012). R^2 is computed through (Equation (19).

$$R^2 = \frac{\sum(Xi-Xav)*\sum(Yi-Yav)}{\sum\sqrt{(Xi-Xav)\,2}*\sum\sqrt{(Yi-Yav)2}} \qquad (19)$$

Where Xi = measured value (m^3/s); Xav = average measured value (m^3/s); Yi = simulated value (m^3/s) and Yav is average simulated value (m^3/s). ENS indicates how well the plots

of observed versus simulated data fits the 1:1 line. It was computed using Equation (20). The ENS value ranges from negative infinity to 1. A value of ENS less than zero depicts that the mean observed value is a better predictor than the simulated value. This indicates unacceptable performance. When the ENS value is greater than 0.5, the simulated value is a better predictor than the mean measured value and is generally viewed as acceptable performance (Arnold *et al.,* 2012).

$$ENS = 1 - \frac{\sum(Xi-Yi)2}{\sum(Xi-Xav)2} \quad (20)$$

Where Xi is the measured value; Yi is the simulated value and X_{av} is the average observed value. According to (Dile and Srinivasan, 2014), the optimal PBIAS value is zero, while positive and negative values indicate model underestimation and overestimation biases, respectively.

$$\text{PBIAS} = \frac{\sum_{i=1}^{n}(Xi-Yi)*100}{\sum_{i=1}^{n}(Xi)} \quad (21)$$

Where Xi is the measured value and Yi is the simulated value.

The Nash-Sutcliffe Efficiency (NSE) of calibration is classified according to the scheme ($0.75 < NSE \leq 1.00$ very good; $0.65 < NSE < 0.75$ good; $0.50 < NSE < 0.65$ satisfactory; $NSE \leq 0.50$ unsatisfactory) for the goodness of fit (Leitinger *et al.,* 2015) and coefficient of determination (R^2) is classified as $0.7 < R^2 \leq 1$ Very good; $0.6 < R^2 \leq 0.7$ Good; $0.5 < R^2 \leq 0.6$ Satisfactory and $R^2 \leq 0.5$ Un satisfactory (Moriasi *et al.,* 2015).

Table 3-7: Performance evaluations for the monthly time step

Performance rating	R^2	NSE	PBIAS (%)
Very good	$0.7 < R^2 \leq 1$	$0.75 < NSE \leq 1.00$	PBIAS < ±10
Good	$0.6 < R^2 \leq 0.7$	$0.65 < NSE \leq 0.75$	±10 ≤ PBIAS < ±15
Satisfactory	$0.5 < R^2 \leq 0.6$	$0.5 < NSE \leq 0.65$	±15 ≤ PBIAS < ±25
Un satisfactory	$R^2 \leq 0.5$	$NSE \leq 0.5$	PBIAS ≥ ±25

Key: R2: coefficient of determination, NSE: Nash-Sutcliffe Efficiency and PBIAS: Percent bias

3.4. Model Running and Simulation Analysis

The calibrated model was then used to simulate hydrological components under changed LULC conditions for the historical and future years. In this case, the hydrological responses to historical LULC change was analyzed using LULC maps of 1990, 2005 and 2020 with the baseline map of 1990 LULC map. Similarly, the hydrological responses to predicted LULC change was analyzed using LULC maps of 2020, 2035 and 2050 with baseline map of 2020 LULC map, using hydrological SWAT model. The generated LULC maps, soil, climatic and stream flow data values were used to evaluate the hydrological responses to LULC changes. To evaluate the hydrological responses to LULC changes from 1990 to 2050, five (5) independent simulation runs were conducted using LULC maps of 1990, 2005, 2020, 2035 and 2050 keeping other input parameters unchanged.

4. RESULTS AND DISCUSSION

4.1. Accuracy Assessment of Classified Historical LULC

The Landsat satellite images, in combination with unsupervised and supervised classification techniques were used to map the LULC in the study watershed of the years 1990, 2005 and 2020.

Table 4-1: Error matrix for the year 1990 classified map

Classified Data	Reference Data						
	GR/RGE	SCRB/BSH	WD	FRST	AGR/SET	Row total	User's accuracy (%)
GR/RGE	13	0	1	0	1	15	86.67%
SCRB/BSH	0	9	0	1	0	10	90.0%
WD	0	1	16	2	1	20	80.0%
FRST	1	0	1	37	1	40	92.5%
AGR/SET	1	2	3	1	23	30	76.67%
Column total	15	12	21	41	26	115	
Producer's accuracy (%)	86.67%	75%	76.19%	90.24%	88.46%		
Kappa coefficient = 81.86%				Overall accuracy = 85.22%			

Table 4-2: Error matrix for the year 2005 classified map

Classified Data	Reference Data						
	GR/RGE	SCRB/BSH	WD	FRST	AGR/SET	Row total	User's accuracy (%)
GR/RGE	12	0	0	2	1	15	80.0%
SCRB/BSH	0	9	1	0	0	10	90.0%
WD	0	0	17	1	2	20	85.0%
FRST	2	0	2	34	2	40	85.0%
AGR/SET	1	2	0	3	24	30	80.0%
Column total	15	11	20	40	29	115	
Producer's accuracy (%)	80%	81.82%	85%	85.0%	82.76%		
Kappa coefficient = 78.34%				Overall accuracy = 83.48%			

Table 4-3: Error matrix for the year 2020 classified map

Classified Data	Reference Data						
	GR/RGE	SCRB/BSH	WD	FRST	AGR/SET	Row total	User's accuracy (%)
GR/RGE	11	1	0	1	2	15	73.33%
SCRB/BSH	1	8	0	1	0	10	80.0%
WD	0	1	19	0	0	20	95.0%
FRST	0	0	4	36	0	40	90.0%
AGR/SET	1	0	0	1	28	30	93.33%
Column total	13	10	23	39	30	115	
Producer's accuracy (%)	84.61%	80%	82.61%	92.31%	93.33%		
Kappa coefficient = 85.1% Overall accuracy = 88.69%							

Key: - AGR/SET: Agriculture/Settlement, FRST: Forest land, WD: Woodland, GR/RGE: Grassland/rangeland, SCRB/BSH: Scrubland/bushland.

The error matrix obtained from the analysis revealed that the overall accuracy of 85.22% and 83.48% with a kappa statistic of 81.86% and 78.34% for the LULC map of 1990 and 2005(Table 4.1 and 4.2) respectively. The overall accuracies of 88.69% and kappa statistics of 85.1% for the LULC maps of 2020 were obtained (Table 4.3). In support, Henok *et al.* (2021) found overall accuracies of 81.21% and 85.16%, kappa statistics of 77.23% and 82.24% for 1988 and 2000 LULC respectively. Moreover, the authors found an overall accuracy of 85.34%, with a kappa statistic of 82.46% for the LULC map of 2018. Nevertheless, the overall accuracy obtained in this study fulfills the minimum criteria for further analysis (Adenew *et al*., 2015; Moriasi *et al.*, 2015).

4.2. Detection of Historical LULC Change

The major types of LULC of the Welmel watershed are forestland, agriculture/settlement, woodland, scrubland/bushland and grassland/rangeland. The classified LULC of Welmel Watershed from 1990 to 2020 showed a significant LULC change. In the period 1990 to

2020, woodland, forest land and grassland/rangeland areas were converted into agriculture/settlement in the downstream, middle and upper stream of the watershed.

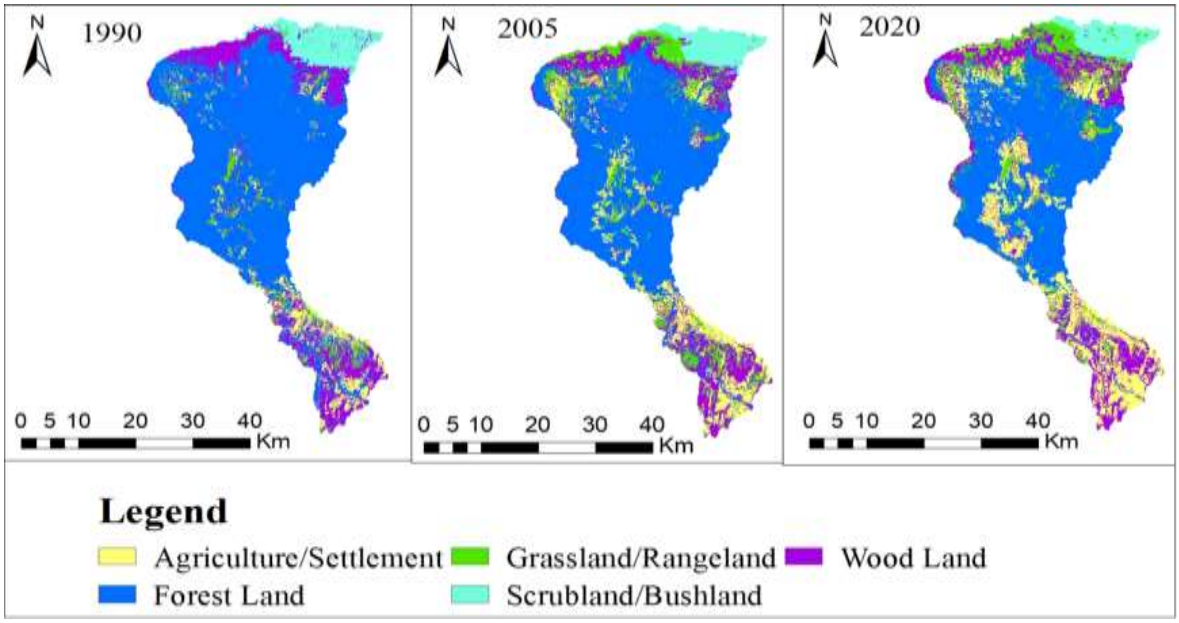

Figure 4-1. LULC maps of 1990, 2005 and 2020 of the study area

Table 4-4: Historical LULC and their percentage from 1990-2020 in the study area

Land Use/Land Cover class	Area extent of Historical LULC in Km^2 and %					
	1990	%	2005	%	2020	%
Grassland/Rangeland	73.84	5.04	156.96	10.74	152.41	10.43
Scrubland/Bushland	113.49	7.78	92.28	6.31	82.75	5.66
Woodland	223.99	15.33	205.36	14.05	245.27	16.78
Forestland	965.13	66.03	848.86	58.08	690.48	47.24
Agriculture/Settlement	85.09	5.82	158.07	10.82	290.64	19.89

Table 4-5: Rate of changes of Historical LULC from 1990-2020 of the study area

Land Use/Land Cover class	Rate of change of Historical LULC (Km^2 /year)		
	1990-2005	2005-2020	1990-2020
Grassland/Rangeland	+5.54	-0.30	+2.62
Scrubland/Bush land	-1.41	-0.64	-1.02
Woodland	-1.24	+2.66	+0.71
Forestland	-7.75	-10.56	-9.16
Agriculture/Settlement	+4.87	+8.84	+6.85

The LULC coverage of forestland, agriculture/settlement, woodland, grassland/rangeland and scrubland/bushland were 965.13Km^2 (66.03%), 85.09Km2 (5.82%), 223.99Km^2 (15.33%), 73.84Km^2 (5.04%) and 113.49 Km^2 (7.78%) respectively, during 1990 LULC map (Table 4.4). However, after 15 years later in 2005, the LULC showed a significant change. Forestland, woodland and scrubland/bushland decreased to 848.86Km^2 (58.08%), 205.36Km^2 (14.05%) and 92.28Km^2 (6.31%) respectively. On contrary, agriculture/settlement and grassland/rangeland increased to 158.07Km^2 (10.82%) and 156.96Km^2 (10.74%) respectively.

The change in LULC continued significantly specially forestland and agriculture/settlement from 2005 to 2020 compared with that of the 1990 to 2005 LULC map. Agriculture/settlement land showed a consistent increase, while scrubland/bushland and forestland showed a decreasing trend throughout the study period (1990 to 2020). Agriculture/settlement and grassland/rangeland increased between 1990 and 2005 with a rate of change of 4.87km^2/year and 5.54km^2/year orderly. This was almost in line with the study conducted by Mesfin *et al.* (2021) in the Shaya catchment, Genale-Dawa River basin, which reported that rangeland increased between 1987 and 2000 while decreased between 2000 and 2015. Adane and Getachew, (2017) in Goba, Harena Buluk and Delo Mena Woreda, reported that the increase in agriculture/settlement throughout the study period from 1986 to 2016, while forestland has decreased. Moreover, the authors specifically reported the expansion in grassland/rangeland areas from 1986 to 2016 and scrubland/bushland declined between 1996 and 2006.

Between 2005 and 2020, agriculture/settlement and woodland increased with a rate of change of 8.84km^2/year and 2.66km^2/year respectively. The increase in woodland was

because of the conversion of forest land into woodland, as woodland converted into agriculture/settlement in other case the reduced woodland area might be compensated from the conversion of forestland into woodland in the study area. However, forestland, scrubland/bushland and grassland/rangeland decreased with a rate of 10.56km^2/year, 0.64km^2/year and 0.30km^2/year. In support of this result, Mesfin *et al.* (2021) in the Genale-Dawa Basin Shaya catchment noted that woodland increased from 2000 to 2015. Moreover, specifically, the author reported that settlement and agricultural land showed increasing trends throughout the study period between 1987 and 2015. Henok *et al*. (2021) observed in the Gidabo River basin in Ethiopia from 2000 to 2018, woodland was increased. Girma *et al.* (2019) noted that, area coverage in agriculture and settlement showed an increasing trend while bushland and forestland declined trend in Delo Mena district from 2000 to 2015. Tewodros *et al.* (2021), in the Upper Baro Basin, Ethiopia, noted that in the last 30 years, agriculture and urban areas increased, while forest and scrubland decreased between 1987 and 2017. Another study conducted by Gemechu *et al.* (2021), reported the expansion of cultivated land and urban built-up areas while a reduction in the forest land and shrub/bushland over 38 years (1979-2017) in Huluka watershed of Oromia Regional State, Ethiopia.

This study indicated that the most significant change has occurred in forestland, agriculture/settlement and grassland/rangeland in the Welmel watershed. Over the last 31 years, agriculture/settlement area had expanded, while forest land area showed a sensational reduction followed by scrubland/bushland. In overall, from 1990 to 2020, forestland declined, while agriculture/settlement increased. The reduction of forest coverage was due to expansion in agriculture/settlement and woodland in the Welmel watershed.

4.2.1. Conversion Matrixes of Historical LULC Changes

Conversions of LULC from one category to another are common phenomena in LULC studies (Fasika *et al.,* 2018; Rientjes *et al.,* 2011). The historical LULC conversion of one LULC category to another between the 1990 and 2020 period was presented in Table 4.6. The diagonals in the matrix from the table are the persistence (remaining unchanged) while the off-diagonals are the conversions from one category to the others. From 1990 to 2020, 124.17km^2 of forest land was converted to agriculture/settlement, 65.65km^2 to grassland/rangeland, 110.27km^2 to woodland and 0.08 km^2 to scrubland/bushland. While 3.16km^2, 4.50km^2 and 16.14km^2 of agriculture/settlement changed to forestland, grassland/rangeland and woodland respectively. The conversion of 110.27km^2 of forest land to woodland might be the result for the incremental in woodland between 2005 and 2020 time period. In line with this result, Adane and Getachew (2017) in Goba, Harena Buluk and Delo Mena Woreda stated that, forest land was mainly converted to agriculture/settlement and woodland between 1986 and 2016.

Table 4-6: Transition area matrix (km^2) of LULC between 1990 and 2020

LULC Class		2020					
		AGR/SET	FRST	GR/RGE	SCRB/BSH	WD	Total
1990	AGR/SET	83.17	3.16	4.50	0	16.14	103.66
	FRST	124.17	661.33	65.65	0.08	110.27	958.19
	GR/RGE	28.00	2.06	15.73	0.16	10.24	56.19
	SCRB/BSH	0.87	2.14	24.25	78.13	9.61	111.7
	WD	69.03	12.17	45.40	3.20	105.30	231.8
	Total	301.94	677.55	152.23	81.57	248.25	1461.54

Key: - AGR/SET: Agriculture/Settlement, FRST: Forest Land, WD: Wood Land, GR/RGE: Grassland/Range Land, SCRB/BSH: Scrubland/Bushland

During the study period 0.87km^2, 2.14km^2, 24.25km^2 and 9.61km^2 of scrubland/bushland changed into agriculture/settlement, forestland, grassland/rangeland and woodland

respectively. Similarly, 69.03km^2, 12.17km^2, 45.40km^2 and 3.20km^2 of woodland changed into agriculture/settlement, forestland, grassland/rangeland and scrubland/bushland respectively. Moreover, 28.00km^2, 2.06km^2, 0.16km^2 and 10.24km^2 of grassland/rangeland has changed to agriculture/settlement, forestland, scrubland/bushland and woodland orderly. Studies conducted in various parts of the country also reported the conversions of one category to others. For instance, research conducted in the Andassa watershed, Blue Nile Basin from 1985 to 2015 (Temesgen *et al.,* 2017); Upper Gilgel Abbay catchment of Blue Nile basin (Rientjes *et al.*, 2011); in northern Afar rangelands (Diress Tsegaye *et al.,* 2010).

4.3. Detection of Predicted LULC Change

The trend of predicted LULC change analysis was examined using LULC maps of 2035 and 2050 with the baseline LULC map of 2020. The result indicated that, from 2020 to 2035 grassland/rangeland will increase as indicated in figure 4.2 and table 4.7. This increase might be due to fallowing of agricultural land and the conversion of scrubland/rangeland and woodland into grassland/rangeland class in the study area. In support of this result, Wakjira *et al.* (2020), stated that the increase in rangeland in Finchaa catchment from 2017 to 2036.

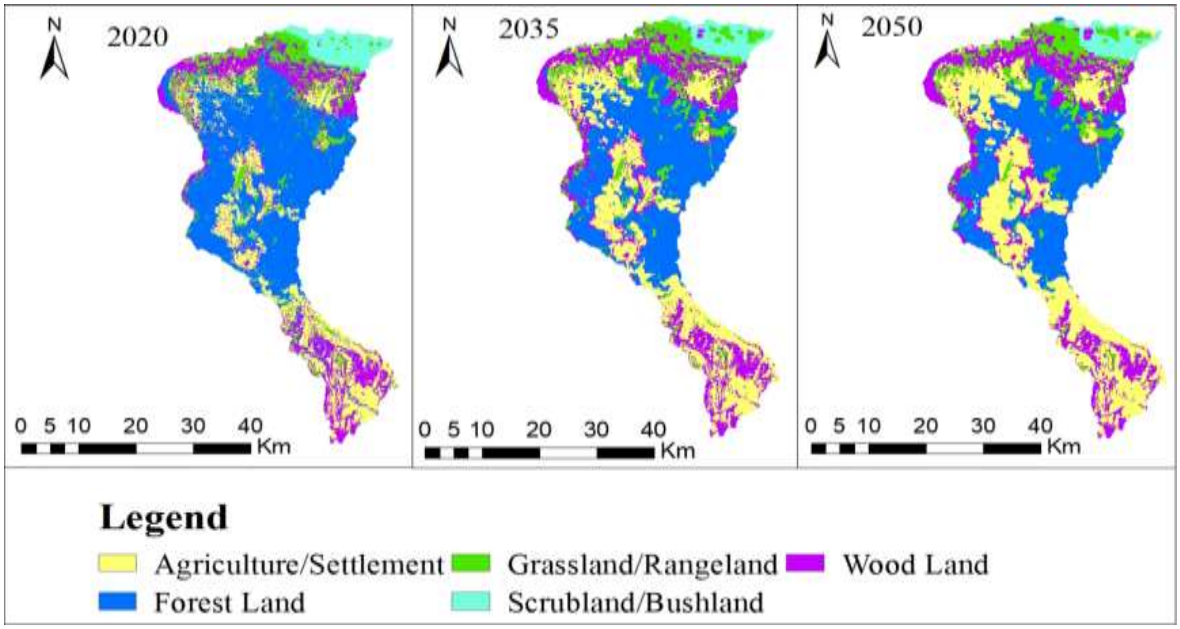

Figure 4-2. Predicted LULC maps from 2035-2050 with the baseline map of 2020

Table 4-7: Predicted LULC and their percentage areas from 2020-2050 in the study area

Land Use/Land Cover class	Area extent of Predicted LULC Km^2 and %					
	2020	%	2035	%	2050	%
Grassland/Rangeland	152.41	10.43	184.26	12.61	178.86	12.24
Scrubland/Bushland	82.75	5.66	62.22	4.26	55.48	3.8
Woodland	245.27	16.78	306.95	21	307.68	21.05
Forestland	690.48	47.24	495.88	33.93	427.01	29.22
Agriculture/Settlement	290.64	19.89	412.23	28.21	492.51	33.7

Table 4-8: Rate of changes of Predicted LULC from 2020-2050 of the study area

Land Use/Land Cover class	Rate of change of Predicted LULC (Km^2 /year)		
	2020-2035	2035-2050	2020-2050
Grassland/Rangeland	+ 2.12	-0.36	+ 0.88
Scrubland/Bushland	-1.37	-0.45	- 0.91
Woodland	+ 4.11	+0.05	+ 2.08
Forestland	-12.97	-4.59	- 8.78
Agriculture/Settlement	+8.11	+5.35	+ 6.73

In the Welmel watershed, woodland will increase with an annual rate of 4.11km^2/year as a result of the conversion of forest to woodland, while forest and scrubland/bushland area

will decrease with a rate of change of 12.97Km^2/year and 1.37Km^2/year respectively. Agriculture/settlement will increase from 290.64Km^2 to 412.23Km^2 with a rate of change of 8.11Km^2/year. The predicted LULC repealed that, agriculture/settlement, woodland and grassland/rangeland classes will increase due to the conversion of scrubland/bushland and forestlands into these LULC classes. This result is in line with the study conducted by Adane and Getachew, (2017), in Goba, Harena Buluk and Delo Mena Woreda by 2026. Another study conducted by Girma *et al.* (2019) in Delo Mena district also suggested that by the year 2030, the forest area will decline between 2010 and 2030, and woodland, farmland and settlement areas will be increased by the year 2030.

In the Welmel watershed, from 2035 to 2050, agriculture/settlement is expected to increase with a rate of change of 5.35Km^2*/year*, while forest land will decrease with a rate of change of 4.59Km^2*/year*. On the other hand, scrubland/bushland and grassland/rangeland will decrease with a rate of change of 0.45Km^2/year and 0.36km^2/year respectively. On contrary, woodland will increase with a rate of change of 0.05km^2/year. This result repealed that, the rate of expansion of agriculture/settlement area from 2020 to 2035 is higher compared to 2035 to 2050, which might be due to the limited areas available for agriculture/settlement expansion in the future. Wakjira *et al.* (2020), in Finchaa catchment, stated that the rate of agricultural land expansion from 2036 to 2055 is lower compared to the result of the previous predicted from 2017 to 2036 might be possible due to the limited area of land for farmland expansion. Semegnew *et al.* (2021) in Gambella, Southwestern Ethiopia, reported that the area of forestland and grassland will show a decreasing trend, while a continuous increase in farmland and settlement between 2032 and 2047. Another study conducted in Nashe Watershed, Blue Nile River Basin, by Megersa *et al.* (2021), reported that forest land will decrease between 2019 and 2050 with a high increasing rate

of urban areas and agricultural land. The rate of reduction of forest area from 2020 to 2035 is higher compared to 2035 to 2050, which might be due to the limited coverage of forest areas between 2035 and 2050. The result of this study shows that in the future between 2020 and 2050, agriculture/settlement will increase at a rate of change of 6.73km^2/year, while forest land will decrease with a rate of change of 8.78km^2/year.

4.3.1. Conversion Matrixes of Predicted LULC Changes

The result of the predicted LULC map from 2020 to 2050 with the baseline LULC map of 2020 indicated that, 113.13km^2 of forest land will convert to agriculture/settlement, 44.19km^2 to grassland/rangeland and 96.74km^2 to woodland. On the other hand, 41.60km^2 of woodland, 4.25km^2 of scrubland/bushland and 33.32km^2 of grassland/rangeland is expected to convert to agriculture/settlement.

Table 4-9: Transition area matrix (Km^2) of LULC between 2020 and 2050

LULC Class		2050					
		AGR/SET	FRST	GR/RGE	SCRB/BSH	WD	Total
2020	AGR/SET	288.26	0.12	1.22	0.00	5.27	294.87
	FRST	113.13	425.84	44.19	0.00	96.74	679.89
	GR/RGE	33.32	0.29	113.75	0.00	8.18	155.54
	SCRB/BSH	4.25	1.23	16.13	55.57	4.41	81.59
	WD	41.60	0.03	13.26	0.00	194.75	249.64
	Total	480.57	427.50	188.54	55.57	309.35	1461.54

Key: - AGR/SET: Agriculture/Settlement, FRST: Forest land, WD: Woodland, GR/RGE: Grassland/Rangeland, SCRB/BSH: Scrubland/Bushland

Similarly, 13.26km^2 of woodland, 16.13km^2 of scrubland/bushland, 44.19km^2 of forest land and 1.22km^2 of agriculture/settlement land will be converted to grassland/rangeland between 2020 and 2050. This will be the reason for the incremental in grassland/rangeland from 2020 to 2050. When we compare the gain and loss of grassland/rangeland, it is expected to gain 74.8km^2 and lose 41.79km^2 of the area with a net gain of 33.01km^2 in the

future. On the contrary, a total area of 26.02km^2 of scrubland/bushland is expected to change to other LULC types in the future. When comparing the gain and loss in woodland, it will gain 114.6km^2 and loss 54.89km^2 which results in a net gain of 59.71km^2. Agriculture/settlement will take 41.60km^2 out of 54.89km^2. In agreement, Tadele *et al.,* (2021), noted that bushland, grassland and agriculture/rural settlement will be converted to forest land. Conversely, forest land will be converted to bushland, agriculture/rural settlement, built-up area, bare land and water body respectively in Coka Watershed Southern Ethiopia, from 2018 to 2060. Similarly, Hamere *et al.,* (2020), stated the conversion of LULC from one type to others from 2017-2047, in Beressa Watershed, Blue Nile basin Ethiopian highlands.

4.4. Modelling of Hydrological Components

4.4.1. Sensitivity Analysis

By utilizing SUFI-2 of SWAT-CUP 2019 version 5.2.1 tool the sensitivity analysis was conducted for hydrological parameters of the SWAT model affecting the hydrological components of the study area. These parameters were calibrated using the observed flows at the Melka Amana gauging station. As the model considered 26 flow parameters for the analysis of sensitivity for calibration and validation of which 12 of them are comparatively sensitive and that were influencing the hydrological processes in the Welmel watershed were chosen (Table 4.10). Some of the selected parameters ranges were taken from the SWAT- CUP manual and works of literature (Tesfahun and Dereje, 2019; Tekalegn *et al.,* 2017; Abdulkerim and Sarma, 2016; Arnold *et al.,* 2012).

Table 4-10: Selected parameters with their Descriptions

Parameter	Descriptions
v__RCHRG_DP.gw	Deep aquifer percolation fraction
v__REVAPMN.gw	Threshold depth of water in the shallow aquifer for "revap" to occur (mm)
v__ESCO.hru	Soil evaporation compensation factor
v__ALPHA_BF.gw	Baseflow alpha-factor(days)
v__GW_DELAY.gw	Groundwater delay(days)
r__SOL_K (.).sol	Saturated hydraulic conductivity (mm/hr)
v__CANMX.hru	Maximum canopy storage (mm)
r__SLSUBBSN.hru	Average slope length(m)
r__SOL_AWC (.).sol	Available water capacity (mm water/mm soil)
v__GW_REVAP.gw	Groundwater revap coefficient
r__CN2.mgt	SCS runoff curve number(dimensionless)
v__GWQMN.gw	Threshold depth of water in the shallow aquifer required for return flow to occur (mm)

Table 4-11: Parameter ranges, sensitivity ranks and optimized values

Parameters	Ranges	t-values	p-values	Ranks	Optimized Values
v__RCHRG_DP.gw	0-1	32.27	0.0000	1	0.55
r__CN2.mgt	±0.25	24.42	0.0000	2	0.17
v__ESCO.hru	0-1	15.38	0.0000	3	0.90
v__GWQMN.gw	±1000	-12.47	0.0104	4	805.0
r__SOL_AWC (.).sol	±0.25	-5.67	0.0135	5	-0.22
v__CANMX.hru	0-10	-5.30	0.0179	6	2.01
v__GW_REVAP.gw	0.02-0.2	-5.01	0.0379	7	0.04
v__GW_DELAY.gw	0-500	-4.22	0.0696	8	8.50
v__REVAPMN.gw	±100	1.96	0.0802	9	61.50
r__SOL_K (.).sol	±0.25	1.01	0.3111	10	-0.14
r__SLSUBBSN.hru	0-0.2	-0.74	0.4619	11	0.08
v__ALPHA_BF.gw	0-1	-0.21	0.8316	12	0.97

4.4.2. Model Calibration and Validation

The calibration and validation of the study were performed using monthly discharge data from 1990-2006 and 2007-2014 respectively with three years of warm-up period.

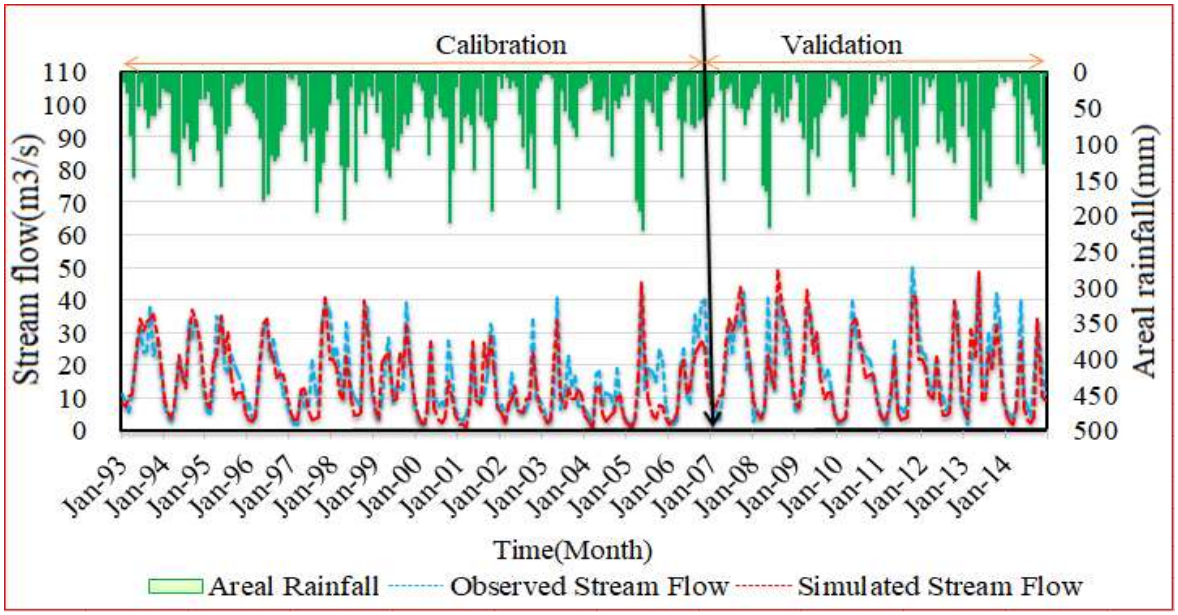

Figure 4-3: Reveals calibration and validation respectively

The sensitive parameters were adjusted in the permissible range to obtain the best fit of the observed and simulated flow. Figure 4.3 shows the hydrograph of monthly calibration and validation flow result with respect to the observed discharge and observed areal rainfall respectively. The hydrograph of measured and simulated stream flow showed that the Arc SWAT model has a good ability to simulate the watershed hydrology of the Welmel River basin. As indicated in figure 4.3 for both calibration and validation, the hydrograph of monthly simulated flow was almost the same as that of hydrograph of measured monthly stream flow.

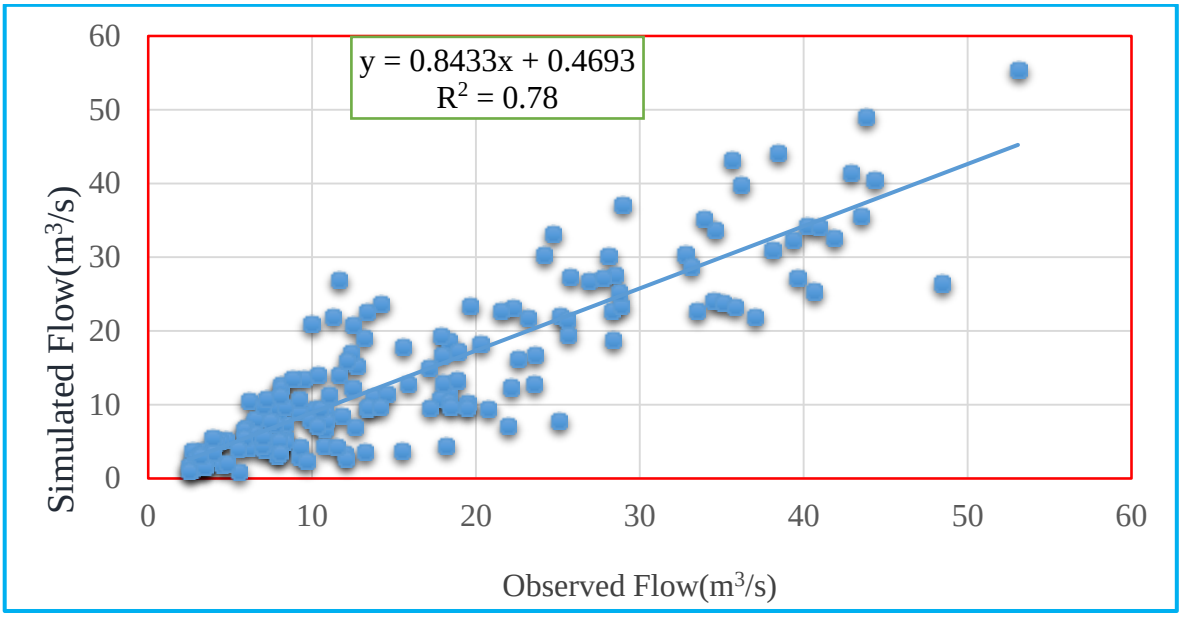

Figure 4-4: Scatter plot of simulated and observed flow for the calibration (1993 - 2006)

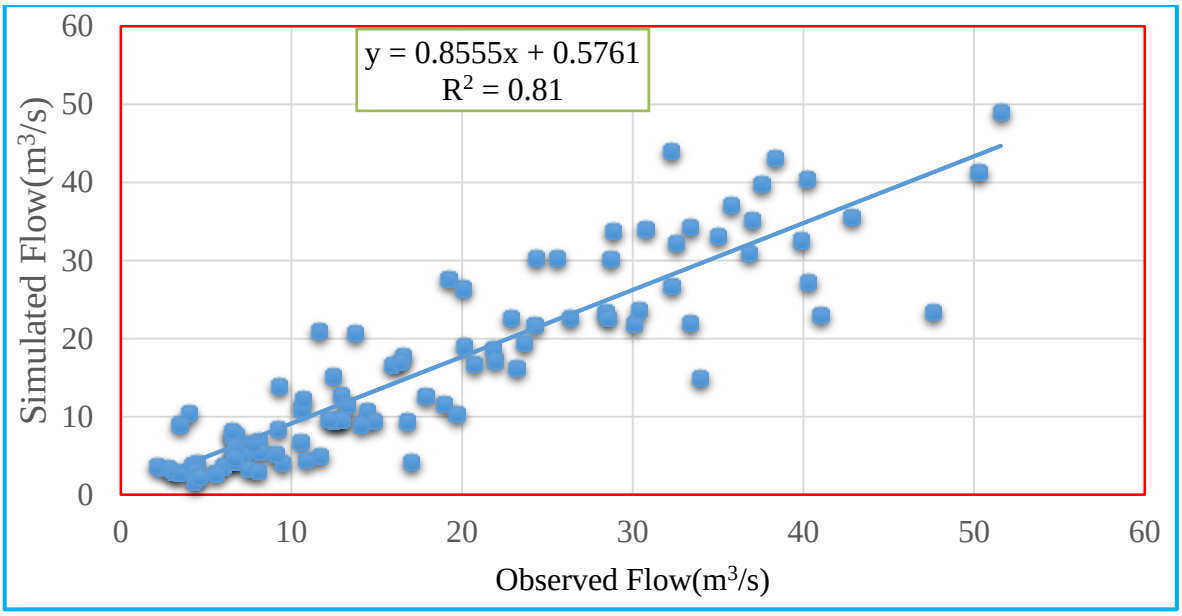

Figure 4-5: Scatter plot of simulated and observed flow for the validation (2007-2014)

4.4.3. Model Performance Evaluation

When comparing the model's performance against the model evaluation criteria introduced in (Table 3.7) for the monthly time step, SWAT simulated the stream flow trends very well both in calibration and validation (Table 4.12).

Table 4-12: SWAT model Performance of the calibration and validation

Period	R^2	NSE	PBIAS
Calibration(1993-2006)	0.78	0.74	12.8
Validation(2007-2014)	0.81	0.78	11.4

R^2: Coefficient of determination; NSE: Nash-Sutcliffe efficiency; PBIAS: Percent bias.

4.5. Responses of hydrological components to LULC Change at Basin level

4.5.1. Responses of Hydrological Components to Historical LULC Change

The evaluation result of the major hydrological components responses of surface runoff, groundwater flow, lateral flow, water yield, evapotranspiration and percolation to LULC change is given in 4.13. The response of hydrological components to historical LULC change for this study was examined with the LULC map of 1990, 2005 and 2020 with the baseline map of 1990.

Table 4-13: Mean annual hydrological components from 1990-2020

Hydrological component (mm)	Historical hydrological components		
	1990	2005	2020
Surface runoff	138.02	153.63	172.96
Lateral flow	53.73	47.40	43.03
Groundwater flow	194.92	178.27	161.46
Water yield	386.67	379.3	377.45
Evapotranspiration	616.47	594.14	614.23
Percolation	264.81	242.18	219.34

Table 4-14: Relative change of mean annual hydrological components from 1990-2020

Hydrological component (mm)	Historical relative change of hydrological components (%)		
	1990-2005	2005-2020	1990-2020
Surface runoff	+ 11.31	+ 12.58	+ 25.32
Lateral flow	-11.78	-9.22	-19.91
Groundwater flow	- 8.54	-9.43	-17.17
Water yield	-1.91	-0.49	-2.38
Evapotranspiration	-3.62	+3.38	-0.36
Percolation	-8.55	-9.43	-17.17

The simulated result using the 1990 LULC map of surface runoff, lateral flow, groundwater flow, water yield, evapotranspiration and percolation were 138.02mm, 53.73mm, 194.92mm, 386.67mm, 616.47mm and 264.81mm respectively. In the same way, surface runoff of 153.63mm, lateral flow of 47.40mm, groundwater flow of 178.27mm, water yield of 379.3mm, evapotranspiration of 594.14mm and percolation of 242.18mm were generated using the LULC map of 2005. Similarly, using the LULC map of 2020, 172.96mm of surface runoff, lateral flow of 43.03mm, groundwater flow 161.46mm, water yield of 377.45mm, evapotranspiration of 614.23mm and percolation of 219.34mm generated. As indicated in table 4.14, surface runoff between 1990 and 2005 increased by a relative change of 11.31% while other hydrological components of lateral flow, groundwater flow, water yield, evapotranspiration and percolation decreased by relative change of 11.78%, 8.54%, 1.91%, 3.62% and 8.55% respectively as a result of changes in LULC.

Between 2005 and 2020, surface runoff increased with a relative change of 12.58%. On contrary, lateral flow, groundwater flow, water yield and percolation decreased by 9.22%, 9.43%, 0.49% and 9.43% respectively. This might be as a result of expansion in agriculture/settlement and contraction in forestland area coverage between 2005 and 2020. In agreement with this result, in Chemoga Catchment, Abay basin (Anmut *et al.*, 2019) from 1994 to 2013 and in Ketar watershed Ziway-Shala basin (Damtew *et al*., 2015) from 1986 to 2010, reported the incremental in surface runoff, while groundwater flow and lateral flow decreased due to the LULC change. Megersa *et al.* (2021) in Nashe catchment, Blue Nile River basin, reported that, due to the LULC change occurred, the average surface runoff has increased though, the average annual lateral flow, groundwater flow, water yield and evapotranspiration showed a decreasing trend from 1990 to 2019. Other research

conducted at Gilgel Gibe, Omo Gibe Basin by Wakjira *et al.* (2016), investigated that from 1987 to 2010, surface runoff increased, while groundwater flow and percolation showed a decreasing trend as a result of changes in LULC between 1987 and 2010. Henok *et al.* (2021), at Gidabo River basin in Ethiopia also reported that, as a result of expansion in cultivated land and urban area and reduction in forest land, the yearly surface runoff increased constantly, whereas lateral flow, groundwater flow, evapotranspiration and percolation decreased from 1988 to 2018. As indicated in Tables 4.13 and 4.14, the change in evapotranspiration was inconsistent in the Welmel Watershed. For instance, the estimated annual average evapotranspiration decreased with a relative change of 3.62% between 1990 and 2005. This might be due to the decline in forestland, woodland and scrubland/bushland and the expansion of agriculture/settlement land. In contrast, the annual average evapotranspiration increased by a relative change of 3.38% from 2005 to 2020 (Table 4.14). This is might be due to the increase in woodland and the gradual decrease of scrubland/bushland. In agreement with this result, Henok *et al.* (2021), at Gidabo River basin concluded that, the increase in agroforestry and the gradual expansion of cultivated land resulted in increase in annual average evapotranspiration between 2000 and 2018. The result of this study indicated that, in response to LULC change, a radical change in hydrological components was observed. During the study period of historical LULC from 1990 to 2020, surface runoff increased by a relative change of 25.32%, while groundwater flow declined by 17.17%. Furthermore, percolation and lateral flow decreased with a relative change of 17.17% and 19.91% respectively.

4.5.2. Response of Hydrological Components to Predicted LULC Change

The response of hydrological components to predicted LULC changes for this study was analyzed using the 2035 and 2050 LULC maps with the baseline map of 2020 LULC.

Table 4-15: Mean annual hydrological components from 2020-2050

Hydrological component (mm)	Predicted hydrological components		
	2020	2035	2050
Surface runoff	172.96	194.01	204.91
Lateral flow	43.03	38.2	31.48
Groundwater flow	161.46	142.31	133.19
Water yield	377.45	374.52	369.58
Evapotranspiration	614.23	607.41	602.52
Percolation	219.34	193.43	181.03

Table 4-16: Relative change of mean annual hydrological components from 2020-2050

Hydrological component (mm)	Predicted relative change (%)		
	2020-2035	2035-2050	2020-2050
Surface runoff	+ 12.17	+ 5.62	+ 18.47
Lateral flow	-11.22	-17.59	- 26.84
Groundwater flow	-11.86	-6.41	- 17.51
Water yield	-0.78	-1.32	- 2.09
Evapotranspiration	-1.11	-0.81	- 1.91
Percolation	- 11.81	- 6.41	-17.47

Due to the will of significant changes in LULC, from 2020 to 2050 (Table 4.15 and 4.16), the average annual surface runoff is expected to increase with a relative change of 18.47%. Conversely, groundwater flow, lateral flow, water yield, evapotranspiration and percolation will decrease consistently. In opposite, Groundwater flow will decrease by 17.51%, lateral flow by 26.84%, water yield by 2.09%, evapotranspiration by 1.91% and percolation by 17.47%. In support of this study, in Andassa watershed, Blue Nile Basin (Temesgen *et al.*, 2017) from 2030 to 2045 and in Finchaa catchment (Wakjira *et al.*, 2020) from 2017 to 2055, noted that due to the LULC changes, surface runoff will be expected to increase, while groundwater flow; lateral flow and evapotranspiration will decline. Megersa *et al.* (2021), in the Nashe catchment, Blue Nile River Basin reported

that due to the expected LULC change from 2019 to 2050, the average annual surface runoff will increase.

The result of this study indicated that, the rate of increase and decline in hydrological components might associate with the rate of LULC changes. For instance, as the rate of LULC change increased the response of hydrological components also increased. When compared the rate of change of agriculture/settlement from 2005 to 2020 with other periods of 1990 to 2005, 2020 to 2035 and 2035 to 2050, its incremental rate of change was higher (8.84%) and the relative change of surface runoff was 12.585 which is higher than other periods. Moreover, comparing the rate of change of agriculture/settlement from 2020 to 2035 with 1990 to 2005 and 2035 to 2050, its incremental rate of change was 8.11% and the relative change of surface runoff was 12.17% which is greater than 1990 to 2005 and 2035 to 2050. Compared 1990 to 2005 with 2035 to 2050, the rate of change of agriculture/settlement from 2035 to 2050 (5.35%) was higher than 1990 to 2005 (4.87%), but the relative change of surface runoff from 1990 to 2005 (11.31%) was higher than that of 2035 to 2050 (5.625). This is might be due to the incremental of grassland/rangeland from 1990 to 2005. Similarly, the relative change of groundwater flow from 2005 to 2020 (9.43%) and 2020 to 2035 (11.86%) was higher than 1990 to 2005 (8.54%) and 2035 to 2050 (6.41%). This could be due to the highest incremental in agriculture/settlement (8.84%) between 2005 and 2020, and (8.11%) between 2020 and 2035 and reduction in forestland (10.56%) between 2005 and 2020, and (12.97%) between 2020 and 2035.

4.6. Response of hydrological components to LULC changes at sub-basin level

4.6.1. Response of Hydrological Components to Historical LULC Changes

The change of hydrological responses in each of the sub-basins under historical LULC change was assessed from1990-2020 with the baseline LULC map of 1990. Spatial distributions of changes in LULC and the hydrological components at the sub-basins level for historical LULC change from 1990 to 2020 are indicated in Figures 4.6 and 4.7 respectively. From the LULC map of 1990 to 2020 (Figures 4.6 and 4.7), the highest increase in surface runoff was observed in the middle especially in the sub-basin (11) and downstream to south and southeast and southwest and northwest parts of the watershed that covered dominantly with agriculture/settlement. In opposite, decreased at the top of the watershed that dominantly characterized by higher scrubland/bushland LULC type. Surface runoff increased almost in all sub-basins, especially in the middle, downstream of southeast and southwest and upper stream of northwest parts of the watershed following the conversion of forest land, woodland and grassland/rangeland LULC types to agriculture/settlement LULC types. The average annual surface runoff in all sub-basin increased by 39.90mm. However, a decrease in surface runoff has also occurred in the upper stream northern part of the watershed. This was due to the increase in grassland/rangeland and the gradual increase in agriculture/settlement land.

While groundwater flows revealed a decreasing pattern almost in all 29 sub-basins between 1990 and 2020, the most significant reduction occurred in the middle of the sub-basin (11), downstream of the South and northwest parts of the watershed. These parts were dominantly characterized with agriculture/settlement LULC type.

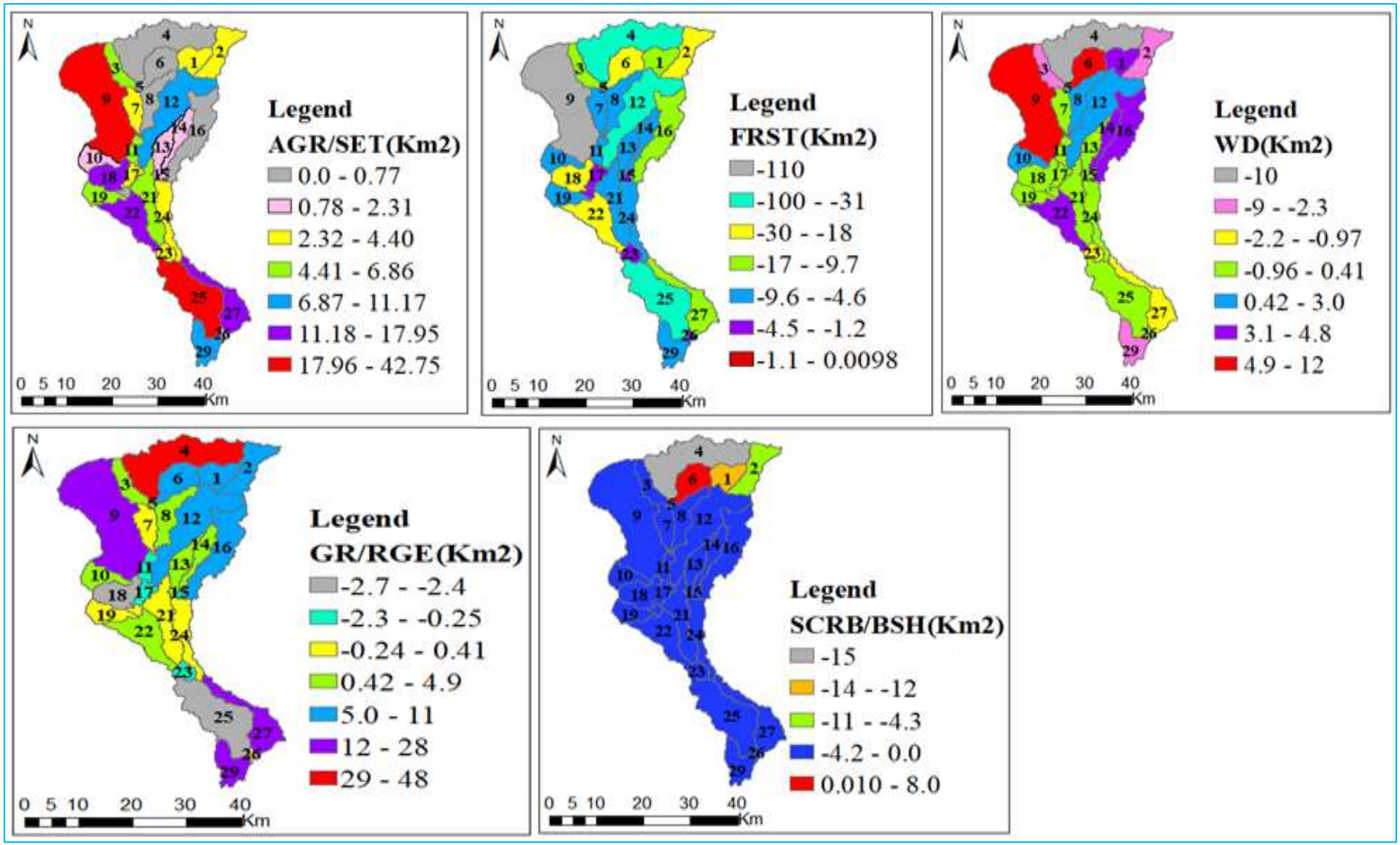

Figure 4-6: Spatial distribution of changes in LULC at the sub-basin level (1990-2020)
Key: AGR/SET: Agriculture/Settlement, FRST: Forest Land, WD: Wood Land, GR/RNG: Grass/Range Land, SCRB/BSH: Scrubland/Bushland

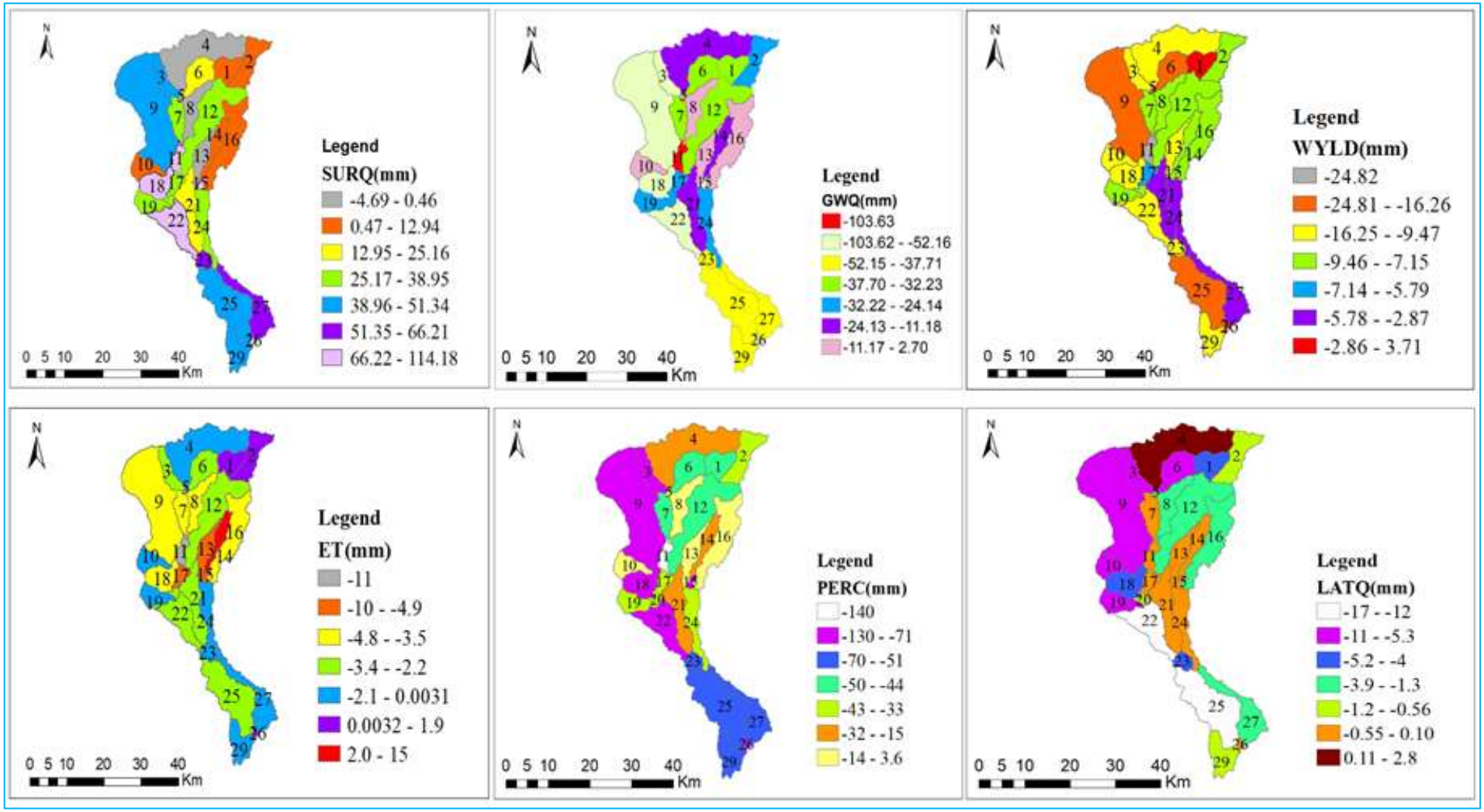

Figure 4-7: Spatial distributions of changes in hydrological components at sub-basin level (1990–2020)

Key: SURQ: Surface runoff; WYLD: Water yield; GWQ: Groundwater flow; LATQ: Lateral flow; PERC: Percolation; ET: Evapotranspiration.

Slight decreasing occurred in northeastern at sub-basin (10), northwest at sub-basin (13, 16) and around the upper stream of the watershed at sub-basin (8). Inversely, in these areas surface runoff has decreased at sub-basin (8, 13) and slightly increased at sub-basin (10, 16). Hence, the increase in groundwater flow in these sub-basins is associated with the decrease in surface runoff and the increase in grassland/range and woodland. The average annual groundwater flows in all sub-basins decreased by 34.57mm. Almost similar result with this finding by Henok *et al.* (2021) at the Gidabo River basin in Ethiopia reported that the groundwater flow in all sub-basins showed a decreasing trend. Moreover, the authors noted that, surface runoff in the basins increased in almost all sub-basins due to the conversion of forest, agroforestry and grassland to cultivated land and urban areas during 1988 and 2018. Another Research conducted in the Gummara watershed, in Lake Tana Basin, reported that due to the expansion of agricultural land use and reduction of forest coverage in most of the sub-basins, resulted in higher surface runoff between 1985 and 2015. Moreover, the authors concluded that the maximum change of surface runoff is associated with the maximum expansion of agricultural land use (Achenafi *et al.*, 2019).

The highest reduction in water yield was observed at the middle of the watershed sub-basin 11 and Northwest and southwest which are covered dominantly with agriculture/settlement. The highest decrease in evapotranspiration observed at the middle of the sub-basin which is dominantly covered with agriculture/settlement and increased in the direction of Northeast parts and middle of the watershed covered with forest and scrubland/bushland. In support, Dias *et al.* (2015), where watersheds with an increase in forest cover tend to have higher evapotranspiration and lower surface runoff. Higher surface runoff and lower evapotranspiration are expected in agricultural land use than forest and shrubs areas (Anaba *et al.*, 2017). Percolation showed a decreasing trend

throughout the study period in all sub-basin levels, with a high decreasing level observed at the middle, northwest, southwest and downstream of the catchment that was dominantly covered with agriculture/settlement and woodland types respectively. On the other hand, a slight decrease in percolation was observed at the upper and Northeastern parts of the watershed that dominantly covered with forest, woodland and scrubland/bushland LULC types respectively.

Lateral flow decreased in all sub-basin levels except at the upper stream of the watershed that characterized in increase of grassland/rangeland. The highest decrease was in the southwest and northwest parts of the catchment that characterized by increasing in agriculture/settlement. The results of this study indicated that sub-basins that were in increasing in agriculture/settlement LULC types cause an increase in surface runoff and decrease in water yield, groundwater flow, percolation, evapotranspiration and lateral flow.

4.6.2. Response of Hydrological Components to Predicted LULC Changes

The projected LULC map between 2020 and 2050 (Figure 4.8), shows that the highest increase in surface runoff is expected in the middle of the watershed (Sub-basin 11) that is expected fully covered with agriculture/settlement in the coming 31 years. This result indicates that, there will be a similar increasing trend in surface runoff within the sub-basin in the future. Megersa *et al.* (2021), found almost similar result that, surface runoff is expected to increase at the sub-basin level with highest increase in the sub-basins characterized with agricultural and urbanization areas in Nashe Watershed, Blue Nile River basin from 2019 to 2050.

While groundwater flow will decrease throughout the sub-basin with the highest decrease is expected in the middle of the watershed (sub-basin 11, 9) and a slight decrease

downstream of sub-basin (29, 27 and 26). This result indicates that, the decrease in groundwater flow is more associated with sub-basins characterized by agriculture/settlement. Water yield will decrease in all sub-basins except at sub-basin-14 in the direction of Northeast parts of the watershed. This might be due to the reduction in groundwater flow and lateral flow. Evapotranspiration will decrease to the northeast and middle parts might be due to the trend of decreasing in forest coverage and increasing in agriculture/settlement (sub-basin 13, 15, 17).

In the study watershed, percolation is expected to show a decreasing trend in the future time at all sub-basin levels. The highest decreasing level in percolation will be observed at the middle parts of sub-basin 11 that characterized by agriculture/settlement. On contrary, a slight decrease will take place downstream of the watershed that characterized in slight decreasing of forest and starting increase in grassland/rangeland. The lateral flow is expected to decrease almost in all sub-basin levels with the highest decrease in the direction of the upper stream of the watershed that is expected to increase in agriculture/settlement and decrease in forest coverage.

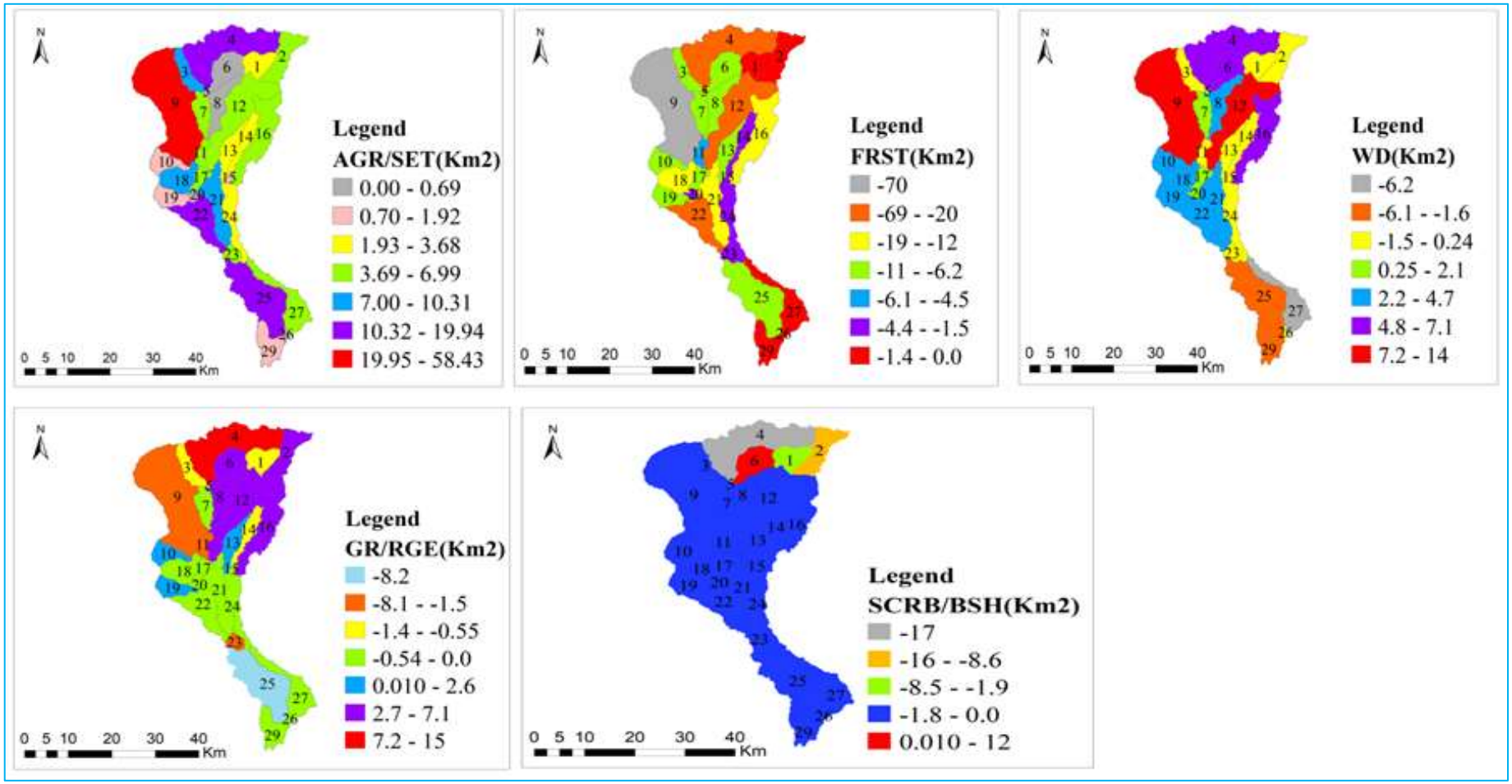

Figure 4-8: Spatial distribution of changes in LULC at the sub-basin level (2020-2050)

Key: AGR/SET: Agriculture/Settlement, FRST: Forest land, WD: Woodland, GR/RNG: Grassland/Rangeland, SCRB/BSH: Scrubland/Bushland

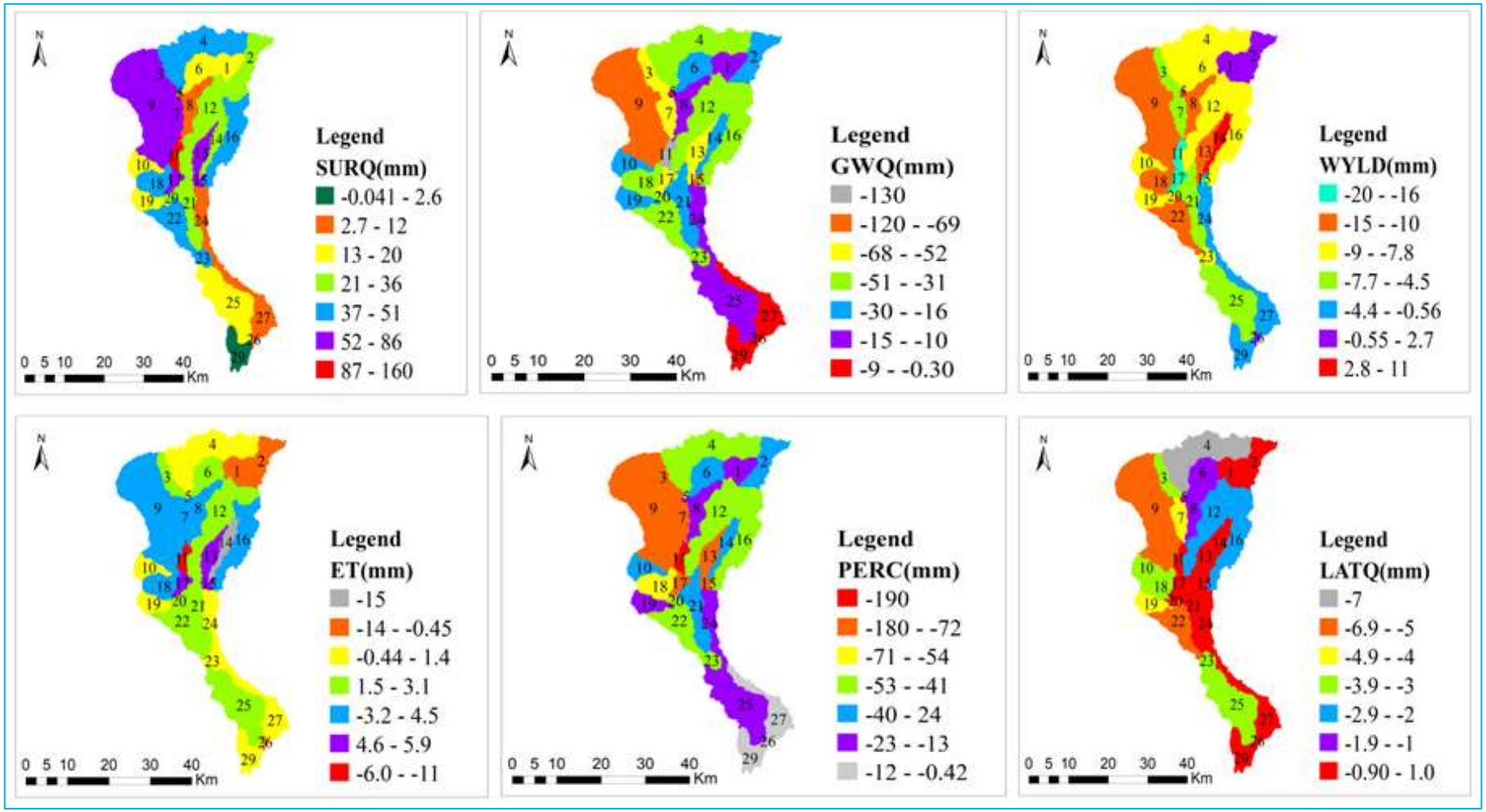

Figure 4-9: Spatial distributions of changes in the hydrological components at the sub-basin level (2020–2050)

Key: SURQ: Surface runoff; WYLD: water yield; GWQ: Groundwater flow; LATQ: Lateral flow; PERC: percolation; ET: Evapotranspiration.

4.7. Evaluation of Stream Flow Change due to LULC Changes

Changes in stream flows due to historical LULC change were evaluated using 1990, 2005 and 2020 LULC maps with the baseline map of 1990. Similarly, predicted stream flow has been assessed using the LULC map of 2020, 2035 and 2050 with the baseline map of 2020.

Table 4-17: Seasonal stream flows from 1990-2020 and 2035-2050

Stream Flow(m^3/s)	Historical seasonal stream flow			Predicted seasonal stream flow	
	1990	2005	2020	2035	2050
Average Annual	854.33	884.96	907.21	963.41	1022.41
Average Wet Season	646.72	682.55	712.79	772.96	841.33
Average Dry Season	207.61	202.41	194.43	190.45	181.08

Table 4-18: Relative change of historical and predicted seasonal stream flow

Stream Flow(m^3/s)	Historical relative change (%)			Predicted relative change (%)		
	1990-2005	2005-2020	2020-1990	2020-2035	2035-2050	2020-2050
Average Annual	+3.58	+2.51	+6.18	+6.19	+6.12	+12.69
Average Wet Season	+5.54	+4.41	+10.21	+8.44	+6.12	+19.67
Average Dry Season	-2.50	-3.94	-6.34	-2.04	-4.91	-6.86

There were significant changes in seasonal stream flow as a result of changes in LULCs in Welmel River (Table 4.17 and 4.18). In the study area, the annual average stream flow for the historical LULC increased with a relative change of 6.18% between the years 1990 to 2020. This is might be due to the change in LULC, especially increasing in agriculture/settlement and reduction in forest areas. In agreement with this result, in Dijo watershed, central rift valley Ethiopia (Ashenafi and Mihret, 2021) from 1985 to 2018; in Shaya River (Mesfin *et al*., 2021) from 1987 to 2015; in Wabe Watershed, Omo-Gibe Basin, Ethiopia (Yonas *et al*., 2020) from 1988 to 2018 and in Gilgel Abay Watershed (Tesfa and Bogale, 2015) from 1986-2011 reported that the stream flow increased due to the contribution of the LULC change.

In the same way, the annual average wet stream flow increased between 1990 and 2020 with a relative change of 10.21%. On contrary, the annual average dry stream flow from 1990 to 2020 decreased with a relative change of 6.34% in responses to LULC change occurred in the Welmel watershed. A similar trend result was found in different parts of the watershed in Ethiopia. For instance, Damtew *et al.* (2015) in Ketar watershed Ziway-Shala basin between 1997 and 2010; Mesfin *et al.* (2021) in Shaya River between 1987 and 2015; Anmut *et al.* (2019), in Chemoga Catchment, Abay Basin between 1994 and 2013, argued that stream flow during dry season decreased, while during wet season increased due to LULC change. In the coming 31 years from 2020 to 2050, the average wet stream flow will increase with a relative change of 19.67%, while the average dry stream flow is expected to decrease with a relative change of 6.86%. In the future from 2020 to 2050, the annual average stream flow in the study area is expected to increase with a relative change of 12.69% in the Welmel watershed.

5. SUMMARY AND CONCLUSION

5.1. Summary

This study was mainly focused on evaluating the hydrological responses to historical (1990-2020) and Predicted (2020-2050) LULC changes at basin and sub-basin levels of Welmel River watershed. The LULC change classification was performed on ERDAS Imagine 2014 by maximum likelihood supervised classification algorism and CA-Markov chain model was used to predict the future LULC change of the study area for the 2050 time period. Arc SWAT model was used for simulation and analysis of the hydrological responses to LULC changes. SUFI-2 of SWAT-CUP 2019 version 5.2.1 tool was employed for the identification of sensitive hydrological parameters of the SWAT model affecting the surface runoff, lateral flow, groundwater flow and evapotranspiration in the study area.

The major LULC of the study area were forestland, woodland, scrubland/bushland, grassland/rangeland, and agriculture/settlement. Agriculture/settlement land showed a consistently increasing trend from 85.09km^2 to 290.64km^2 with a rate of change of 6.85km^2/year. However, forest and scrubland/bushland showed a decreasing trend throughout the study period between 1990 and 2020. Forest land declined from 965.13km^2 to 690.48km^2 with a rate of change of 9.16km^2/yea and scrubland/bushland from 113.49km^2 to 82.75km^2 with a rate of change of 1.02km^2/year. The LULC change trend analysis of this study showed that, between 1990 and 2020, 124.17km^2 of forestland, 28.0km^2 of grassland/rangeland, 0.87km^2 of scrubland/bushland and 69.03km^2 of woodland converted into agriculture/settlement. For the whole study of the historical period (1990-2020), 124.17km^2, 65.65km^2, 110.27km^2, 0.08 km^2 of forest land were converted to agriculture/settlement, grassland/rangeland, woodland and scrubland/bushland

respectively. Similarly, between 2020 and 2050, agriculture/settlement will increase from 290.64Km^2 to 492.51Km^2 with a rate of change of 6.73Km^2/year, while forest and scrubland/bushland areas are expected to decline from 690.48Km^2 to 427.01Km^2 and 82.75km^2 to 55.48km^2 with a rate of change of 8.78Km^2/year and 0.91km^2/year, respectively. The result of the predicted LULC map from 2020 to 2050 with the baseline LULC map of 2020 indicated that, 113.13km^2 of forest land will convert to agriculture/settlement, 44.19km^2 to grassland/rangeland and 96.74km^2 to woodland. On the other hand, 41.60km^2 of woodland, 4.25km^2 of scrubland/bushland and 33.32km^2 of grassland/rangeland is expected to convert to agriculture/settlement.

During Model performance evaluation, the model showed good performance R^2 of 0.78, NSE of 0.74 and PBIAS of 12.8 for calibration while for validation R^2 of 0.81, NSE of 0.78 and PBIAS 11.4 were obtained. Due to LULC change in the Welmel River watershed, Surface runoff increased by relative change of 25.32% while lateral flow, groundwater flow, water yield, evapotranspiration and percolation declined by 19.91%, 17.17%, 2.38%, 0.36% and 17.17% respectively from 1990 to 2020. Similarly, the predicted LULC map from 2020 to 2050 is expected to show an increase in surface runoff and decreasing trends in other hydrological components. The results of this study indicated that sub-basins that were in increasing in agriculture/settlement LULC types cause increasing in surface runoff and decreasing in water yield, groundwater flow, percolation, evapotranspiration and lateral flow. The result indicated that, the average annual stream flow increased with a relative change of 6.18% from 1990 to 2020 and is expected to increase with a relative change of 12.69% by 2050. In overall, the average wet annual and dry annual stream flow for historical LULC increased and decreased respectively. Also, the

average wet and dry annual stream flow is expected to show increase and decline trends by 2050 respectively.

5.2. Conclusion

It can be concluded that the Welmel watershed has undergone significant LULC change in the last 31 years and it is expected to continue into the near future of the coming 31 years. In particular, it can be concluded that the expansion of agriculture/settlement areas at the expense of forestland, woodland, grassland/rangeland and scrubland/bush land affected the hydrologic system of the Watershed. Moreover, the result of this study revealed that the hydrological response to LULC changes is more obvious at the sub-basin level than the basin level. For instance, sub-basins characterized by increasing in agriculture/settlement LULC types cause an increase in surface runoff and decrease in water yield, groundwater flow, percolation, evapotranspiration and lateral flow. Generally, the stream flow of the welmel watershed showed an increase in annual average during wet and decreasing during the dry season throughout the study period for historical and predicted LULC changes.

5.3. Recommendations

Based on the finding of this study, the following basic recommendations are drawn:

- During validation, the CA-Markov model was showed a high level of agreement which was reliable for further prediction. Nevertheless, it is important to compare with other LULC models to integrate with hydrological models to analyze the hydrological responses to future LULC changes to make better choices for land and water resource planning and management in the future.

- This study revealed expansion of agriculture/settlement at the expense of forest and woodlands including sloppy areas in the study area. Therefore, the Woredas in and around the watershed, the regional government and the Bale Mountains National Park should integrate to design and implement a proper strategy for protecting and managing the existing forest and woodlands in addition to rehabilitating the degraded areas to maintain the hydrological balance of the watershed.

- The result of this study at the sub-basins level indicated that grassland/rangeland has a positive relation with groundwater and negative with surface runoff. Hence, it is recommended to integrate grassland/range with cultivated land and conserve it.

- This study addressed only the impact of Land Use/Land Cover changes on the hydrology of the watershed. However, climate change and variability may affect the hydrology of the watershed. Thus, further research needs to be done on hydrological responses to historical and future climate change and variability, and driving forces behind LULC changes of Welmel River Watershed.

6. REFERENCES

Abate Shiferaw and K.L.Singh. 2011. Evaluating the Land Use and Land Cover Dynamics in Borena Woreda of South Wollo Highlands, Ethiopia. Journal of Sustainable Development in Africa 13 (1): 87-107.

Abbaspour, K.C., S.A. Vaghefi and R. Srinivasan. 2017. A guideline for successful calibration and uncertainty analysis for soil and water assessment: a review of papers from the 2016 international SWAT conference. Water, 10 (1), 6. doi:10.3390/w10010006.

Abdulkerim Bedewi and A.K. Sarma. 2016. Evaluation of the Arc SWAT model in simulating catchment hydrology: in Weyib River basin, bale mountainous area of southeastern Ethiopia. Int. J, Inov. Emrg. Res. Eng, 3(2), pp.3-11.

Abdulrahman, A.I. and S.A. Ameen, 2020. Predicting Land use and land cover spatiotemporal changes utilizing CA-Markov model in Duhok district between 1999 and 2033. *Academic Journal of Nawroz University*, *9*(4), pp.71-80.

Achenafi Teklay, Dileb Yihun, Shimelis Gebriye, Demissie Solomon, Asfaw Dereje .2019. Evaluation of static and dynamic land use data for watershed hydrologic process simulation: a case study in Gummara watershed, Ethiopia. Catena, 172, pp.65-75.

Adane Mezgebu and Getachew Workineh. 2017. Changes and drivers of afro-alpine forest ecosystem: future trajectories and management strategies in Bale eco-region, Ethiopia. Ecological Processes, 6(1), pp.1-13.

Adenew Taffa, J. van Vliet and P.H. Verburg. 2015. Land-use and land-cover changes in the Central Rift Valley of Ethiopia: Assessment of perception and adaptation of stakeholders. Applied Geography, 65, pp.28-37

Adilah, A.N. and H. Hannani. 2021, February. Comparison of Methods to Estimate Missing Rainfall Data for Short Term Period at UMP Gambang. In IOP Conference Series: Earth and Environmental Science (Vol. 682, No. 1, p. 012027). IOP Publishing.

Alam, A., M.S. Bhat and M. Maheen. 2019. Using Landsat satellite data for assessing the land use and land cover change in Kashmir valley. Geo Journal, 85(6), pp.1529-1543.

Alemayehu Muluneh. 2010. Synthesis of Research on Land Use and Land Cover Dynamics in the Ethiopian Highlands. UNU-Land Restoration Training Programme, Keldnaholt, 112 Reykjavik, Iceland.

Alemayehu Shawul, Chakma, S., and Melesse Assefa. 2019. The response of water balance components to land cover changes based on hydrologic modeling and partial least squares regression (PLSR) analysis in the Upper Awash basin. Journal of Hydrology: Regional Studies, 26, 100640.

Alemayehu Shawul, Tena Alamirew, Melesse Assefa and Chakma, S. 2016. Climate change impact on the hydrology of Weyib River watershed, Bale mountainous area, Ethiopia. In Landscape dynamics, soils and hydrological processes in varied climates (pp. 587-613). Springer, Cham.

Alemayehu Shawul. 2014. Climate Change Impact on the Hydrology of Weyib River Watershed, Bale Mountainous Area, Ethiopia: In book: Landscape Dynamics, Soils and Hydrological Processes in Varied Climates, Chapter: 27, Publisher: Springer International Publishing, Editors: Assefa M. Melesse, Wossenu Abtew, pp.587-613: DOI: 10.1007/978-3-319-18787-7_27

Alemtsehay Jima. 2010. Determinating factors for a successful establishment of participatory forest management: a comparative study of Goba and Dello districts, Ethiopia (Master's thesis, Universiteteti Agder, University of Agder).

Anaba, L.A., N. Banadda, N. Kiggundu, J. Wanyama, B. Engel and D. Moriasi. 2017. Application of SWAT to Assess the Effects of Land Use Change in the Murchison Bay Catchment in Uganda. Computational Water, Energy, and Environmental Engineering, 6, 24-40.

Anmut Enawgaw, Tesfu Abebe and Negash Wagesho. 2019. Evaluation of stream flow under land use land cover change: A case study of Chemoga Catchment, Abay Basin, Ethiopia. African Journal of Environmental Science and Technology, 14(1), pp.26-39.

Araya, Y.H. and P. Cabral. 2010. Analysis and modeling of urban land cover change in Setúbal and Sesimbra, Portugal. *Remote Sensing*, *2*(6), pp.1549-1563.

Ariti, A.T., J. van Vliet and P.H., Verburg. 2015. Land-use and land-cover changes in the Central Rift Valley of Ethiopia: Assessment of perception and adaptation of stakeholders. *Applied Geography*, *65*, pp.28-37.

Arnold, J. G., P. M. Allen and G. Bernhardt. 1993. A comprehensive surface ground water flow model. Journal of Hydrology, 142: 47-69.

Arnold, J., J. Kiniry, R. Srinivasan, J.Williams, E. Haney and S. Neitsch. 2012. Soil and Water Assessment Tool. Input/Output. Documentation Version 2012.Texas Water Resources Institute TR-439.654 pp.

Arnold, J.G. 2014. The potential for agricultural land use change to reduce flood risk in a large watershed. Hydrological processes, 28(8), pp.3314-3325.

Arnold, J.G., D.N. Moriasi, P.W. Gassman, K.C. Abbaspour, M.J. White, R., Srinivasan, C. Santhi, R.D. Harmel, A. Van Griensven, M.W. Van Liew and N. Kannan. 2012.

SWAT: Model use, calibration, and validation. Transactions of the ASABE, 55(4), pp.1491-1508.

Arnold, J.G., R. Srinivasan, R.R. Muttiah, J.R. Williams. 1998. Large Area Hydrologic Modeling and As-sessment Part I: Model Development. Journal of the American Water Resources Association, 34(1): 73-89.

Ashenafi Nigusie and Mihret Dananto. 2021. Impact of land use/land cover change on hydrologic processes in Dijo watershed, central rift valley, Ethiopia. International Journal of Water Resources and Environmental Engineering, 13(1), pp.37-48.

Asimamaw Nigusie. 2013. Assessing the impacts of land use and land cover change on hydrology of watershed: A case study on GILGEL-ABAY watershed, Lake Tana basin Ethiopia. MSC thesis, Consortium Universities, Washington.

Asimamaw Nigusie. 2020. Impact of Land Use/Land Cover Change on Reservoir Sedimentation: The Case of Ribb Dam Reservoir, Lake Tana Sub Basin, Ethiopia.

Asmamaw Adamu. 2013. Assessing the impacts of land use and land cover change on hydrology of watershed: a case study on Gigel-Abbay Watershed, Lake Tana Basin, Ethiopia.

Atasoy, M., C. Biyik, H. Ayaz, F. Karsli, O. Demir, E. Z. Baskent. 2006. Monitoring land use changes and determinating the suitability of land for different uses with digital Photogrammetry, Remote Sensing and Photogrammetry, Cairo, Egypt.

Baker, T.J. and S.N. Miller. 2013. Using the soil and water assessment tool (SWAT) to assess land use impact on water resources in an East African watershed. Journal of Hydrology, 486, 100–111. doi:10.1016/j. jhydrol.2013.01.041

Bauwe, A., P. Kahle and B. Lennartz. 2016. Hydrologic evaluation of the curve number and Green and Ampt infiltration methods by applying Hooghoudt and Kirkham tile drain equations using SWAT. Journal of Hydrology, 537, pp.311-321.

Behera, M. D., S. N. Borate, S. N. Panda, P. R. Behera and P. S. Roy. 2012. Modelling and analyzing the watershed dynamics using Cellular Automata (CA)-Markov model - A geo-information-based approach. Journal of Earth System Science, 121(4), 1011–1024.https://doi.org/10.1007/s12040-012-0207-5

Belward, A.S. and J.O. Skøien. 2015. Who launched what, when and why; trends in global land-cover observation capacity from civilian earth observation satellites. ISPRS Journal of Photogrammetry and Remote Sensing, 103, pp.115-128.

Berhan Gessesse, Woldeamlak Bewket and A. Bräuning, 2015. Model based characterization and monitoring of runoff and soil erosion in response to land use/land cover changes in the Modjo watershed, Ethiopia. Land Degradation & Development, 26 (7), 711–724. https://doi.org/10.1002/ldr.

Binyam Alemu, Efrem Garedew, Zewdu Eshetu, Habtemariam Kassa. 2015. Land Use and Land Cover Changes and Associated Driving Forces in North Western Lowlands of Ethiopia. International Research Journal of Agricultural Science and Soil Science 5(1):28-44.

Birhan Asmame and Assefa Abegaz. 2018. Estimating soil loss for sustainable land management planning at the Gelana sub-watershed, northern highlands of Ethiopia, International Journal of River Basin Management, DOI: 10.1080/15715124.2017.1351978

Briassoulis, H. 2011. Factors Influencing Land Use Land Cover Change. Journal of Land Use, Land Cover and Soil Science.

Caldas, M.M., D. Goodin, S. Sherwood, J.M. Campos Krauer and S.M. Wisely. 2015. Land-cover change in the Paraguayan Chaco: 2000–2011. Journal of Land Use Science, 10(1), pp.1-18.

Caldera, H.P.G.M., V.R.P.C. Piyathisse and K.D.W., Nandalal. 2016. A comparison of methods of estimating missing daily rainfall data. Engineer: Journal of the Institution of Engineers, Sri Lanka, 49(4).

Caletka, M., M. Šulc, P. Karásek and P. Fučík. 2020. Improvement of SCS-CN initial abstraction coefficient in the Czech Republic: a study of five catchments. Water, 12(7), p.1964.

Camara, M., N.R.B. Jamil, A.F.B. Abdullah and R.B. Hashim, 2020. Integrating cellular automata Markov model to simulate future land use change of a tropical basin. *Global Journal of Environmental Science and Management*, *6*(3), pp.403-414.

Chow, V. T., D. R. Maidment, and L. W. Mays. 1988. Applied Hydrology, McGraw-Hill Book Company, Singpore.

Cunderlik, J. 2003. Hydrological model selection for CFCAS project, Assessment of water resource risk and vulnerability to change in climate condition, University of Western Ontario.

Daggupati, P., N. Pai,, S. Ale, K.R. Douglas-Mankin, , R.W. Zeckoski, J. Jeong, P.B. Parajuli, D. Saraswat and M.A. Youssef. 2015. A recommended calibration and validation strategy for hydrologic and water quality models. Transactions of the ASABE, 58(6), pp.1705-1719.

Damtew Fufa, Y. Abbulu and G. V. R. Srinivasa Rao. 2015. Hydrological Impacts due to Land-Use and Land-Cover Changes of Ketar Watershed, Lake Ziway Catchment, Ethiopia. International Journal of Civil Engineering and Technology, 6(10), 2015, pp.3645.http://www.iaeme.com/.

Dayamba, S.D., H. Djoudi, M. Zida, L. Sawadogo and L. Verchot. 2016. Biodiversity and carbon stocks in different land use types in the Sudanian Zone of Burkina Faso, West Africa. Agriculture, Ecosystems & Environment, 216, pp.61-72.

Demel Teketay. 2001.Vegetation Types and Forest Fire Management in Ethiopia", Addis Ababa, Ethiopia

Dereje Dargie. 2010. Impact of land use change on reservoir sedimentation (case study of Karadobi). Msc thesis, Addis Ababa University, Ethiopia.

Dhami, B. S. and A. Pandey. 2013. Comparative Review of Recently Developed Hydrologic Models. Journal of Indian Water Resources Society, 33(3), 34–42.

Dias, L.C.P., M.N. Macedo, M.H. Costa, M.T. Coe, C. Neill. 2015. Effects of land cover change on evapotranspiration and stream flow of small catchments in the Upper Xingu River Basin, Central Brazil. J. Hydrol. 4, 108–122.

Dile, Y.T. and R. Srinivasan. 2014. Evaluation of CFSR climate data for hydrologic prediction in data-scarce watersheds: an application in the Blue Nile River Basin. JAWRA Journal of the American Water Resources Association, 50(5), pp.1226-1241.

Ebrahim Esa and Mohamed Assen. 2017. Land use/cover dynamics and its drivers in Gelda catchment, Lake Tana watershed, Ethiopia. Environ. Syst. Res. 6 (4), 1–13.

Efrem Garedew. 2010. Land-use and land-cover dynamics and rural livelihood perspectives, in the semi-arid areas of Central Rift Valley of Ethiopia (Vol. 2010, No. 2010: 7).

Eleni Yeshaneh, Wagner, W., Exner-Kittridge, M., Dagnachew Legesse and Blöschl, G. 2013. Identifying land use/cover dynamics in the Koga catchment, Ethiopia, from multi-scale data, and implications for environmental change. ISPRS International Journal of Geo-Information, 2(2), pp.302-323.

Eskider Gidey, Dikinya, O., Sebego, R.E. Segosebe and Amanuel Zenebe. 2017. Cellular automata and Markov Chain (CA-Markov) model-based predictions of future land use and land cover scenarios (2015–2033) in Raya, northern Ethiopia. Modeling Earth Systems and Environment, 3(4), pp.1245-1262.

Eyayu Molla, Heluf Gebrekidan, Tekalign Mamo and Mohammed Assen. 2010. Patterns of Land Use/Cover Dynamics in the Mountain Landscape of Tara Gedam and Adjacent Agro-Ecosystem, Northwest Ethiopia. J. Sci. 33(2): 75-88.

Farley, K.A., E.G. Jobbágy and R.B. Jackson. 2005. Effects of afforestation on water yield: a global synthesis with implications for policy. Global change biology, 11(10), pp.1565-1576.

Farm-Africa-SOS Sahel Ethiopia. 2010. Annual Accomplishment Report for 2009. Submitted to Charities and Societies Agency (CSA), Addis Ababa, Ethiopia.

Fasika Alemayehu, Motuma Tolera and Gizaw Tesfaye. 2018. Land use land cover change trend and its drivers in somodo watershed south western, Ethiopia. African Journal of Agricultural Research, 14(2), pp.102-117.

Fisher, J.I. and J.F. Mustard. 2004. High spatial resolution sea surface climatology from Landsat thermal infrared data. Remote Sensing of Environment, 90(3), pp.293-307.

Food and Agriculture Organization of the United Nations. 2010. Global Forest Resources Assessment Main report, FAO Forestry Paper 163, Food and Agriculture Organization of the United Nations, Rome.

Gao, P., Li, P., Zhao, B., Xu, R., Zhao, G., Sun, W. and X. Mu. 2017. Use of double mass curves in hydrologic benefit evaluations. Hydrological Processes, 31(26), pp.4639-4646.

Garg, V., B.R. Nikam, P.K. Thakur, S.P. Aggarwal, P.K. Gupta and S.K. Srivastav. 2019. Human-induced land use land cover change and its impact on hydrology. HydroResearch, 1, pp.48-56.

Gemechu Shale, Amare Bantider and Davide Geneletti. 2021. Dynamics of land use and land cover changes in Huluka watershed of Oromia Regional State, Ethiopia. https://doi.org/10.1186/s40068-021-00218-4.

Ghaffari G, S. Keesstra, J. Ghodousi and H. Ahmadi 2010. SWAT-simu- lated hydrological impact of land-use change in the Zanjanrood Basin, Northwest Iran. Hydrol Process 24(7):892–903. https:// doi.org/10.1002/hyp.7530

Ghoraba, S. 2015. Hydrological modeling of the Simly Dam watershed (Pakistan) using GIS and SWAT model. Alex. Eng. J. 54, 583–594.

Gibbard, S., K. Caldeira, G. Bala, T.J. Phillips. and M. Wickett. 2005. Climate effects of global land cover change. Geophysical Research Letters, 32(23). doi.org/10.1029/2005GL024550

Girma Ayele, Hussein Hayicho and Mersha Alemu. 2019. Land Use Land Cover Change Detection and Deforestation Modeling: In Delomena District of Bale Zone, Ethiopia. Journal of Environmental Protection, 10, 532-561.https://doi.org/10.4236/jep.2019.104031.

Girum Getachew and Tesfa Gebrie. 2018. Application of remote sensing for evaluation of land use change responses on hydrology of Muga Watershed, Abbay River Basin, Ethiopia. J. Earth Sci. Clim. Change, 9(2). DOI: 10.4172/2157-7617.1000493

Guan. D, H. Li, T.Inohae, W.Su, T.Nagaie and K. Hokao. 2011. Modeling urban land use change by the integration of cellular automaton and Markov model. Ecol. Model. 222, 3761–3772.

Gyamfi, C., J.M. Ndambuki , R.W.Salim, 2016. Hydrological responses to land use/cover changes in the Olifants Basin, South Africa. Water 8, 588.

Habtamu Temesgen, Wei Wu, Abiyot Legesse and Eshetu Yirsaw. 2021. Modeling and prediction of effects of land use change in an agroforestry dominated southeastern Rift-Valley escarpment of Ethiopia. Remote Sensing Applications: Society and Environment, 21, p.100469.

Hagos Gebreslassie. 2014. Land use-land covers dynamics of Huluka watershed, Central Rift Valley, Ethiopia. International Soil and Water Conservation Research, 2(4), 25-33.

Hajkowic z, S. 2003. Exploring future land scapes: a conceptual framework for planned change. Land and water. Australia: Canberra, Australia.

Hajkowicz, S. 2009. The evolution of Australia's natural resource management programs: towards improved targeting and evaluation of investments. Land Use Policy, 26(2), pp.471-478.

Hamere Yohannes, Teshome Soromessa, Mekuria Argaw and Ashraf Dewan. 2020. Changes in landscape composition and configuration in the Beressa watershed, Blue Nile basin of Ethiopian Highlands: historical and future exploration. Heliyon, 6(9), p.e04859.

Hamza, I.A. and A. Iyela. 2012. Land use pattern, climate change, and its implication for food security in Ethiopia: A review. Ethiopian Journal of Environmental Studies and Management, 5(1), pp.26-31.http://dx.doi.org/10.4314/ejesm.v5i1.4

Han, E., V. Merwade and G.C. Heathman. 2012. Implementation of surface soil moisture data assimilation with watershed scale distributed hydrological model. Journal of hydrology, 416, pp.98-117.

Harssema Solomon. 2005. GIS based surface runoff modeling and analysis of contributing factors: a case study of Nam Chun watershed, Thailand. ITC.

He, C., Z. Liu, S. Gou, Q. Zhang, J. Zhang and L. Xu. 2019. Detecting global urban expansion over the last three decades using a fully convolutional network. Environmental Research Letters, 14(3), p.034008.

Henok Mekonen, M.K. Goel and S.K. Mishra. 2021. Hydrological responses to human-induced land use/land cover changes in the Gidabo River basin, Ethiopia. Hydrological Sciences Journal, 66(4), pp.640-655.

Hindall, S. 1991. Temporal trends in fluvial-sediment discharge in Ohio, 1950–1987. Journal of Soil and Water Conservation, 46, 311–313.

Hiywot Menker. 2014. Drivers of Land Use Change and Forest Conservation Under Uncertain Markets for Forest Ecosystem Services in Ethiopia. Doctoral thesis, University of Pretoria, Pretoria.

Hooke, R.L., J.F. Martín Duque and J.D. Pedraza Gilsanz. 2012. Land transformation by humans: a review. GSA today, 22(12), pp.4-10.

Hua, A.K. 2017. Application of Ca-Markov model and land use/land cover changes in Malacca River Watershed, Malaysia. Applied Ecology and Environmental Research, 15(4), pp.605-622.)

Hudson. 1995. Bridging the Gap between Communities and GIS Participatory 3D Modelling, India.

Hurni, H. Solomon Abate, Amare Bantider, Berhanu Debele, Eva Ludi, Brigitte Portner, Birru Yitaferu, and Gete Zeleke. 2010. Land degradation and sustainable land management in the highlands of Ethiopia.187-207.

Hyandye, C. and L. W. Martz, 2017. A Markovian and cellular automata land-use change predictive model of the Usangu Catchment. International Journal of Remote Sensing, 38(1), 64–81. https://doi.org/10.1080/01431161.2016.1259675.

Institute of Biodiversity Conservation. 2005. National Biodiversity Strategy and Action Plan", Addis Ababa, Ethiopia.

Intergovernmental Panel on Climate Change (IPCC). 2007. Climate change synthesis report. Contribution of Working Groups I, II and III to the fourth assessment report of the Intergovernmental Panel on Climate Change. Pachauri RK and Reisinge, A (Eds.). Geneva, Switzerland, 104pp.

Karki, R., P. Srivastava and T.L.Veith. 2020. Application of the Soil and Water Assessment Tool (SWAT) at field scale: categorizing methods and review of applications. Transactions of the ASABE, 63(2), pp.513-522.

Kassa Tadele. 2009. Watershed hydrological responses to changes in land use and land cover and management practices at Hare watershed. Ethiopia: PhD dissertation. Siegen University.

Kaul, H.A. and I. Sopan. 2012. Land use land cover classification and change detection using high resolution temporal satellite data. Journal of Environment, 1(4), pp.146-152.

Keshtkar, H. and W. Voigt. 2016. A spatiotemporal analysis of landscape change using an integrated Markov chain and cellular automata models. Modeling Earth Systems and Environment, 2(1), pp.1-13.

Kiptala, J.K., Y. Mohamed, M.L. Mul and P. Van Der Zaag. 2013. Mapping evapotranspiration trends using MODIS and SEBAL model in a data scarce and heterogeneous landscape in eastern Africa. Water Resour. Res. 49, 8495–8510.

Kotei, R., E, Ofori., N., Kyei-Baffour and W.A. Agyare. 2013. Landuse changes and their impacts on the hydrology of the Sumampa catchment in Mampong-Ashanti, Ghana.

Kumar N, SK. Singh, PK. Srivastava and B. Narsimlu. 2017. SWAT model calibration and uncertainty analysis for stream flow prediction of the Tons river basin, India, using sequential uncertainty fitting (SUFI-2) algorithm. Model Earth System Environ. https://doi. org/10.1007/s40808-017-0306.

Kumar, S., N. Radhakrishnan and S. Mathew, 2014. Land use change modelling using a Markov model and remote sensing. *Geomatics, Natural Hazards and Risk*, *5*(2), pp.145-156.

Kushwaha, A. and M.K. Jain. 2013. Hydrological simulation in a forest dominated watershed in Himalayan region using SWAT model. Water resources management, 27(8), pp.3005-3023.

Lambin, E.F. and P. Meyfroidt. 2011. Global land use change, economic globalization, and the looming land scarcity. Proceedings of the National Academy of Sciences, 108(9), pp.3465-3472.

Lambin, E.F., Geist, H. and Rindfuss, R.R. 2006. Introduction: local processes with global impacts. In Land-use and land-cover change (pp. 1-8). Springer, Berlin, Heidelberg.

Leitinger, G.; R. Ruggenthaler, A. Hammerle, S. Lavorel, U. Schirpke, J.-C. Clement, P. Lamarque, N. Obojes and U. Tappeine. 2015. Impact of droughts on water provision in managed alpine grasslands in two climatically different regions of the Alps. Ecohydrology 2015, 8, 1600–1613.

Lewoye Tsegaye. 2014. Analysis of Land Use and Land Cover Change and Its Drivers Using GIS and Remote Sensing: The Case of West Guna Mountain, Ethiopia. International Journal of Remote Sensing and GIS 3(3): 53-63

Liu J, C. Zhang, L. Kou and Q. Zhou. 2017. Effects of Climate and Land Use Changes on Water Resources in the Taoer River. Advances in Meteorology DOI: 10.1155/2017/1031854.

Manandhar R. 2009. Improving the accuracy of land use and land cover classification of Landsat data using post classification enhancement. Remote Sensing.;1:330-344.

Mango, L.M., Melesse Assefa, M.E. McClain, D. Gann and Shimelis Gebriye. 2011. Land use and climate change impacts on the hydrology of the upper Mara River Basin, Kenya: results of a modeling study to support better resource management. Hydrology and Earth System Sciences, 15(7), pp.2245-2258.

Marhaento, Hero, J. Martijn, Booij and A.Y. Hoekstra. 2017. "Attribution of changes in stream flow to land use change and climate change in a mesoscale tropical catchment in Java, Indonesia." Hydrology research 48, no. 4 (2017): 1143-1155.

Marland, G., R.A. Pielke Sr, M. Apps, R. Avissar, R.A. Betts, K.J. Davis, P.C. Frumhoff, S.T. Jackson, L.A. Joyce, P. Kauppi and J. Katzenberger. 2003. The climatic impacts of land surface change and carbon management, and the implications for climate-change mitigation policy. Climate policy, 3(2), pp.149-157.

Maviza. A and F.Ahmed. 2020. Analysis of past and future multi-temporal land use and land cover changes in the semi-arid Upper- Mzingwane sub-catchment in the Matabeleland south province of Zimbabwe. Int. J. Remote Sens. 41, 5206–5227.

McCuen, R.H. 1998. Hydrologic Analysis and Design. Upper Saddle River,N.J.: Prentice Hall. Setegn

Megersa Kebede, Tamene Adugna and J. Tränckner. 2021. Hydrological Responses of Watershed to Historical and Future Land Use Land Cover Change Dynamics of Nashe Watershed, Ethiopia. Water 2021, 13, 2372. https://doi.org/10.3390/w13172372.

Mengistie Kindu, T. Schneider, Demel Teketay and T. Knoke. 2013. Land use/land cover change analysis using object-based classification approach in Munessa-Shashemene landscape of the Ethiopian highlands. Remote Sensing, 5, pp.2411-2435.

Mesfin Reta, Samuel Dagalo and S.M. Pingale. 2021. Modeling the rainfall-runoff using MIKE 11 NAM model in Shaya catchment, Ethiopia. Modeling Earth Systems and Environment, pp.1-7. doi.org/10.1007/s12517-021-06447-2.

Messay Mulugeta. 2011. Land use/land cover Dynamics in Nonno District, Central Ethiopia. Journal of Sustainable Development in Africa 13(1): 123-141.

Meyer, W. B. 1995. Past and Present Land-Use and Land –Cover in the U.S.A. Consequences PP. 24-33.

Miller, S.N., W.G. Kepper, M.H. Mehaffey, M. Hemandez, R.C. Miller, D.C. Goodrich, K.K. Dovonald, D.T. Heggem, and W.P. Miller. 2002. Integrating landscape assessment and hydrological modelling for land cover change analysis. J. of Amer. Water Res. Assoc. 38(4):915-929.

Ministry of Water Resources. 2007. Genale Dawa River Basin Integrated Resources Development Master Plan, Vo. I-IV (21 volumes)", Addis Ababa, Ethiopia

Mishra, V.N. and P.K. Rai. 2016. A remote sensing aided multi-layer perceptron-Markov chain analysis for land use and land cover change prediction in Patna district (Bihar), India. Arabian Journal of Geosciences, 9(4), p.249.

Mishra, V.N., Rai, P.K. and K.Mohan, 2014. Prediction of land use changes based on land change modeler (LCM) using remote sensing: a case study of Muzaffarpur (Bihar), India. *Journal of the Geographical Institute" Jovan Cvijic", SASA*, *64*(1), pp.111-127.

Molina-navarro E, D. Trolle, S. Martínez-pérez, A. Sastre-merlín and E. Jeppesen. 2014. Hydrological and water quality impact assessment of a Mediterranean limno-reservoir under climate change and land use management scenarios. J Hydrol 509:354–366. https://doi.org/10.1016/j.jhydrol.2013.11.053.

Moriasi, D.N., B.N.Wilson, K.R. Douglas-Mankin, J.G. Arnold and P.H. Gowda. 2012. Hydrologic and water quality models: Use, calibration, and validation. Transactions of the ASABE, 55(4), pp.1241-1247.

Moriasi, D.N., M.W. Gitau, N. Pai and P. Daggupati. 2015. Hydrologic and water quality models: Performance measures and evaluation criteria. Transactions of the ASABE, 58(6), pp.1763-1785.

Mu, X.M., X.Q. Zhang, P. Gao and F. Wang. 2010. Theory of double mass curves and its applications in hydrology and meteorology. Journal of China Hydrology, 30(4), pp.47-51.

Mulatu Liyew, Atsushi Tsunekawa, Nigussie Haregeweyn, Derege Tsegaye, Enyew Adgo, Mitsuru Tsubo, Tsugiyuki Masunaga, Ayele Almaw, Dagnenet Sultan and Mesenbet Yibeltala. 2019. Hydrological responses to land use/land cover change and climate variability in contrasting agro-ecological environments of the Upper Blue Nile basin, Ethiopia. Science of the Total Environment, 689, pp.347-365. doi:10.1016/j.scitotenv.2019.06.338.

Mulugeta Lemeneh and Tadesse Woldemariam. 2010. Review of Forest, Woodland and Bushland Resources. In Forum for Environment Addis Ababa, Ethiopia.

Nath, B., Z. Wang, Y.Ge, K. Islam, R. P. Singh and Z. Niu. 2020. Land use and land cover change modeling and future potential landscape risk assessment using Markov-CA model and analytical hierarchy process. ISPRS International Journal of Geo-Information, 9(2), p.134.

Nauman, S. and Z. Zulkafli. 2021. Auto-calibration and uncertainty analysis of SWAT Model for Haro River Watershed using Sequential Uncertainty Fitting (SUFI-2) algorithm. Hydrology and water resources.

Neitsch SL, JG. Arnold JR. Kiniry, JR. Williams. 2005. Soil and Water Assessment Tool, Theoretical Documentation: Version 2005. Temple, TX.USDA Agricultural Research Service and Texas A & M Black land Research Centre.

Neitsch, S., J. Arnold, J. Kiniry and J. Williams. 2011. Soil and Water Assessment Tool Theoretical Documentation Version 2009 Texas Water Resources Institute Technical Report No. 406.618 pp.

Ngo, T.S., D.B. Nguyen and P.S. Rajendra. 2015. Effect of land use change on runoff and sediment yield in Da River Basin of Hoa Binh province, Northwest Vietnam. Journal of Mountain Science, 12(4), pp.1051-1064.

Nigussie Haregeweyn, A.Tsunekawa, J. Poesen, M. Tsubo, Derege Tsegaye, Ayele Almaw, J. Nyssen and E. Adgo. 2017. Comprehensive assessment of soil erosion risk for better land use planning in river basins: Case study of the Upper Blue Nile River. *Science of the Total Environment*, *574*, pp.95-108.

Nigussie Haregeweyn, Samuel Tesfaye, Atsushi Tsunekawa, Mitsuru Tsubo, Derege Tsegaye Meshesha, Enyew Adgo and Asres Elias. 2014. Dynamics of land use and land cover and its effects on hydrologic responses: case study of the Gilgel Tekeze catchment in the highlands of Northern Ethiopia. Environmental monitoring and assessment, 187(1), pp.1-14.

Nyssen, J., A.Frankl, M. Haile, H. Hurni, K. Descheemaeker, D. Crummey, A. Ritler, B. Portner, B. Nievergelt, J. Moeyersons and N. Munro. 2014. Environmental conditions and human drivers for changes to north Ethiopian mountain landscapes over 145 years. Science of the total environment, 485, pp.164-179.

Omar, N.Q., M.S.S. Ahamad, W.M.A.W. Hussin, N. Samat and S.Z.B. Ahmad. 2014. Markov CA, multi regression, and multiple decisions making for modeling historical changes in Kirkuk City, Iraq. Journal of the Indian Society of Remote Sensing, 42(1), pp.165-178.

Orkodjo, T.P. 2014. Impact of Land Use/Land Cover Change on Catchment Hydrology (A case Study of Awassa Catchment). Arba Minch University.

Parsa, V.A., A. Yavari and A. Nejadi, 2016. Spatio-temporal analysis of land use/land cover pattern changes in Arasbaran Biosphere Reserve: Iran. *Modeling earth systems and environment*, *2*(4), pp.1-13.

Rahman K, AG. da Silva, EM. Tejeda, A. Gobiet, M. Beniston and A. Lehmann. 2015. An independent and combined effect analysis of land use and climate change in the upper Rhone River watershed, Switzerland. Applied Geography 63 : 264–272 DOI: 10.1016/j.apgeog.2015.06.021.

Razak, M.F.A. and M. Firdaus. 2013. Evaluation of Land Cover Changes in Sultan Azlan Shah Dam Catchment Using Remote Sensing Techniques (Doctoral dissertation, Universiti Sains Malaysia).

Reddy and Gebreselassie. 2011. Analyses of land cover changes and major driving forces assessment in middle highland Tigray,Ethiopia: the case of areas around Laelay-Koraro. Journal of biodiversity and Environmental sciences, 22-29.

Rientjes TH, AT. Haile, E. Kebede, CM. Mannaerts, E. Habib and TS. Steenhuis. 2011. Changes in land cover, rainfall and stream flow in Upper Gilgel Abbay catchment, Blue Nile basin-Ethiopia. Hydrol Earth Syst Sci 15:1979–1989.

Rutledge, A. T. 1985. Use of double mass curves to determine drawdown in a long-term aquifer test in North Central Volusia County.Florida HSSS. Water Resources Investigations Report, 84–4309.

Saah, D., G. Johnson, B. Ashmall, G. Tondapu, K. Tenneson, M. Patterson, A. Poortinga K. Markert, N.H. Quyen, K. San Aung and L. Schlichting. 2019. Collect Earth: An online tool for systematic reference data collection in land cover and use applications. Environmental Modelling & Software, 118, pp.166-171.

Sang, L., C. Zhang, J.Yang, D.Zhu and W.Yun, 2011. Simulation of land use spatial pattern of towns and villages based on CA–Markov model. *Mathematical and Computer Modelling*, *54*(3-4), pp.938-943.

Savenije, H.H., A.Y. Hoekstra and P.Van der Zaag. 2014. Evolving water science in the Schilling, K.E., Gassman, P.W., Kling, C.L., Campbell, T., Jha, M.K., Wolter, C.F.

Schilling, K.E., P.W. Gassman, C.L, Kling, T. Campbell, M.K. Jha, C.F. Wolter and J.G. Arnold. 2014. The potential for agricultural land use change to reduce flood risk in a large watershed. Hydrological processes, 28(8), pp.3314-3325. doi:10.1002/hyp.9865.

Semegnew Tadese, Teshome Soromessa, and Tesefaye Bekele. 2021. Analysis of the Current and Future Prediction of Land Use/Land Cover Change Using Remote Sensing and the CA-Markov Model in Majang Forest Biosphere Reserves of Gambella, Southwestern Ethiopia. https://doi.org/10.1155/2021/6685045.

Seto, K.C., B. Güneralp and L.R. Hutyra. 2012. Global forecasts of urban expansion to 2030 and direct impacts on biodiversity and carbon pools. Proceedings of the National Academy of Sciences, 109(40), pp.16083-16088.

Sexton, A.M., A.M. Sadeghi, X. Zhang, R. Srinivasan and A. Shirmohammadi. 2010. Using NEXRAD and rain gauge precipitation data for hydrologic calibration of SWAT in a northeastern watershed. Transactions of the ASABE, 53(5), pp.1501-1510.

Shrestha, S. 2012. Drivers of Land Use Change: A Study from Sundarijal Catchment, Shivapuri Nagarjun National Park. MSc. thesis, Kathmandu University.

Šimunek, J., M.T. Van Genuchten and M. Šejna. 2012. HYDRUS: Model use, calibration, and validation. Transactions of the ASABE, 55(4), pp.1263-1274.

Singh, S.K., P.B. Laari, S.K. Mustak, P.K. Srivastava and S. Szabó. 2018. Modelling of land use land cover change using earth observation data-sets of Tons River Basin, Madhya Pradesh, India. Geocarto international, 33(11), pp.1202-1222.

Sisay Nune, Teshome Soromessa and Demel Teketay. 2016. Land use and land cover change in the Bale Mountain Eco-Region of Ethiopia during 1985 to 2015. Land, 5(4), p.41.

Solomon Gebreyohannis, Ayele Taye and K. Bishop. 2010. Forest cover and stream flow in a headwater of the Blue Nile: complementing observational data analysis with community perception. Ambio 39 (4), 284–294.

Srinivasan, R., X. Zhang and J. Arnold. 2010. SWAT un-gauged: hydrological budget and crop yield predictions in the Upper Mississippi River Basin. Trans. of American Society of Agricultural and Biological Engineers 53(5): 1533-1546.

Stefanov, W. L., M. S. Ramsey and P. R. Christensen. 2001. Monitoring urban land cover change: An expert system approach to land cover classification of semiarid to arid urban centers. Remote sensing of Environment 77 (2001) 173-185.

Subedi, P., K. Subedi and B. Thapa. 2013. Application of a hybrid cellular automaton Markov (CA-Markov) Model in land-use change prediction: a case study of saddle creek drainage Basin, Florida. – Applied Ecology and Environmental Sciences 1(6): 126-132.

Subedi, P., K. Subedi and B.Thapa, 2013. Application of a hybrid cellular automaton–Markov (CA-Markov) model in land-use change prediction: a case study of Saddle

Creek Drainage Basin, Florida. *Applied Ecology and Environmental Sciences*, *1*(6), pp.126-132.

Subedi, P., K. Subedi and B.Thapa, 2013. Application of a hybrid cellular automaton–Markov (CA-Markov) model in land-use change prediction: a case study of Saddle Creek Drainage Basin, Florida. *Applied Ecology and Environmental Sciences*, *1*(6), pp.126-132.

Tadele Buraka Eyasu Elias and Alemu Lelago. 2021. Analysis and Prediction of Land Use/land Cover Changes and Driving Forces by Using GIS and Remote Sensing in the Coka Watershed, Southern Ethiopia. DOI: https://doi.org/10.21203/rs.3.rs-884581/v1.

Taelman, S.E., T. Schaubroeck, S. De Meester, L. Boone and J. Dewulf 2016. Accounting for land use in life cycle assessment: the value of NPP as a proxy indicator to assess land use impacts on ecosystems. Science of the Total Environment, 550, pp.143-156.

Tang, Z., C.E. Hull and S. Rothenberg, 2012. How corporate social responsibility engagement strategy moderates the CSR–financial performance relationship. Journal of management Studies, 49(7), pp.1274-1303.

Tekalegn Ayele, N.A. Elagib, L. Ribbe and J. Heinrich. 2017. Hydrological responses to land use/cover changes in the source region of the Upper Blue Nile Basin, Ethiopia. Science of the Total Environment, 575, pp.724-741.

Temesgen Desalegn, F. Cruz, Meigistu Kindu, M. B. Turrión and J. Gonzalo. 2014. Land-Use/Land-Cover (LULC) Change and Socioeconomic Conditions of Local Community in the Central Highlands of Ethiopia. International Journal of Sustainable Development & World Ecology.

Temesgen Gashaw, Amare Bantider and Abraham Mahari. 2014. Evaluations of land use/land cover changes and land degradation in Dera District, Ethiopia: GIS and remote sensing based analysis. Int. J. Sci. Res. Environ. Sci. 2 (6), 199–208.

Temesgen Gashaw, Taffa Tulu, Mekuria Argawa and Worqlul Abeyou. 2017. Evaluation and prediction of land use/land cover changes in the Andassa watershed, Blue Nile Basin, Ethiopia. Environmental Systems Research, 6(1), pp.1-15.

Temesgen Gashaw, Taffa Tulu, Mekuria Argawa and Worqlul Abeyou. 2018. Modeling the hydrological impacts of land use/land cover changes in the Andassa watershed, Blue Nile Basin, Ethiopia. Science of the Total Environment, 619, pp.1394-1408.

Tesfa Gebrie and Bogale Gebremariam. 2015. Impact of land use land covers change on stream flow and sediment yield: a case study of Gilgel Abay watershed, Lake Tana sub-basin, Ethiopia. Int. J. Technol. Enhanc. Merg. Eng. Res, 3, pp.28-42.

Tesfahun Addisu and Dereje Tolosa. 2019. Modeling change of Land use on Hydrological Response of River by Remedial Measures using Arc SWAT: Case of Weib Catchment, Ethiopia. DOI:10.35940/ijitee.J9531.0981119.

Tesfay Gebretsadkan, Y.A. Mohamed ,G.D. Betrie, P. Van Der Zaag and E. Teferi. 2013. Trend analysis of runoff and sediment fluxes in the Upper Blue Nile basin: A combined analysis of statistical tests, physically-based models and land use maps. Journal of Hydrology, 482, pp.57-68.

Tesfay Gebretsadkan, Y.A. Mohamed and P. Van der Zaag. 2019. Attributing the hydrological impact of different land use types and their long-term dynamics through combining parsimonious hydrological modelling, alteration analysis and PLSR analysis. Science of the Total Environment, 660, pp.1155-1167.

Tewodros Getu, Tewodros Assefa, Abreham Berta and John Barnabas. 2021. Land Use/Land Cover Change Impact on Hydrological Process in the Upper Baro Basin, Ethiopia. https://doi.org/10.1155/2021/6617541.

Tibebe Degefie and Woldeamlak Bewket. 2011. Surface runoff and soil erosion estimation using the SWAT model in the Keleta watershed, Ethiopia. Land Degrad. Dev. 22, 551–564.

Verheye, W. 2011. Land Cover, Land Use and the Global Change. Journal of Land Use, Land Cover and Soil Science I.

Vilaysane, B., K. Takara, P. Luo, I. Akkharath and W. Duan, 2015. Hydrological stream flow modelling for calibration and uncertainty analysis using SWAT model in the Xedone river basin, Lao PDR. Procedia Environmental Sciences, 28, pp.380-390.

Wagner, P.D., S. Kumar and K. Schneider. 2013. An assessment of land use change impacts on the water resources of the Mula and Mutha Rivers catchment upstream of Pune, India. Hydrology and Earth System Sciences, 17 (6), 2233–2246. doi:10.5194/hess-17-2233-2013.

Wakjira Takala, Tamene Adugna and Dawud Tamam. 2016. The effects of land use land cover change on hydrological process of Gilgel Gibe, Omo Gibe Basin, Ethiopia. Int. J. Sci. Eng. Res, 7(8), p.2020.

Wakjira Takala, Tamene Adugna and Konrad Miege. 2020. Watershed hydrological response to combined land use/land cover and climate change in highland Ethiopia: Finchaa catchment. Water, 12(6), p.1801.

Wang, Y., P. Yu, K.H. Feger, X. Wei, G. Sun, M. Bonell, W. Xiong, S. Zhang and L. Xu. 2011. Annual runoff and evapotranspiration of forestlands and non-forestlands in selected basins of the Loess Plateau of China. Ecohydrology, 4(2), pp.277-287.

Woldeamlak Bewket. 2002. Land covers dynamics since the 1950s in Chemoga watershed, Blue Nile Basin, Ethiopia. Mountain Research and Development 22, No. 3: 263–269.

Wolka Kebede, Mengistu Tefera, Taddese Habitamu and Tolera Alemayehu. 2014. Impact of land cover change on water quality and stream flow in lake Hawassa watershed of Ethiopia. Agricultural Sciences, 2014.

World Meteorological Organization. 2005. Climate and Land Degradation. Soil conservation- Land Management- Flood forecasting- Food Security. WMO- No 989.

Yan, R., X. Zhang, S. Yan, J. Zhang and H. Chen. 2018. Spatial patterns of hydrological responses to land use/cover change in a catchment on the Loess Plateau, China. Ecological Indicators, 92, pp.151-160. doi:10.1016/j.ecolind. 2017.04.013.

Yang, X.; X.Q. Zheng and L.N. Lv. 2012. A spatiotemporal model of land use change based on ant colony optimization, Markov chain and cellular automata. Ecol. Model. 233, 11–19.

Yang. X, X.Q. Zheng and R. Chen. 2014. A land use change model: Integrating landscape pattern indexes and Markov-CA. Ecol. Model. 283, 1–7.

Yesserie, A. G. 2009. Spatio-Temporal Land Use/Land Cover Changes Analysis and Monitoring in the Valencia Municipality, Spain. M.Sc Thesis, University of Jaume.

Yonas Mathewos and Teshale Ayano. 2020. Evaluations of Stream Flow Response to Land use and Land Cover Changes in Wabe Watershed, Omo-Gibe Basin, Ethiopia.

Zhang, M., X. Huang, X. Chuai, H.Yang, L. Lai and J. Tan. 2015. Impact of land use type conversion on carbon storage in terrestrial ecosystems of China: A spatial-temporal perspective. Scientific reports, 5(1), pp.1-13.

Zhou, F., Y.Xu, Y.Chen, C.Y. Xu, Y. Gao and J. Du. 2013. Hydrological response to urbanization at different spatio-temporal scales simulated by coupling of CLUE-S and the SWAT model in the Yangtze River Delta region. Journal of Hydrology, 485, pp.113-125. doi:10.1016/j.jhydrol.2012.12.040.

7. APPENDICES

Appendix 1: Coordinates for the Ground Control Points of Welmel River Basin

No	Easting	Northing	Class Name	No	Easting	Northing	Class Name
1	566953.57	734713.4	Grass/Range Land	26	587997.21	691664.34	Forest Land
2	583392.35	696713.71	Grass/Range Land	27	587600.91	689995.46	Forest Land
3	582831.21	699019.25	Grass/Range Land	28	565271.38	730429.66	Forest Land
4	574068.04	708277.23	Grass/Range Land	29	562262.36	728892.25	Forest Land
5	572351.18	732481.16	Grass/Range Land	30	561060.37	729178.63	Forest Land
6	564941.2	733304.03	Grass/Range Land	31	566640.68	746909.12	Forest Land
7	574085.12	708254.66	Grass/Range Land	32	564460.74	746719.77	Forest Land
8	573925.71	709863.84	Grass/Range Land	33	566446.18	752782.9	Forest Land
9	564848.76	732659.64	Grass/Range Land	34	564201.4	746091.04	Forest Land
10	565137.25	734052.13	Grass/Range Land	35	568830.65	741206.56	Forest Land
11	557191.68	732938.26	Grass/Range Land	36	582734.81	702825.32	Forest Land
12	566822.59	752972.7	Grass/Range Land	37	583435.5	701987.98	Forest Land
13	562845.78	751863.97	Grass/Range Land	38	570776.45	711184.79	Forest Land
14	582066.26	753893.36	Grass/Range Land	39	575333.96	712279.38	Forest Land
15	571242.15	744816.46	Grass/Range Land	40	566087.78	727575.68	Forest Land
1	586293.61	756067.82	Scrub/Bush Land	1	566518.85	737971.49	Agriculture/Set
2	583922.64	757467.7	Scrub/Bush Land	2	565020.39	735844.25	Agriculture/Set
3	577487.69	743985.09	Scrub/Bush Land	3	569586.66	730254	Agriculture/Set
4	576871.45	757844.71	Scrub/Bush Land	4	572237.83	726778.85	Agriculture/Set
5	574373.67	761160.69	Scrub/Bush Land	5	565745.09	718887.32	Agriculture/Set
6	567393.03	758426.5	Scrub/Bush Land	6	577499.23	705737.63	Agriculture/Set
7	565239.98	758112.81	Scrub/Bush Land	7	577665.4	705457.81	Agriculture/Set
8	584721.85	744841.11	Scrub/Bush Land	8	586162.29	691832.05	Agriculture/Set
9	562066.28	756566.39	Scrub/Bush Land	9	585958.28	691083.13	Agriculture/Set
10	587968.7	758213.06	Scrub/Bush Land	10	586808.64	690450.01	Agriculture/Set
1	557389.29	743949.83	Wood Land	11	584963.54	689974.16	Agriculture/Set
2	556979.63	744689.97	Wood Land	12	584495.55	690338.96	Agriculture/Set
3	565643.7	750231.86	Wood Land	13	561895.62	725689.23	Agriculture/Set
4	564925.12	753010.47	Wood Land	14	561720.17	724568.38	Agriculture/Set
5	574530.38	756335.78	Wood Land	15	564930.05	721627.69	Agriculture/Set
6	587236.83	695505.27	Wood Land	16	565292.57	719773.04	Agriculture/Set
7	588052.03	695215.54	Wood Land	17	574458.01	707317.14	Agriculture/Set
8	583276.57	692970.66	Wood Land	18	574906.54	706671.92	Agriculture/Set
9	590175.33	695891.22	Wood Land	19	576605.48	705444.89	Agriculture/Set
10	579243.82	740262.52	Wood Land	20	576680.47	702566.44	Agriculture/Set
11	557201.88	744586.16	Wood Land	21	588525.72	690806.97	Agriculture/Set
12	558029.4	743551.04	Wood Land	22	590167.48	697585.48	Agriculture/Set
13	579653.7	756603.25	Wood Land	23	586213.13	700105.24	Agriculture/Set
14	566578.68	755068.44	Wood Land	24	582253.56	700018.99	Agriculture/Set
15	572539.05	753660.54	Wood Land	25	575778.91	705076.81	Agriculture/Set
16	576126.68	750694.83	Wood Land	26	579186.2	738862.38	Agriculture/Set
17	577286.71	752467.87	Wood Land	27	578495.89	748228.71	Agriculture/Set
18	579454	744647.84	Wood Land	28	580996.26	751519.48	Agriculture/Set
19	580803.13	744166.67	Wood Land	29	577470.49	748880.87	Agriculture/Set
20	578831.95	740378.31	Wood Land	30	578664.73	751613.08	Agriculture/Set
1	575379.84	736290.14	Forest Land	31	566099.49	732982.78	Settlement/Set
2	569307.19	741895.27	Forest Land	32	564468.04	733357.63	Settlement/Set

3	570379.9	754688.52	Forest Land	33	565046.42	733773.7	Settlement/Set
4	572618.8	719628.07	Forest Land	34	577216.45	708797.32	Settlement/Set
5	572230.34	716737.58	Forest Land	35	569823.5	711542.83	Settlement/Set
6	568265.04	747012.02	Forest Land	36	569475.36	712397.24	Settlement/Set
7	571446.66	749285.49	Forest Land	37	564412.87	733287.71	Settlement/Set
8	574592.29	752256.13	Forest Land	38	576610.35	709164.33	Settlement/Set
9	582048.57	738027.08	Forest Land	39	577184.96	708799.06	Settlement/Set
10	572329.55	749438.16	Forest Land	40	576609.35	709327.69	Settlement/Set
11	575606.5	707222.08	Forest Land				
12	564437.94	733122.31	Forest Land				
13	582379.97	742188.09	Forest Land				
14	581281.04	741122.97	Forest Land				
15	581567.07	738920.61	Forest Land				
16	579228.25	736301.9	Forest Land				
17	576799.47	739084.3	Forest Land				
18	577852.2	734584.12	Forest Land				
19	574914.76	729578.77	Forest Land				
20	567828.64	724194.74	Forest Land				
21	569089.59	717043.76	Forest Land				
22	574382.4	714412.09	Forest Land				
23	573139.22	710857.46	Forest Land				
24	575645.98	707180.26	Forest Land				
25	575522.23	704301.57	Forest Land				

Appendix 2: Station Annual Rainfall from 1990 to 2020

Station Annual Rainfall				
Year	**Adaba**	**Angetu**	**Delo Mena**	**Rira**
1990	833.74	742.18	680.61	872.63
1991	976.99	732.18	819.64	752.92
1992	1092.13	932.59	934.36	512.92
1993	940.85	809.40	567.00	792.92
1994	942.39	874.59	775.80	749.57
1995	853.34	931.98	981.21	697.80
1996	942.96	909.96	1018.70	864.20
1997	768.59	806.04	1491.19	966.20
1998	849.97	928.14	1110.65	805.10
1999	765.12	729.83	759.30	865.10
2000	546.00	766.51	1301.65	804.30
2001	753.72	955.06	1191.10	768.50
2002	875.68	738.17	940.20	671.10
2003	735.13	866.13	877.45	691.90
2004	630.58	679.88	879.60	656.80
2005	637.24	836.38	1150.53	841.15
2006	1025.74	924.78	999.00	798.42
2007	899.39	875.83	1310.95	817.62
2008	790.77	963.47	921.60	838.36
2009	877.28	953.51	942.85	925.50
2010	971.30	998.13	810.45	879.20
2011	643.75	904.47	690.30	644.70

2012	864.47	765.01	1004.60	818.40
2013	1067.63	967.63	1209.50	724.50
2014	887.62	987.50	767.62	692.55
2015	1045.64	902.31	916.29	702.52
2016	850.20	904.00	1159.35	878.32
2017	757.17	835.12	905.10	898.20
2018	837.54	747.18	882.64	879.90
2019	858.66	904.61	960.27	895.35
2020	821.93	969.44	981.88	821.07

Appendix 3: Average Maximum and Minimum Temperature from 1990 to 2020

Year	**Delo Mena**		**Angetu**		**Adaba**		**Rira**	
	Av.TMAX	**Av.TMIN**	**Av.TMAX**	**Av.TMIN**	**Av.TMAX**	**Av.TMIN**	**Av.TMAX**	**Av.TMIN**
1990	28.87	15.81	26.54	14.43	23.62	10.55	19.67	10.47
1991	28.57	15.94	27.39	14.60	24.92	10.55	20.41	10.91
1992	29.27	15.72	26.97	14.53	23.86	10.52	19.18	10.77
1993	29.28	15.72	26.39	14.41	23.85	10.38	19.32	10.62
1994	30.46	14.60	26.82	14.82	23.18	10.50	20.08	10.79
1995	29.96	15.52	26.76	14.76	23.49	10.77	19.75	10.71
1996	29.23	15.72	25.62	14.45	23.63	10.53	19.48	10.73
1997	30.81	16.38	26.18	14.78	24.06	10.93	20.36	10.62
1998	30.51	16.16	26.57	15.22	23.32	10.94	19.61	10.72
1999	30.71	14.95	26.93	14.91	24.23	10.46	19.53	10.66
2000	30.72	15.91	27.99	15.07	24.08	10.77	21.90	10.67
2001	29.17	15.74	27.92	15.00	23.79	11.11	19.32	10.63
2002	30.68	15.72	28.07	15.14	24.57	11.18	20.18	10.69
2003	31.24	15.92	28.13	15.03	24.54	11.12	22.28	10.62
2004	29.95	16.27	28.42	15.10	24.59	11.18	22.45	10.71
2005	29.06	16.14	27.47	15.29	24.17	11.07	21.80	10.58
2006	30.35	16.31	24.77	14.91	23.95	10.97	19.43	10.62
2007	29.85	16.19	26.79	14.60	24.15	10.81	19.80	10.53
2008	30.28	15.94	26.94	14.63	23.81	10.83	22.09	10.70
2009	29.78	16.27	25.18	15.48	23.65	11.00	20.13	10.71
2010	30.31	16.35	24.37	15.32	23.58	11.01	19.38	10.62
2011	30.16	16.11	24.21	15.64	23.44	11.05	22.37	10.64
2012	31.23	15.96	25.19	15.65	23.51	10.80	22.11	10.73
2013	31.03	16.08	25.84	15.53	23.46	10.93	19.82	10.77
2014	30.66	15.47	25.42	14.78	23.12	10.92	19.86	10.66
2015	29.80	15.04	26.46	14.91	23.37	10.99	21.86	10.86
2016	29.86	16.03	25.24	14.92	23.92	10.94	20.64	10.85
2017	29.56	15.55	25.47	14.54	23.83	10.96	21.49	10.64
2018	29.66	15.96	23.98	15.22	25.96	10.93	21.10	10.37
2019	29.94	16.08	25.78	15.44	26.31	11.29	21.84	10.83
2020	27.40	16.30	26.11	15.38	23.83	10.93	21.00	10.14
Av.T°C	**29.35°C**	**15.87°C**	**26.32°C**	**14.98°C**	**23.99°C**	**10.87**°C	**20.59°C**	**10.66°C**

Appendix 4: Average Annual Simulated Stream flow

Month	Year				
	1990 LULC	**2005 LULC**	**2020 LULC**	**2035 LULC**	**2050 LULC**
Jan	21.51	20.42	18.55	19.82	17.69
Feb	17.32	16.64	15.37	14.67	13.60
Mar	48.36	51.53	54.95	57.42	65.82
Apr	93.03	96.90	99.84	106.34	110.83
May	129.89	132.98	136.76	147.79	161.19
Jun	70.78	69.66	66.95	65.57	62.56
Jul	61.65	59.39	57.57	55.16	53.22
Aug	95.55	99.90	104.39	112.10	122.53
Sep	97.75	104.66	107.36	118.26	134.62
Oct	108.91	115.85	123.24	137.23	143.51
Nov	73.23	80.73	86.26	93.81	102.82
Dec	36.34	36.30	35.99	35.23	34.01
Total	854.33	884.96	907.21	963.41	1022.41

Appendix 5. Area Coverage of Welmel Watershed

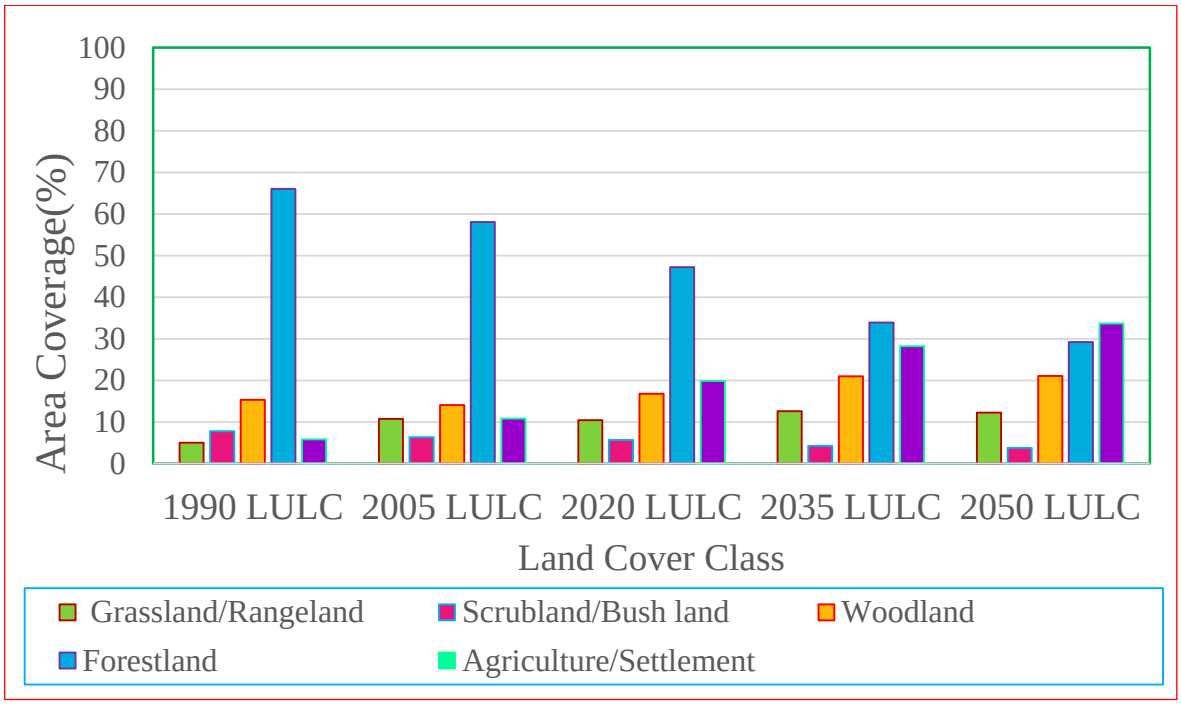

Appendix 7. Thiessen Polygon of Meteorological stations

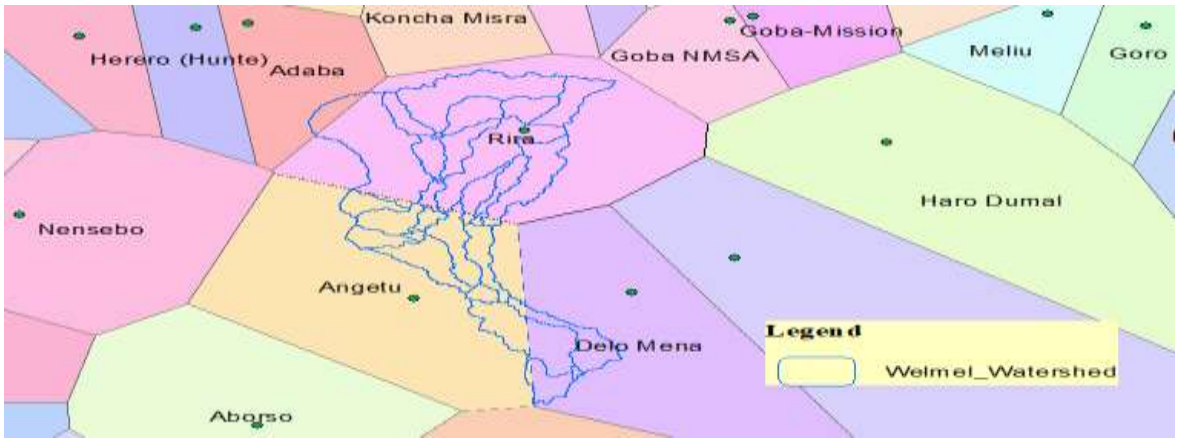

Appendix 8: Gauged Station of Welmel River at Melka Amana

Appendix 9: Landsat satellite Image of: A) 1990 B) 2005 C) 2020